Copyright

by

Daric John Wible

2015

The Dissertation Committee for Daric John Wible certifies that this is the approved version of the following dissertation:

Regulation of ATG5 and the ATG12–ATG5-ATG16L1 Complex in Prostate Cancer

Committee:

_____
Casey W. Wright, Supervisor

_____
Shawn B. Bratton, Co-supervisor

_____
Arturo De Lozanne

_____
Janice A. Fischer

_____
Dean G. Tang

Regulation of ATG5 and the ATG12–ATG5-ATG16L1 Complex in Prostate Cancer

by

Daric John Wible, B.A.

Dissertation

Presented to the Faculty of the Graduate School

of The University of Texas at Austin

in Partial Fulfillment

of the Requirements

for the Degree of

Doctor of Philosophy

The University of Texas at Austin

May 2015

Acknowledgments

I am of course very grateful for my Ph.D. advisor, Dr. Shawn Bratton, who took me on even though I came in without much experience in the lab. I struggled mightily at the beginning having joined a project that was new and exciting, but was not directly related to the main focus of the lab. Despite spending most of the first couple years essentially beating my head against the wall, Shawn never gave up on me. It would eventually be one single interesting finding that Shawn helped me nurture into a stand-alone project that would become the entirety of this dissertation. I'm very appreciative of the freedom that he gave to me in the lab. He instilled confidence in my own ability to drive this project and make it into my own, even though I was starting it several years already into my graduate career. It certainly didn't come together as quickly as we had all hoped, but I'm proud of what I've developed and I owe Shawn a lot for his guidance. I hope this project lives on in the form of multiple RO1s and the lab becomes known as a premier autophagy lab.

I need to thank our collaborators, especially Dean for his unique expertise and for always challenging me on the basketball court. Also, his lab members Tammy and Eva were very kind in helping with the mice and bioinformatics work. I also need to acknowledge my committee for giving their time and advice and to everyone in neighboring labs from old pharmacy, BME and at Science Park.

Finally, I need to thank my friends and family. To everyone in the lab currently: Ting for being there with me the whole time, Sophie for being the nicest person ever, Nick for being the lab clown who eats packing peanuts, and Crystal for teaching me Chinese swears. To the ghosts of the past: Srinivas, Madhavi, John and Shankar. To Mike and James, for being the most normal people in the building, even though they are both far from normal. To my parents for supporting me and not constantly hounding me about when I'm going to graduate and get a real job. And, of course, to Cari who made it so that I was the only one in the lab not pissed about moving to Science Park. She has stuck with me through all the late nights in the lab, all the random 3 AM time points and basically kept me alive while I tried to work full-time on experiments and write this dissertation simultaneously. For that, I'm very thankful for her.

Regulation of ATG5 and the ATG12–ATG5-ATG16L1 Complex in Prostate Cancer

by

Daric John Wible, Ph.D.

The University of Texas at Austin, 2015

Supervisor: Casey W. Wright

Co-Supervisor: Shawn B. Bratton

Autophagy is a highly conserved pathway in which an autophagosome envelops cytoplasmic cargo and delivers it to the lysosome for degradation in order to maintain cellular homeostasis or survival in response to stress. The ATG12–ATG5-ATG16L1 complex functions as an essential regulator of autophagosome formation. We have discovered that DU145 prostate cancer (PCa) cells have a splice donor-site mutation that triggers aberrant splicing of *ATG5* and leads to the proteasomal degradation of ATG12 and ATG16L1, thus completely inactivating autophagy. We demonstrate that ATG5, ATG12, and ATG16L1 are coordinately degraded when not associated with the complex and that the ATG5-ATG16L1 interaction is essential for preventing ubiquitination and turnover, thereby facilitating ATG12 conjugation. We also show that this

interaction can be disrupted through alternative *ATG5* splicing and by *ATG5* genetic mutations that have been identified in human tumors. Meta-analysis of available mRNA expression data indicates that ATG5 is significantly downregulated in PCa. We confirmed previous reports that found prostate cancers have frequent deletions of the 6q21 locus containing *ATG5*. However, mRNA expression of neighboring genes is largely unaffected, indicating *ATG5* can also be selectively downregulated though other mechanisms. Together, this suggests that *ATG5* functions as a tumor suppressor gene that can be inactivated by a variety of different mechanisms. *ATG5* is more significantly underexpressed than many established PCa tumor suppressor genes and is also underexpressed in PCa metastases compared to primary tumors. This implies that *ATG5* is also a tumor suppressor in advanced PCa. *ATG5* re-expression in *ATG5*-deficient DU145 PCa cells resulted in dramatic suppression of xenograft tumor growth, indicating that *ATG5* is a functional PCa tumor suppressor gene. Therefore, autophagy may actually be tumor suppressive at both early and late stages of prostate tumorigenesis, which suggests that autophagy inhibition may be counterproductive for the treatment of advanced prostate cancers.

Table of Contents

List of Tables

List of Figures

List of Abbreviations

3-MA	3-methyladenine
AIM	Atg8-interacting motif
ALS	amyotrophic lateral sclerosis
AMBRA1	autophagy/Beclin 1 regulator 1
AMPK	AMP-activated protein kinase
AR	androgen receptor
Arg	arginine
APF-1	ATP-dependent proteolysis factor-1 (ubiquitin)
apg1	autophagy-related 1
ATG	autophagy-related
ATG16L1	autophagy-related 16-like 1
ATG16L2	autophagy-related 16-like 2
Baf A1	Bafilomycin A1
BAX	BCL2-associated X protein
BECN1	Beclin 1, autophagy-related
Bcl-2	B-cell CLL/lymphoma 2
BCR-ABL1	breakpoint cluster region–c-abl oncogene 1-ABL proto-oncogene 1 gene fusion
Bif-1	SH3-domain GRB2-like endophilin B1 (*SH3GLB1*)
BNIP3	BCL2/adenovirus E1B 19kDa-interacting protein 3

BRAF	V-raf murine sarcoma viral oncogene homolog B
BRCA1	breast cancer 1, early onset
BVES	blood vessel epicardial substance
Cas9	CRISPR associated protein 9
CDKN1B	cyclin-dependent kinase inhibitor 1B (*p27*)
cBioPortal	cBioPortal for Cancer Genomics
CGH	comparative genomic hybridization
CMA	chaperone-mediated autophagy
COSMIC	Catalogue of Somatic Mutations in Cancer
cpm	counts per minute
CRISPR	clustered regularly interspaced short palindromic repeat
DAPK	death-associated protein kinase 1
DFPC1	double FYVE domain-containing protein 1
DLBC1	diffuse large B-cell lymphoma
DMSO	dimethyl sulfoxide
DUB	deubiquitinase
ECM	extracellular matrix
EM	electron microscopy
EMT	epithelial-mesenchymal transition
ER	endoplasmic reticulum
EV	empty vector
ERGIC	ER-golgi intermediate compartment

FACS	fluorescence-activated cell sorting
FBS	fetal bovine serum
FIP200	200 kDa FAK family kinase-interacting protein (RB1CC1)
FUNDC1	FUN14 domain-containing protein 1
GABARAP	GABA(A) receptor-associated protein
GABARAPL1	GABA(A) receptor-associated protein like 1
GABARAPL2	GABA(A) receptor-associated protein like 2 (GATE-16)
GATE-16	GABA(A) receptor-associated protein like 2 (GABARAPL2)
Gln	glutamine
Glu	glutamate
HBSS	Hank's buffered saline solution
HGPIN	high-grade prostatic intraepithelial neoplasia
HEK	human embryonic kidney
HSC70	heat shock cognate protein 70
HSP90	heat shock protein 90
ICGC	International Cancer Genome Consortium
JNK1	JUN N-terminal kinase (JNK1) kinase
KRAS	Kristen rat sarcoma viral oncogene homolog
LAMP-2A	lysosome-associated membrane protein 2A
LC3	microtubule-associated protein 1 light chain 3 (MAP1LC3)
LC3-I	cytosolic form of LC3
LC3-II	lipid conjugated form of LC3

LIR	LC3-interacting region
Lys	lysine
MAP1LC3	microtubule-associated protein 1 light chain 3 (LC3)
MAP3K7	mitogen-activated protein kinase kinase kinase 7 (*TAK1*)
MEF	mouse embryonic fibroblast
Mcl-1	myeloid cell leukemia 1
MCS	multiple cloning site
Mhtt	mutant huntingtin
MHC	major histocompatibility complex
MOMP	mitochondrial outer-membrane permeabilization
MSI	microsatellite instability
mTORC1	mammalian target of rapamycin complex 1
MVB	multi-vesicular body
MYC	v-myc avian myelocytomatosis viral oncogene homolog
Na-Caco	sodium cacodylate
NBR1	neighbor of BRCA1 Gene 1
NCBI	National Center for Biotechnology Information
NF-κB	nuclear factor kappa-light-chain-enhancer of activated B cells
NFT	neurofibrillary tangles
NIX	NIP3-like protein X
NKX3-1	NK3 homeobox 1

NMD	nonsense-mediated decay
NOD	non-obese diabetic
NRF2	nuclear factor, erythroid 2-like 2
ORF	open reading frame
p27	cyclin-dependent kinase inhibitor 1B (*CDKN1B*)
p53	tumor protein p53 (*TP53*)
p62	sequestosome-1 (SQSTM1)
p150	phosphatidylinositol 3-kinase, regulatory subunit 4 (VPS15)
Parkin	parkin RBR E3 ubiquitin protein ligase
PB	rat probasin
PCa	prostate cancer
PE	phosphatidylethanolamine
PGAM5	phosphoglycerate mutase family member 5
Phe	phenylalanine
PI3K	phosphatidylinositol 3-kinase
PIK3C3	phosphatidylinositol 3-kinase, catalytic subunit type 3 (VPS34)
PI(3)P	phosphatidylinositol 3-phosphate
PINK1	PTEN induced putative kinase 1
PML-RARA	promyelocytic leuikemia–retinoic acid receptor, alpha gene fusion
POPDC3	popeye domain containing 3

PREP	prolyl endopeptidase
Prkdc	protein kinase, DNA-activated, catalytic polypeptide
PtdIns3P	phosphatidylinositol 3-phosphate
PTEN	phosphatase and tensin homolog
RB1	retinoblastoma 1
RB1CC1	RB1-inducible coiled coil 1 (FIP200)
ROS	reactive oxygen species
scid	severe combined immunodeficiency mutation
SH3GLB1	SH3-domain GRB2-like endophilin B1 (*Bif-1*)
shRNA	short hairpin RNA
SILAC	stable isotope labeling by amino acids in cell culture
SLE	systemic lupus erythematosus
SMAD4	SMAD family member 4
SNARE	soluble NSF attachment protein receptor
SNP	single-nucleotide polymorphism
SPOP	speckle-type POZ protein
SQSTM1	sequestosome-1/p62
STAT3	signal transducer and activator of transcription 3
TAK1	mitogen-activated protein kinase kinase kinase 7 (*MAP3K7)*
TEM	transmission electron microscopy
TCA	Trichloroacetic acid
TCGA	The Cancer Genome Atlas

TECPR1	tectonin beta-propeller repeat containing 1
TMPRSS2-ETS	transmembrane protease, serine 2 – E twenty-six transcription factor family gene fusions
TP53	tumor protein p53
TRAF6	TNF receptor-associated factor 6, E3 ubiquitin protein ligase
TWIST1	Twist-related protein 1
Ub	ubiquitin
UBL	ubiquitin-like
UFD	ubiquitin-fold domain
ULK1	unc-51 like autophagy activating kinase 1
ULK2	unc-51 like autophagy activating kinase 2
uORF	upstream open reading frame
UPS	ubiquitin-proteasome system
USP9X	ubiquitin specific peptidase 9, X-linked
USP13	ubiquitin specific peptidase 13
UTR	untranslated region
UVRAG	UV radiation resistance associated gene
VPS15	phosphatidylinositol 3-kinase, regulatory subunit 4 (p150)
VPS34	phosphatidylinositol 3-kinase, catalytic subunit type 3 (PIK3C3)
WIPI2	WD repeat domain, phosphoinositide-interacting protein 2
WT	wild-type

Chapter 1: Introduction

1.1 Mechanisms of Proteolysis

1.1.1 Early history of proteolysis research – Decades of groundbreaking research have lead to our current understanding that protein synthesis and proteolysis exist in equilibrium within the cells of all forms of life. Early studies on DNA and the discovery of the DNA double-helix structure by James Watson and Francis Crick essentially established the field of molecular biology in the early 1950s. In the years following, several groups raced to determine how genetic information coded in DNA could result in the synthesis of diverse and complex proteins within the cell. With the main focus of scientific interest on the understanding of the genetic code and protein synthesis, the importance of protein degradation was largely overlooked.

Today we can appreciate that all proteins are continuously degraded and resynthesized and that complex mechanisms exist to ensure this degradation occurs in a highly controlled manner. However, the idea that structural proteins unrelated to cellular metabolism were degraded was not well accepted until several scientists applied new technologies and used new experimental techniques to make significant advancements in the understanding of protein catabolism in the mid-1950s (Ciechanover, 2005). The most important contribution was the discovery and biochemical characterization of the lysosome

by Christian de Duve in 1955, for which he would later win a Nobel Prize in Physiology or Medicine in 1974 (Bowers, 1998). By optimizing the newly developed technique of cellular fractionation, de Duve discovered that certain fractions of rat liver homogenates contained latent acid phosphatase activity. He determined that the latent activity was due to the sequestration of the active enzyme by a membrane barrier that could be mechanically or chemically disrupted. Analyzing the activity of several acid hydrolases led de Duve to propose that these enzymes were contained within a novel subcellular particle that he termed the *lysosome*, due its hydrolytic properties (De Duve et al., 1955).

Later that year, Alex Novikoff fixed Dr. de Duve's lysosome-enriched fractions of rat liver and examined them with an electron microscope, a technology that at that time was only just beginning to see biological applications. Using a histochemical technique that labeled sites of acid phosphatase activity with electron-dense lead sulfide deposits, Novikoff and de Duve revealed the morphology of the lysosome, *in situ*, for the first time (Novikoff et al., 1956). Dr. de Duve's discovery of the lysosome was a defining moment in cell biology and would lead to the identification of a multitude of degradative pathways that converge at the lysosome.

1.1.2 Discovery of autophagy – The pairing of histochemistry and electron microscopy (EM) became a powerful tool for characterizing the morphology of cellular structures that had been previously only inferred biochemically. Early

studies revealed lysosomes and other membrane-bound vesicles, initially identified as immature or pre-lysosomes, exhibited significant functional and morphological diversity. A process called *heterophagy*, referring to the uptake and degradation of extracellular material (now broadly referred to as endocytosis), was initially characterized by the engulfment of exogenous material into distinct membrane vesicles initially termed *heterophagosomes*. These structures were shown to eventually merge with the acid phosphate-positive lysosomes to form hybrid *phago-lysosomes*, where the internalized material was degraded (De Duve and Wattiaux, 1966). Currently, the term *endocytosis* is used to encompass several different cellular processes that all originate from the plasma membrane. These include: phagocytosis, which is the uptake and extracellular material; pinocytosis, which is the uptake of extracellular fluid; and receptor-mediated endocytosis, which is the selective uptake of substrates that bind to cell-surface receptors. Generally, these endocytic pathways terminate at the lysosome where the contents are degraded, although in some cases material can be recycled to the cell surface or secreted out of the cell (Mukherjee et al., 1997).

Early EM studies also indicated that, in addition to the delivery of exogenous substrates to the lysosome, intracellular material could also be degraded upon engulfment within double-membrane bound vesicles that subsequently fuse with lysosomes. In 1963, Christian de Duve coined this process as *autophagy*, which is derived from Greek for “self-eating”, to contrast it

with the term *heterophagy* that defines the degradation of exogenous material (Ohsumi, 2014). In 1968, Antti Arstila and Benjamin Trump eloquently illustrated the process of autophagy by using EM to image double and single membrane structures containing diverse intracellular material, including mitochondria and endoplasmic reticulum (ER), at various stages of degradation (Arstila and Trump, 1968). The double-membrane structure, called an *autophagosome*, lacks acid hydrolases necessary for proteolysis and instead serves to sequester portions of the cytoplasm and deliver it to the lysosome where the cargo is exposed to proteolytic enzymes and degraded. It was initially determined that autophagosomes form *de novo* in the cytosol rather than originating directly from the plasma membrane or some other membrane vesicle, although it is now believed that autophagosomes form in close association with the ER and can receive membrane contributions from a variety of sources including the outer mitochondrial membrane, the plasma membrane, the ER-golgi intermediate compartment (ERGIC) and recycling endosomes (Shibutani and Yoshimori, 2014). The fusion of the autophagosome and lysosome results in the degradation of the both the sequestered cytoplasmic material as well as the inner membrane of the autophagosome, creating a single membrane structure dubbed the *autolysosome* or *autophagolysosome* (Klionsky, 2007) (Fig. 1.1*A*).

1.1.3 Types of autophagy – The landmark 1966 review on lysosomes written by Christian de Duve and Robert Wattiaux referred to another form of autophagy

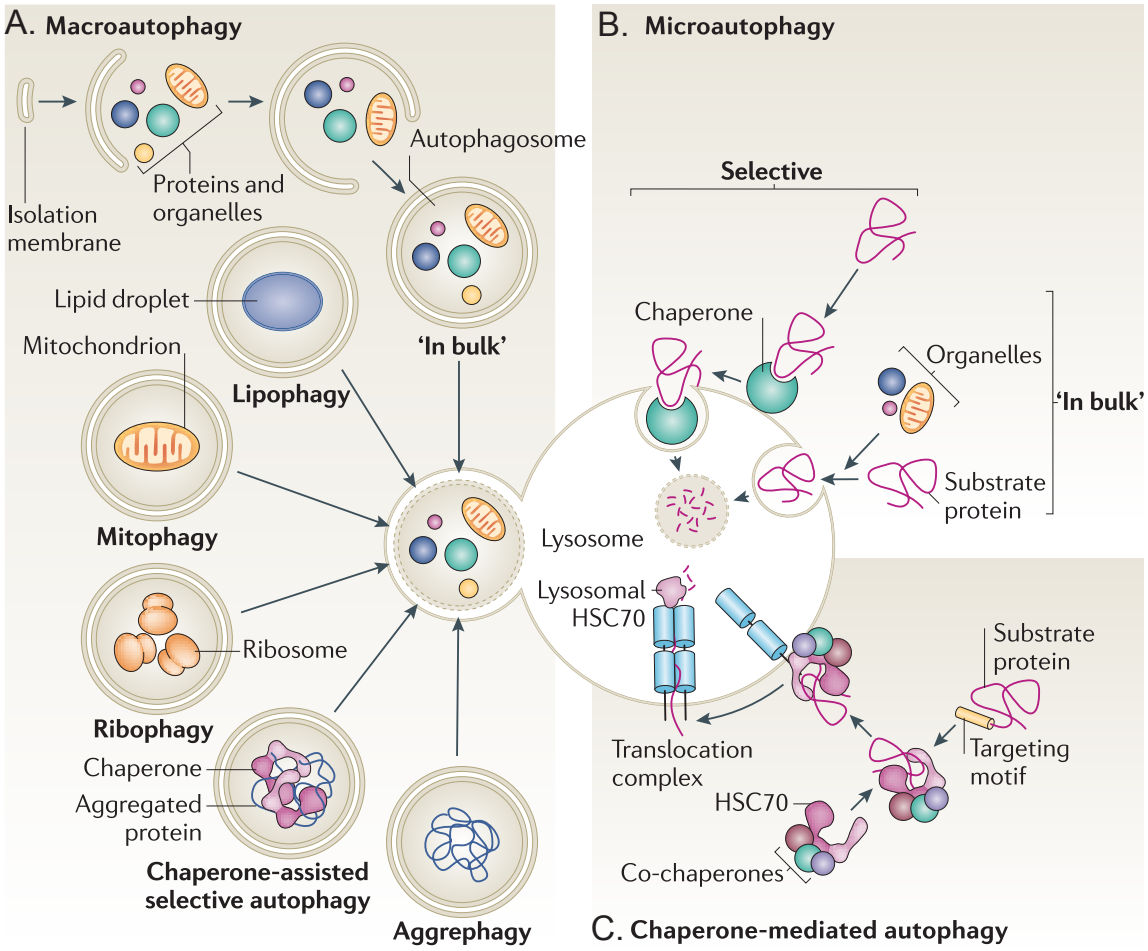

Figure 1.1 – Overview of autophagy pathways. (*A*) Macroautophagy (herein referred to as autophagy) begins with the formation of a double-membrane sheet called the isolation membrane or the phagophore. The phagophore/isolation membrane elongates and envelops either bulk or selective cytoplasmic cargo including: lipid droplets, mitochondria, ribosomes, protein aggregates, etc., before eventually closing to form a mature, double-membrane autophagosome. The autophagosome then fuses with a lysosome where the sequestered material is degraded and can be recycled. (*B*) Microautophagy involves bulk and selective degradation of cytoplasmic material by direct invagination of the lysosomal membrane. (*C*) Chaperone-mediated autophagy (CMA) requires unfolding and translocation of proteins containing a KFERQ motif across the lysosomal membrane via the HSC70/LAMP-2A translocation complex. Adapted from: Cuervo, A.M. (2011). Nat Rev Mol Cell Biol **12**(8): 535-541.

called *microautophagy* that is used to describe the direct invagination or sequestration of cytoplasmic material by the lysosomal membrane (De Duve and Wattiaux, 1966) (Fig. 1.1*B*). Despite a lack of concrete evidence of its existence in 1966, the term *microautophagy* was used to differentiate the process from the more pronounced pathway of *macroautophagy*, which involves the formation of the autophagosome and subsequent fusion with the lysosome (Fig. 1.1*A*). Generally, the term *autophagy* is used to specifically refer to *macroautophagy* and this terminology will be hereafter used, unless otherwise indicated.

To date, very little is known about microautophagy. The most conclusive examples have been found in yeast where the yeast vacuole is considered roughly analogous to the mammalian lysosome. Using electron microscopy, the yeast vacuole has been imaged invaginating and surrounding non-specific portions of the cytosol as well as a variety of cellular components including mitochondria, peroxisomes, and portions of the nucleus (Mijaljica et al., 2011). Microautophagy-like lysosomal structures have also been captured by EM in mammalian cells (de Waal et al., 1986), however the mechanism for how these structures form is not known. The invagination of the endosomal membrane during formation of MVBs has been shown to, at times, include cytosolic proteins and has been described as a microautophagy-like process (Sahu et al., 2011).

The 1980s saw the discovery of another mechanism for transporting specific proteins from the cytoplasm, across the lysosomal membrane and into the lumen of the lysosome. This process would eventually be named *chaperone*-

mediated autophagy (CMA), after the chaperone protein, heat shock cognate protein 70 (HSC70), was found to promote the unfolding of the target proteins and their translocation across the membrane via the multimerization of the lysosomal membrane protein, lysosome-associated membrane protein 2A (LAMP-2A) (Chiang et al., 1989; Cuervo and Dice, 1996) (Fig. 1.1*C*). The Lys-Phe-Glu-Arg-Gln (KFERQ) pentapeptide motif was identified as an HSC70 binding site and was found to be both necessary and sufficient to target proteins for CMA, which to date has only been shown to occur in mammalian cells (Chiang and Dice, 1988; Chiang et al., 1989; Cuervo, 2011).

Crosstalk has been reported between macroautophagy and CMA where inhibition of either form of autophagy leads to the strong activation of the remaining functional pathway (Cuervo and Wong, 2014). While macroautophagy and CMA have distinct, non-overlapping functions, it is believed they can partially compensate for one another in response to cellular stress. However, no such connections have been reported with microautophagy (Mijaljica et al., 2011).

1.1.4 Selective autophagy – Since the observation that autophagosomes and autolysosomes contained a variety of intracellular material, there has been keen interest in determining precisely what serves as a suitable target for autophagy and what determines the type of sequestered cargo. CMA is an example of a selective mechanism for degrading specific cytosolic proteins containing the KFERQ motif. However, unlike CMA, it is generally thought that both micro and

macroautophagy can either selectively or non-selectively sequester intact cytoplasmic material of a wide range of sizes and deliver it to the lumen of the lysosome. Most evidence suggests non-specific autophagy is activated as a survival mechanism in response to starvation conditions where bulk cytoplasmic material can be degraded and recycled for use in essential cellular processes. However, one examination of starvation-induced protein turnover by stable isotope labeling by amino acids in cell culture (SILAC) and mass spectrometery suggested some cytoplasmic components might be more preferentially degraded than others (Kristensen et al., 2008). In contrast, selective autophagy is believed to be a homeostatic mechanism, regulating the quantities of specific organelles according to cellular needs and removing deleterious protein aggregates, damaged organelles and invading pathogens. Usually the selective process is named based on the specific cargo that is enveloped and degraded such as aggrephagy for protein aggregates or xenophagy for pathogens. Organellophagy, a broad term for the autophagic degradation of organelles, includes, but is not limited to: mitophagy for the selective degradation of mitochondria, pexophagy for peroxisomes, ribophagy for ribosomes, lipophagy for lipid droplets, nucleophagy for portions of the nucleus, reticulophagy/ER-phagy for the ER and even lysophagy for autophagic degradation of lysosomes (Okamoto, 2014) (Fig. 1.1*A*).

The most studied form of selective autophagy is mitophagy, which eliminates excess mitochondria in times of nutrient surplus and removes

defective mitochondria that release reactive oxygen species (ROS) that can damage lipids, proteins or DNA within the cell (Murphy et al., 2011). Mammalian cells have two known mechanisms of mitophagy, both of which involve recruitment of the mitochondrion to the autophagosome by receptor proteins that bind to a family of proteins called the microtubule-associated protein 1 light chain 3 (MAP1LC3 or LC3) family, which are homologous to yeast autophagy-related protein 8 (Atg8) and are found exclusively on autophagosome membranes (Moyzis et al., 2015). BCL2/adenovirus E1B 19kDa-interacting protein 3 (BNIP3), NIP3-like protein X (NIX/BNIP3L) and FUN14 domain-containing protein 1 (FUNDC1) are mitochondrial outer membrane proteins whose affinity for LC3 family members are both positively and negatively regulated by different phosphorylation events that ultimately control the sequestration of the mitochondrion by the autophagosome (Novak et al., 2010; Liu et al., 2012; Zhu et al., 2013) (Fig. 1.2*A* and 1.2*B*).

Loss of mitochondrial membrane potential leads to a second mitophagy mechanism initiated by the stabilization of the protein kinase, PTEN induced putative kinase 1 (PINK1), on the outer membrane of depolarized mitochondria. PINK1 recruits and phosphorylates parkin RBR E3 ubiquitin protein ligase (Parkin), stabilizing it on the outer membrane where it promotes the ubiquitin conjugation of multiple mitochondrial outer membrane proteins. Ubiquitin is a 76-amino acid protein that is covalently conjugated to lysine residues as a post-translational modification and serves as a destruction signal. The relevant

Receptor-mediated mitophagy

A. BNIP3/NIX

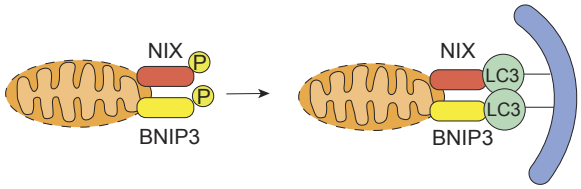

B. FUNDC1

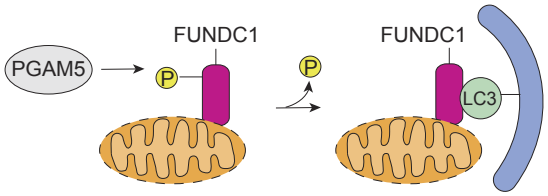

Ubiquitin-mediated mitophagy

C. PINK1/Parkin

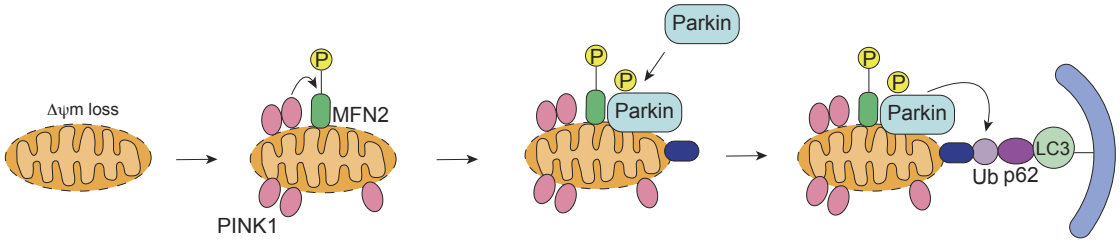

Figure 1.2 – Mechanisms of mitophagy. (*A*) Phosphorylation of mitochondrial outer membrane proteins, BNIP3 and BINP3L(NIX), increases their affinity for the autophagosome-associated protein, LC3, resulting in recruitment of the mitochondrion into the autophagosome. (*B*) FUNDC1 affinity for LC3 is increased by phosphoglycerate mutase family member 5 (PGAM5)-mediated dephosphorylation in response to mitochondrial stress, which also leads to recruitment of the mitochondrion into the autophagosome. (*C*) PINK1 is stabilized on the outer membrane of depolarized mitochondria where it phosphorylates the E3 ligase, Parkin, stabilizing it on the outer membrane and stimulating its ubiquitin ligase activity. Adapter proteins such as p62, bind Parkin-ubiquitinated substrates and target the mitochondrion to the autophagosome via interaction with LC3. Adapted from: Moyzis et al. (2015). Am J Physiol Heart Circ Physiol **308**(3): H183-192.

ubiquitinated target proteins are not well characterized, however the adapter proteins sequestosome-1 (SQSTM1/p62) and neighbor of BRCA1 Gene 1 (NBR1), are known to bind the ubiquitinated outer membrane proteins as well as LC3 on the autophagosomal membrane, thus incorporating the defective mitochondrion into the autophagosome (Okamoto, 2014) (Fig. 1.2*C*). Ubiquitin, p62 and NBR1 have been shown to be essential for the selective autophagic clearance of a variety of other ubiquitinated substrates including peroxisomes, protein aggregates, as well as intracellular bacteria (Rogov et al., 2014). While ubiquitin plays an important role in selective autophagy, it is also essential for another intracellular and lysosome-independent proteolysis pathway called the ubiquitin-proteasome system (UPS).

1.1.5 Ubiquitin-proteasome (UPS) system – For many years, the only known location for intracellular protein degradation was the lysosome via autophagy. The late 1970s saw the development and use of lysosomotropic weak bases, such as chloroquine and ammonium chloride, which freely enter the lumen of the lysosome and neutralize the low pH, thus inactivating the acid hydrolase enzymes. These agents inhibited both heterophagy/endocytosis and autophagy, but surprisingly did not completely prevent intracellular proteolysis (Poole et al., 1977). Based on this, it was proposed that a lysosome-independent mechanism for intracellular proteolysis must exist.

In 1980, in a series of elegant biochemical studies reminiscent of De Duve's fractionation experiments that led to the discovery of the lysosome, Avram Hershko and Aaron Ciechanover used fractionation of reticulocytes (immature red blood cells that lack lysosomes) and found two distinct fractions that contained energy-dependent proteolytic activity when combined together. Further characterization of one fraction would lead to the discovery of ATP-dependent proteolysis factor-1 (APF1), which turned out to be the previously identified, but functionally unknown protein, ubiquitin (Wilkinson et al., 1980). Hershko and Ciechanover observed that ubiquitin (APF1) covalently conjugated to a variety of proteins and stimulated their degradation (Ciechanover, 2005).

Shortly after, Hershko and Ciechanover used affinity chromatography of immobilized ubiquitin and discovered three enzymes responsible for this covalent conjugation reaction: enzyme-1 (E1) that activates ubiquitin; E2, which is a ubiquitin-conjugating enzyme and facilitates transfer of ubiquitin to the substrate; and E3, which is a ubiquitin-ligase that specifically binds a target protein as well as the ubiquitin–E2 and catalyzes the transfer of ubiquitin to the substrate (Ciechanover et al., 1982; Hershko et al., 1983) (Fig. 1.3). Hershko and Ciechanover would share the Nobel Prize in Chemistry in 2004 for their characterization of the ubiquitin system. It is now estimated the human genome contains two E1 enzymes, approximately 40 E2 enzymes and more than 600 different E3 ligases which provides remarkable substrate diversity for the ubiquitin conjugation reaction (Komander, 2009).

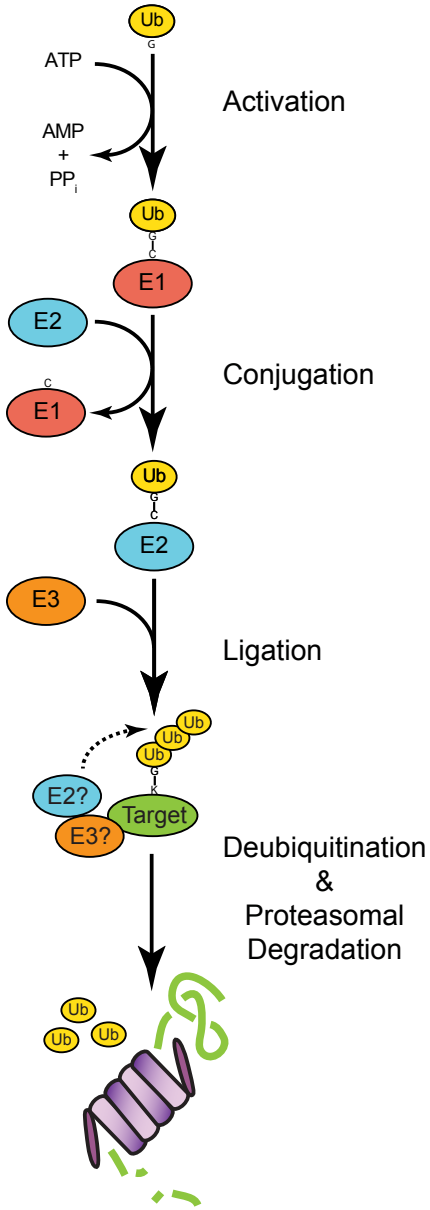

Figure 1.3 – Ubiquitin conjugation reaction. Ubiquitin is activated by ATP and the ubiquitin-activating (E1) enzyme creating a thioester bond between its catalytic cysteine and the C-terminal glycine of ubiquitin. Next, a ubiquitin-conjugating (E2) enzyme attacks the E1–ubiquitin thioester bond, resulting in transfer of ubiquitin to the catalytic cysteine of the E2 enzyme. An E3 ubiquitin-ligase enzyme then binds the E2–ubiquitin intermediate and a target protein, catalyzing the transfer of ubiquitin to a lysine residue on either the target protein or another ubiquitin molecule to form linear or branched polyubiquitin chains. Linear polyubiquitin chains direct the target protein to the proteasome where ubiquitin is deconjugated and recycled and the target protein is unfolded and degraded.

By the early 1990s, a large multicatalytic protease called the proteasome was determined to be responsible for the ATP-dependent proteolytic activity of the second fraction initially isolated by Hershko and Ciechanover in 1980. The 26S proteasome consists of a 20S core particle, a hollow cylindrical structure that contains proteolytic activity and two 19S regulatory particles that act like a "cap" to regulate protease activity by specifically recognizing ubiquitinated proteins, unfolding them and directing them into the pore of the core particle. Proteasome-associated deubiquitinases (DUBs) remove the ubiquitin tags from target proteins prior to their entrance into the core particle, which allows ubiquitin to be recycled rather than degraded along with the target protein (Ciechanover, 2005) (Fig. 1.3).

Ubiquitin is conjugated via its C-terminal glycine residue to the ε-amino groups of lysine residues on target proteins as well as to lysines within other ubiquitin molecules. The seven internal lysine residues of ubiquitin allow the formation of a variety of different isopeptide linkages that result in both linear polyubiquitin chains, branched ubiquitin chains or mixtures of each. These chains have a variety of degradative and non-degradative functions. Lys^{48} is the most common polyubiquitin linkage and is primarily responsible for promoting the proteasomal degradation of protein substrates (Komander, 2009). Branched ubiquitin chains are resistant to degradation, while it is thought that all types of linear ubiquitin chains can promote proteasomal degradation, with the possible exception of Lys^{63}-linkages (Kim et al., 2007; Komander, 2009).

Based on the specific length and type of the linkage, ubiquitin can also promote lysosomal degradation through either endocytosis or autophagy. Lys^{63} ubiquitin chains are thought to trigger the endocytosis and sorting of plasma membrane proteins into MVBs that ultimately fuse with lysosomes where the targets are degraded (Clague and Urbe, 2010). Lys^{63}-linked ubiquitination was also found to promote the autophagic removal of protein aggregates, while monoubiquitination was shown to be sufficient to target a soluble, cytosolic protein to the autophagosome (Kim et al., 2008; Tan et al., 2008). The ubiquitin adapter protein, p62, reportedly has higher affinity for monoubiquitin and Lys^{63} polyubiquitin chains than other forms of ubiquitin, suggesting these specific forms may promote autophagic degradation over proteasomal degradation (Seibenhener et al., 2004; Long et al., 2008). This may not always be the case as both Lys^{27} and Lys^{63} polyubiquitin chains have a reported role in Parkin-mediated mitophagy (Geisler et al., 2010). Thus, while the specific functions of different ubiquitin linkages are not entirely clear, the unifying role of ubiquitin in both the proteasome and the autophagy-lysosome systems is indicative of the importance and the degree of crosstalk between these two intracellular degradation pathways.

1.1.6 Crosstalk between autophagy and the UPS – Early studies characterizing the kinetics of protein turnover found widely differing rates of protein degradation (Goldberg and St John, 1976). The UPS specializes at

selectively degrading short-lived, soluble, cytosolic proteins while long-lived proteins as well as organelles or large protein aggregates that are unable to be partially unfolded and enter into proteasomes can instead be selectively sequestered by the autophagosome and delivered to the lysosome for degradation. Still, there is evidence of overlapping substrates between the two pathways, particularly with misfolded or aggregate-prone proteins such as alpha-synuclein (Shaid et al., 2013).

There are also numerous instances of cross-regulation between the two intracellular degradation pathways. Most examples of crosstalk between autophagy and the UPS are based on observations that perturbation of one pathway affects the other. Pharmacological and genetic inhibition of the proteasome results in the upregulation of autophagy in many different contexts, however the mechanisms involved in this compensation are largely unknown (Park and Cuervo, 2013). In contrast, one report found that long term inactivation of autophagy actually impairs proteasomal degradation due to a build up of p62, which is normally degraded by autophagy and was proposed to be responsible for impeding delivery of ubiquitinated proteins to proteasomes (Korolchuk et al., 2009).

Proteasomes are a reported target for starvation-induced autophagy, suggesting that stress-induced autophagy can directly regulate the UPS (Kristensen et al., 2008). Countless examples of ubiquitination and proteasomal degradation of autophagy-related proteins indicate the UPS is also an important

regulator of autophagy. Some examples of specific regulation of autophagy-related proteins by ubiquitination will be discussed in more detail in the next section, which focuses on the molecular mechanisms regulating autophagy. Interestingly, autophagosome formation involves a number of ubiquitin-like (UBL) proteins that share similar structures and undergo multi-step conjugation reactions analogous to ubiquitin. The molecular similarities between ubiquitin and the autophagy-related UBL proteins suggest a possible evolutionary link between the ubiquitin-proteasome pathway and autophagy that could potentially account for the extent of crosstalk between them.

1.2 Molecular Mechanisms of Autophagy

1.2.1 Identification of autophagy-related (*ATG*) genes – Electron microscopy was indispensible for determining the morphological characteristics of the forming autophagosome and its subsequent fusion with the lysosome. For decades, scientific understanding of autophagy was almost entirely based on the early EM-based morphological descriptions of the basic autophagy pathway. Still, researchers had no way of quantifying the amount of actual autophagic protein degradation and a specific biochemical marker, such as acid phosphatase activity, did not exist for autophagosomes. With no biochemical marker for autophagy and no knowledge of the molecular machinery involved in autophagosome formation, the field remained largely stagnant until the early

1990s when the discovery of autophagy in yeast brought the field into the molecular age.

The yeast vacuole is considered roughly analogous to the mammalian lysosome and contains an acidic lumen with hydrolytic enzymes. However, the power of yeast genetics and the specific characteristics of the yeast vacuole made yeast an ideal model system for identifying the genes involved in autophagy. Besides the wealth of genetic tools, one major advantage is that the yeast vacuole is the only organelle visible by phase contrast microscopy and it has a low refractive index due to its low protein content (Ohsumi, 2014). This attribute led Yoshinori Ohsumi to observe that “autophagic bodies”, consisting of a single membrane vesicle containing cytoplasmic material, visibly accumulated within the vacuole of nutrient starved *Saccharomyces cerevisiae* containing a genetic deficiency in several vacuolar hydrolases (Takeshige et al., 1992). This marked the first evidence of macroautophagy outside of mammalian cells. A follow up EM study by Ohsumi confirmed that, similar to mammalian autophagy, double membrane autophagosomes form in the cytoplasm and fuse with the vacuole where the inner membrane and cargo, which together comprise the reported “autophagic bodies”, are then rapidly degraded in wild-type cells (Baba et al., 1995).

The ease with which these “autophagic bodies” could be visualized accumulating in the vacuole upon nitrogen starvation in vacuolar hydrolase-deficient cells made it conducive to genetic screens and would finally unveil the

genes involved in autophagy. Using this approach, the first genetic screen for autophagy mutants was performed by Ohsumi in 1993 and yielded the first autophagy-related gene, *apg1*, which was later renamed autophagy-related 1 (*atg1*) upon unification of autophagy-related gene nomenclature (Tsukada and Ohsumi, 1993; Klionsky et al., 2003).

In addition to the accumulation of autophagic bodies in the vacuole, the *atg1* mutant strain was found to be sensitive to long term nitrogen starvation. On this basis, a follow up primary screen was performed based on viability following long-term nitrogen deprivation, followed by a secondary screen for the build up of autophagic bodies within the vacuole (Tsukada and Ohsumi, 1993). This clever genetic approach yielded a total of 15 autophagy-related genes (*atg1-15*) that, remarkably, comprised nearly all of the genes responsible for the core autophagy machinery that mediates formation of the autophagosome (Table 1.1).

Saccharomyces cerevisiae was the first eukaryotic genome to be fully sequenced in 1996, which greatly facilitated the cloning and identification of the genes identified in the Yoshinori screen. Surprisingly, only one of the identified autophagy-related genes was previously known at the time, sparking great interest in identifying the molecular functions of the autophagy-related gene products as well as their mammalian homologs (Ohsumi, 2014). The core autophagy machinery can be divided into several functional groups that control distinct stages of autophagosome formation including: (1) initiation, (2) nucleation, (3) elongation and (4) closure. The proteins comprising these

Table 1.1 – Core autophagy-related (ATG) proteins

	Yeast	Mammalian	Function
Atg1/ULK1 complex	Atg1	ULK1/2	initiation of autophagosome formation; recruits/activates other ATG proteins
	Atg13	ATG13	regulatory subunit
	Atg17	FIP200 (RB1CC1) (functional homology)	scaffold protein important for complex localization
	Atg29		forms scaffold with Atg17/Atg31
	Atg31		forms scaffold with Atg17/Atg29
	Atg11		scaffold protein
		ATG101	required for complex stability
Beclin 1-Vps34 complex	Vps34	PIK3C3	PI-3 kinase; nucleation of phagophore
	Vps15	PIK3R4/VPS15/p150	regulatory subunit; Ser/Thr protein kinase
	Vps30/Atg6	Beclin 1	regulatory subunit of core complex
	Atg14	ATG14L (Barkor)	accessory subunit; directs complex to autophagosome formation sites
Atg9 vesicle system	Atg2	ATG2	interacts with Atg18
	Atg9	ATG9A/B	nucleation of the phagophore; traffics to phagophore via vesicles; interacts with Atg18/WIPI1/2; possibly involved in membrane fusion
	Atg18	WIPI1/2	PI3P binding protein; interacts with Atg9; recruits Atg12–Atg5-Atg16 complex
Atg12 UBL conjugation system	Atg12	ATG12	conjugates to Atg5; binds Atg3, catalyzes Atg8/LC3 conjugation
	Atg7	ATG7	E1-like enzyme
	Atg10	ATG10	E2-like enzyme
	Atg5	ATG5	conjugates to Atg12
	Atg16	ATG16L1	binds ATG5; involved in complex localization
Atg8 UBL conjugation system	Atg8	LC3A/B/C; GABARAP/L1/L2	conjugates to PE; required for phagophore elongation/closure; serves as cargo adapter
	Atg7	ATG7	E1-like enzyme
	Atg3	ATG3	E2-like enzyme
	Atg4	ATG4A/B/C/D	deconjugates Atg8/LC3 family proteins

different functional groups will be highlighted below, with a particular emphasis on the mammalian system.

1.2.2 Atg1/ULK1 complex – Atg1, and its mammalian homologs unc-51 like autophagy activating kinase 1 and 2 (ULK1 and ULK2), integrate several upstream signaling pathways and control the initiation of autophagosome formation. Over 40 residues are known to be phosphorylated on ULK1 alone, although the functions of only a few are well characterized (Russell et al., 2014). Unlike the yeast Atg1 complex, the mammalian ULK1 complex has been shown to remain intact independent of nutrient status and includes: ATG13, an Atg13 homolog that acts as a regulatory subunit; RB1-inducible coiled coil 1 (RB1CC1/FIP200), a functional homolog of Atg17 thought to be a scaffold protein involved in complex localization; and ATG101, which is not conserved in yeast, but is required for complex stability (Hosokawa et al., 2009b; Mercer et al., 2009; Wirth et al., 2013).

In nutrient replete conditions, the nutrient sensing complex, mammalian target of rapamycin complex 1 (mTORC1), associates with and phosphorylates ULK1 and ATG13, thereby suppressing ULK1 kinase activity and autophagy initiation (Ganley et al., 2009; Hosokawa et al., 2009a; Jung et al., 2009). Nutrient deprivation inactivates mTORC1, liberating the ULK1 complex and allowing it to localize to autophagosome formation sites thought to form on the ER in proximity to ER-mitochondria contact sites (Hamasaki et al., 2013; Wirth et

al., 2013). Active ULK1 then phosphorylates itself as well as other members of the ULK1 complex, although the specific functions of these later phosphorylation events remain unknown (Dunlop and Tee, 2013). Active ULK1 also phosphorylates and inactivates mTORC1, thus creating an amplification loop for autophagy initiation (Dunlop et al., 2011; Jung et al., 2011) (Fig. 1.4).

Another energy-sensing kinase, AMP-activated protein kinase (AMPK), which is activated by a drop in cellular energy levels dictated by the AMP:ATP ratio, serves as another level of control over autophagy initiation. In addition to directly inhibiting mTORC1 complex activity, AMPK also positively regulates ULK1 activity through the phosphorylation of multiple residues (Egan et al., 2011; Kim et al., 2011; Shang et al., 2011). Interestingly, active ULK1 phosphorylates and inactivates AMPK forming a negative feedback loop that may serve to prevent overactivation of ULK1 and autophagy (Loffler et al., 2011). Thus, ULK1, mTORC1 and AMPK form a "kinase triad" that intricately maintains cellular energy levels through tight regulation of cell growth and autophagy (Dunlop and Tee, 2013) (Fig. 1.4). Despite this, certain stimuli such as glucose starvation or ammonia treatment reportedly activate autophagy independent of ULK1 and ULK2 (Cheong et al., 2011; McAlpine et al., 2013).

Beyond its role in autophagy signaling, the exact function of the ULK1 complex in autophagosome formation is not fully understood. The yeast Atg1 complex phosphorylates Atg9, which is required for Atg18 localization to the phagophore (Papinski et al., 2014). Independent of its kinase activity, yeast Atg1

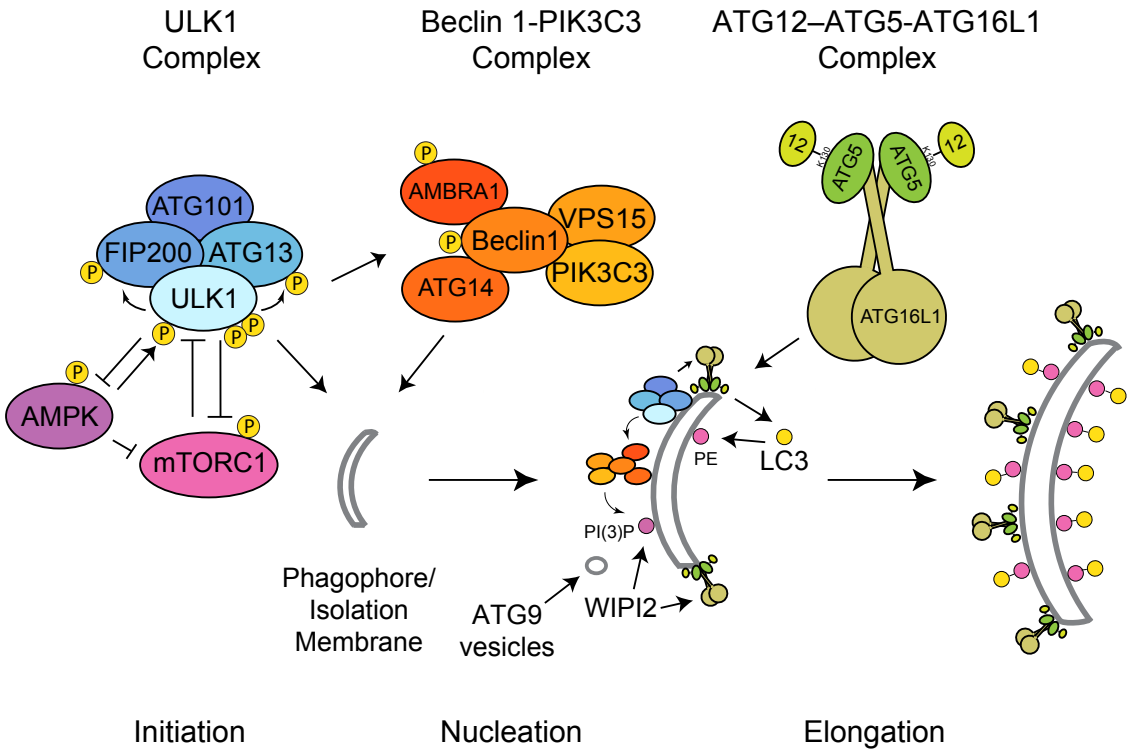

Figure 1.4 – Formation and elongation of the phagophore. Initiation of autophagosome formation is controlled by the ULK1 complex which integrates AMPK and mTORC1 nutrient-related signaling pathways. Both positive and negative feedback loops exist between ULK1, AMPK and mTORC1, ensuring tight regulation of cell growth and autophagy. Active ULK1 phosphorylates AMBRA1 and Beclin 1, which activates PI3KC3 lipid kinase activity and allows the Beclin 1-PI3KC3 complex to localize to the phagophore where it produces phosphatidylinositol 3-phosphate or PI(3)P. ULK1 also plays a role in the trafficking of ATG9-containing vesicles that contribute to phagophore nucleation. ATG9 binds the PI(3)P effector protein, WIPI2, which recruits the ATG12–ATG5-ATG16L1 complex. The ATG12–ATG5-ATG16L1 complex may also be recruited to the phagophore by FIP200 where it catalyzes the ubiquitin-like conjugation of LC3 to phosphatidylethanolamine (PE). PE-conjugated LC3 is essential for phagophore elongation and closure and is involved in the recruitment of cargo into the mature autophagosome.

is also proposed to act as a scaffold for the tethering and fusion of Atg9-containing vesicles. These vesicles are involved in the nucleation of the double-membrane, cup-shaped precursor of the autophagosome called the *phagophore* (Stanley et al., 2014). It remains unknown if the mammalian ULK1 complex tethers mammalian ATG9 vesicles in a similar way, although ATG9 trafficking is known to be ULK1-dependent (Young et al., 2006).

The mammalian ULK1 complex, including its kinase activity, has been implicated in the recruitment of other ATG proteins to autophagosome formation sites (Chan et al., 2009). Temporal analysis of ATG protein recruitment to autophagosome formation sites upon amino acid starvation indicates that ULK1 and ATG5 are recruited simultaneously, with ATG14 following shortly thereafter (Koyama-Honda et al., 2013). ATG5 is part of the ATG12–ATG5-ATG16L1 complex that catalyzes conjugation of LC3 to the autophagosomal membrane. Direct binding between FIP200 and autophagy-related 16-like 1 (ATG16L1) is thought to be responsible for the recruitment of the ATG12–ATG5-ATG16L1 complex to the phagophore (Nishimura et al., 2013). On the other hand, ATG14 associates with the class III phosphatidylinositol 3-kinase (PI3K) complex containing, in part, the catalytic subunit 3 (PIK3C3/VPS34), regulator subunit 4 (p150/VPS15) as well as the Atg6 homolog and regulatory factor, Beclin 1, whose phosphorylation by ULK1 is required for PIK3C3 lipid kinase activity (Russell et al., 2013) (Fig. 1.4).

1.2.3 Beclin 1-PIK3C3 complex – Beclin 1, p150 (VPS15), and PIK3C3 (VPS34) form the core complex whose function is altered by association with a diverse array of accessory subunit proteins (Wirth et al., 2013). Autophagy/Beclin 1 regulator 1 (AMBRA1) binds Beclin 1 and normally sequesters the complex to microtubules through interaction with the Dynein motor complex. Active ULK1 phosphorylates AMBRA1, which disrupts the interaction with dynein and allows translocation of the Beclin 1-PIK3C3 complex to autophagosome formation sites (Di Bartolomeo et al., 2010). Recently, ULK1 phosphorylation was also reported to stabilize AMBRA1 by disrupting its interaction with Cullin-4, an E3 ligase that normally mediates its ubiquitination and proteasomal degradation (Antonioli et al., 2014).

Interestingly, it has also been shown that active AMBRA1 promotes the Lys^{63}-linked polyubiquitination of both ULK1 and Beclin 1. Lys^{63}-linked polyubiquitination of ULK1 increases ULK1 stability and kinase activity, while Lys^{63}-linked polyubiquitination of Beclin 1 enhances its interaction with PIK3C3 and stimulates its lipid kinase activity (Nazio et al., 2013; Xia et al., 2013). Thus, it appears a positive feedback loop exists in which active ULK1 phosphorylates and liberates stable AMBRA1 which facilitates the recruitment of the Beclin 1-PIK3C3 complex to autophagosome formation sites and results in further activation of both ULK1 and PIK3C3 kinase activity through Lys^{63}-linked polyubiquitination.

The association of other subunit proteins with the core Beclin 1-PIK3C3 complex is also heavily regulated by ubiquitin and phosphorylation post-translational modifications. Lys^{63}-polyubiquitination of Beclin 1 by TNF receptor-associated factor 6, E3 ubiquitin protein ligase (TRAF6) is proposed to activate autophagy by disrupting its interaction with the antiapoptotic protein, B-cell CLL/lymphoma 2 (Bcl-2), which normally sequesters Beclin 1 away from PIK3C3 and suppresses its kinase activity (Shi and Kehrl, 2010; Russell et al., 2014). Dissociation of Bcl-2 from Beclin 1 is also enhanced upon phosphorylation of Beclin 1 by death-associated protein kinase 1 (DAPK) and JUN N-terminal kinase (JNK1) kinases (Funderburk et al., 2010). Another Bcl-2 family member, myeloid cell leukemia 1 (Mcl-1), was shown to promote Beclin 1 ubiquitination and degradation by sequestering the ubiquitin specific peptidase 9, X-linked (USP9X) DUB involved in Beclin 1 stabilization (Elgendy et al., 2014). Inhibition of another DUB, ubiquitin specific peptidase 13 (USP13), with the small-molecule inhibitor, Spautin-1, also leads to Beclin 1 ubiquitination and proteasomal degradation along with the rest of Beclin 1-PIK3C3 complex (Liu et al., 2011). Additionally, inhibition of heat shock protein 90 (HSP90) using Geldanamycin disrupts the HSP90-Beclin 1 interaction and results in Lys^{48}-linked polyubiquitination and proteasomal turnover of Beclin 1 (Xu et al., 2011). Together, these findings indicate that multiple types of ubiquitination combine to positively and negatively regulate Beclin 1 and the Beclin 1–PIK3C3 complex.

Another accessory protein, ATG14 (also named Barkor), binds to the ER-resident soluble NSF attachment protein receptor (SNARE), syntaxin-17, and recruits the Beclin 1-PIK3C3 complex to autophagosome formation sites thought to be located at ER-mitochondria contact sites (Hamasaki et al., 2013). With the complex localized to the ER, PIK3C3 then phosphorylates the 3´-position of the inositol ring of phosphatidylinositol, forming phosphatidylinositol 3-phosphate (PtdIns3P or PI(3)P) that is essential for formation of the phagophore (Shibutani and Yoshimori, 2014).

The exact function of PI(3)P in phagophore formation is unclear, however it is required for the formation of the ER-associated, Ω-like structure named the *omegasome*, which serves as a membrane cradle for the expanding phagophore. The PI(3)P effector protein, double FYVE domain-containing protein 1 (DFPC1), is recruited by PI(3)P and is used as a molecular marker for the omegasome, although its specific role in autophagosome formation is unknown (Axe et al., 2008). WD repeat domain, phosphoinositide-interacting protein 2 (WIPI2) is another PI(3)P effector protein that binds PI(3)P and was recently reported to recruit the ATG12–ATG5-ATG16L1 complex to autophagosome formation sites through interaction with ATG16L1 (Dooley et al., 2014) (Fig. 1.4). ATG16L1 interacts with WIPI2 and FIP200 through adjacent regions, however it is unclear how these two interactions affect one another and if the ATG12–ATG5-ATG16L1 complex is recruited to autophagosome formation sites through two distinct mechanisms.

1.2.4 Ubiquitin-like (UBL) conjugation systems – Of the fifteen genes originally identified in the Yoshinori yeast genetic screen, eight turned out to be directly involved in two UBL conjugation reactions that are essential for the formation of the autophagosome (Fig. 1.5). Atg12 and Atg8 are both UBL proteins that have ubiquitin-like structures and undergo multistep conjugation reactions (Mizushima et al., 1998a; Ichimura et al., 2000). Similar to ubiquitin, the C-terminal glycine residue of ATG12 is activated by adenylation allowing it to form a thioester bond with the active-site cysteine residue of the E1-like enzyme, ATG7 (Klionsky and Schulman, 2014). ATG12 is then transferred to the E2-like enzyme, ATG10, which interacts directly with ATG5 and mediates ATG12–ATG5 conjugation independent of a known E3-like enzyme (Kaiser et al., 2012; Yamaguchi et al., 2012). ATG12–ATG5 reversibly binds ATG16L1, which is proposed to target the ATG12–ATG5-ATG16L1 complex to the phagophore through interaction with FIP200 and/or WIPI2 (Nishimura et al., 2013; Dooley et al., 2014). The same region of ATG12–ATG5 also interacts with tectonin beta-propeller repeat containing 1 (TECPR1), which reportedly functions in cargo selection as well as during autophagosome-lysosome fusion (Ogawa et al., 2011; Chen et al., 2012; Kim et al., 2015).

The ATG12–ATG5-ATG16L1 complex primarily functions as an E3-like enzyme to catalyze the ubiquitin-like conjugation of LC3 to phosphatidylethanolamine (PE) at the phagophore. In addition, the ATG12–

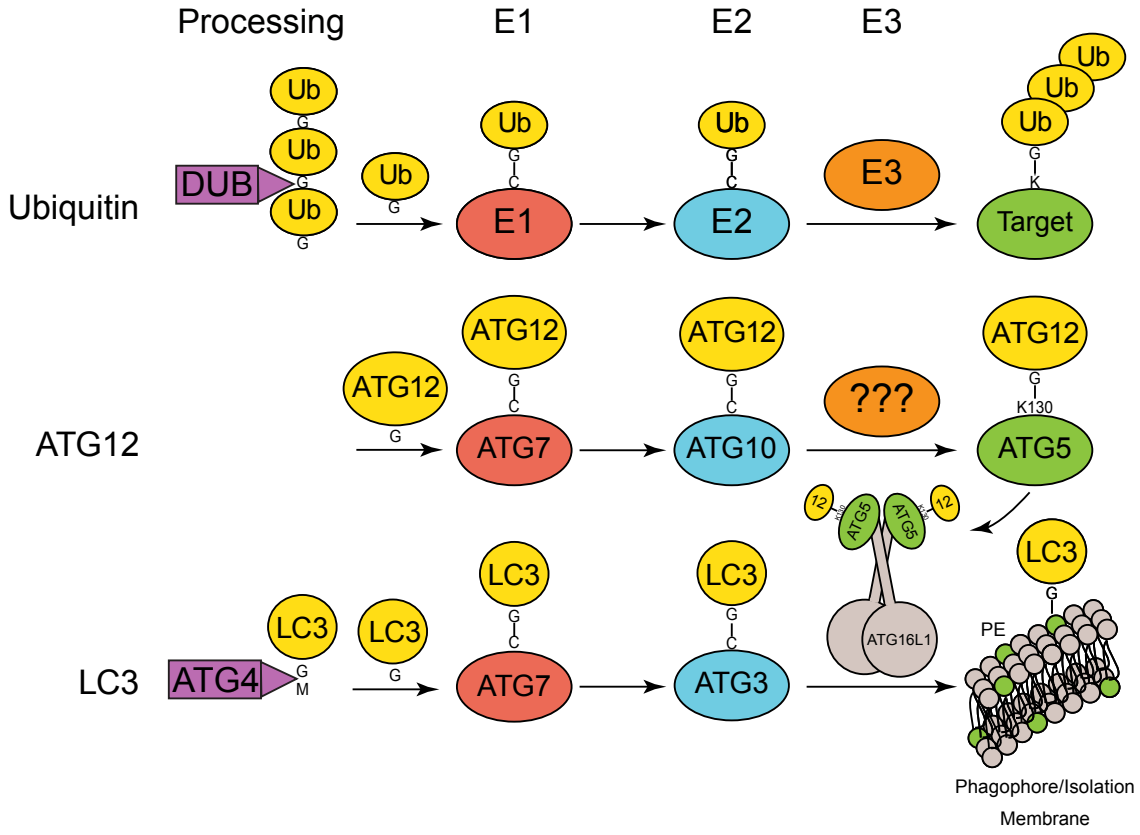

Figure 1.5 – ATG12 and LC3 ubiquitin-like conjugation reactions. Two ubiquitin-like conjugation reactions are required for phagophore extension and autophagosome formation. ATG12 and LC3 are ubiquitin-like (UBL) proteins that share structural similarity to ubiquitin and undergo similar multi-step conjugation reactions. Ubiquitin is processed by deubiquitinase (DUB) enzymes that release monomeric ubiquitin and expose a C-terminal glycine residue that is targeted by the active-site cysteine of an E1 ubiquitin-activating enzyme. While ATG12 does not undergo processing, LC3 must be cleaved by ATG4 in order to expose its C-terminal glycine residue. Both ATG12 and LC3 ubiquitin-like conjugation reactions share the same E1-like enzyme, ATG7. The E2-like enzymes for ATG12 and LC3 conjugation are ATG10 and ATG3, respectively. There is no known E3-like enzyme for catalyzing ATG12 conjugation to ATG5, although the ATG12–ATG5-ATG16L1 complex acts as an E3-like enzyme and catalyzes LC3 conjugation to phosphatidylethanolamine (PE) on the phagophore/isolation membrane. ATG12 conjugation is believed to be irreversible; however, deconjugation of LC3 from the outer membrane of the phagophore by ATG4 is required for final maturation of the autophagosome.

ATG5-ATG16L1 complex has been reported to both tether giant unilamellar vesicles and act as a flexible membrane scaffold for autophagosome formation *in vitro* (Romanov et al., 2012; Kaufmann et al., 2014). However, no direct evidence of either of these functions has been found *in vivo*.

Atg8/LC3 is unique amongst UBLs in that it is conjugated to the primary amine from the head group of the phospholipid, PE, rather than the typical ε-amino group of a lysine residue. Mammalian homologs of Atg8 can be classified into two families, each consisting of three related proteins that are similarly conjugated to PE. MAP1LC3A (LC3), LC3B, and LC3C are proposed to be essential for phagophore elongation, while GABA(A) receptor-associated protein (GABARAP), GABA(A) receptor-associated protein like 1 (GABARAPL1), and GABA(A) receptor-associated protein like 2 (GABARAPL2/GATE-16) may function at later stages (Weidberg et al., 2010). While little is known about either group's specific role in autophagosome formation, disruption of any of the upstream genes involved in Atg8/LC3 lipid-conjugation blocks formation of functional autophagosomes.

Unlike Atg12, Atg8 must be cleaved by the cysteine protease Atg4 in order to expose the C-terminal glycine residue targeted for the ubiquitin-like conjugation reaction. There are 4 mammalian Atg4 homologs (ATG4A, ATG4B, ATG4C and ATG4D), which may possess selectivity for certain LC3 family members (Li et al., 2011). ATG7 is the E1 activating enzyme for both ATG12 and LC3, whereas ATG3 serves as the E2-like enzyme for LC3 conjugation

rather than ATG10 (Hong et al., 2011; Taherbhoy et al., 2011). It is thought that the ATG3–LC3 intermediate is recruited to the phagophore by ATG12 where binding to the ATG12–ATG5 conjugate triggers a conformational change within the ATG3 catalytic site that promotes the conjugation of LC3 to PE (Noda et al., 2013; Sakoh-Nakatogawa et al., 2013).

Atg8/LC3 is initially conjugated to both the inner and outer membranes of the expanding phagophore and is the only Atg protein that remains attached to the either membrane upon completion of autophagosome biogenesis (Klionsky and Schulman, 2014). Interestingly, whereas the Atg12–Atg5 isopeptide bond is thought to be irreversible, Atg4-mediated deconjugation of Atg8 from the outer membrane of the immature autophagosome is required for full maturation and closure of the autophagosome for reasons that are unclear (Nair et al., 2012; Yu et al., 2012). Atg8/LC3 still remains associated with the inner membrane of the phagophore, which allows it to serve as a platform for cargo recruitment into the autophagosome via adapter proteins, such as the previously mentioned p62 and NBR1. These adapters bind Atg8/LC3 through short hydrophobic domains called Atg8-interacting motifs (AIMs) in yeast or LC3-interacting regions (LIRs) in mammals (Noda et al., 2010). Proteomic analysis indicates at least 67 different proteins, many of which contain LIRs, interact with the six mammalian Atg8 homologs (Behrends et al., 2010). This includes several members of the ULK1 and Beclin 1-PIK3C3 complexes, which suggests an additional role for Atg8

proteins in the recruitment of other Atg proteins involved in autophagosome formation (Kraft et al., 2012).

Since the Yoshinori screen, interest in the field of autophagy has exploded and significant progress has been made in our mechanistic understanding of how autophagy occurs and is regulated. Still, many important questions remain, the largest of which relate to the role(s) of autophagy in normal physiological functions and its contribution to the development and progression of human disease.

1.3 Autophagy in Physiology and Human Disease

1.3.1 Neurodegeneration – The homeostatic function of autophagy is particularly important in the brain where the unique architecture and lack of cell division by postmitotic neurons exacerbates the burden of accumulating deleterious proteins and organelles (Wong and Cuervo, 2010). Mice with neural-specific genetic defects in autophagy display progressive neurodegeneration with features common to human neurodegenerative diseases including the accumulation of intracellular protein aggregates and inclusions (Hara et al., 2006; Komatsu et al., 2006). Conversely, stimulation of autophagy was found to reduce levels of neuronal cell death in mouse models of neurodegeneration (Ravikumar et al., 2004; Schaeffer et al., 2012).

Deregulation of autophagy is associated with several human neurodegenerative diseases including Alzheimer's, Huntington's and Parkinson's diseases as well as amyotrophic lateral sclerosis (ALS) (Choi et al., 2013). Evidence suggests the accumulation of neurofibrillary tangles (NFTs), comprised of hyperphosphorylated and ubiquitinated tau, correlates with the extent of cognitive loss in Alzheimer's patients (Giannakopoulos et al., 2003). Tau NFTs appear in several other neurodegenerative diseases, together classified as tauopathies, where their accumulation most likely contributes to neurotoxicity. Tau can be degraded by the ubiquitin-proteasome system as well as through macroautophagy or chaperone-mediated autophagy. As discussed previously, these pathways are highly interrelated and it is not clear which pathway contributes more to tau degradation, although it is likely that lager aggregates of tau can only be degraded by macroautophagy (Lee et al., 2013).

Mutations in *PINK1* and *PARK2,* which encode the previously discussed mitophagy regulating factors PINK1 and Parkin, are highly associated with an autosomal recessive, early-onset form of Parkinson's disease. Therefore, it has been suspected that defects in mitophagy may lead to a buildup of damaged mitochondria that contribute to Parkinson's disease. However *PINK1/PARK2* deficient mouse models do not develop significant neurodegeneration, indicating that there are likely additional factors involved (Pickrell and Youle, 2015). Lewy bodies are a hallmark of Parkinson's disease and are comprised primarily of α-synuclein aggregates that are a reported target of autophagy. However, α-

synuclein aggregation may also suppress macroautophagy (Winslow et al., 2010). Similarly, aggregated mutant huntingtin (mhtt) is a characteristic of Huntington's disease and is a reported target of autophagy, yet mhtt aggregates also appear to interfere with the autophagic degradation of protein aggregates, damaged mitochondria and lipid droplets (aggrephagy, mitophagy and lipophagy) through an unknown mechanism (Ravikumar et al., 2002; Martinez-Vicente et al., 2010). The negative effects of α-synuclein and mhtt protein aggregates on autophagy may increase the buildup of other aggregates and damaged organelles, further exacerbating neurotoxicity in Parkinson's and Huntington's patients.

1.3.2 Immunity – Autophagy also plays a key role in both innate and adaptive immunity. It is activated upon infection by a wide range of cytokine and immuno-related signaling pathways and has been shown to help protect against several pathogens *in vivo* (Choi et al., 2013). The suppression of autophagy increases the susceptibility of organisms to infection in many different model systems (Levine et al., 2011). Pathogens that escape into the cytoplasm are ubiquitinated and recruited into LC3-coated autophagosomes by adapter proteins, such as p62 or NBR1, which bind both ubiquitin and LC3. This version of selective autophagy is called xenophagy and serves to sequester intracellular bacteria, viruses and parasites and target them to lysosomes for destruction (Gomes and Dikic, 2014). The mechanism(s) for the autophagic elimination of pathogens that do not escape into the cytoplasm and instead remain within phagosomes or endosomes

is less understood. A few possibilities have been proposed, such as the sequestration of pathogen-containing phagosomes/endosomes by large autophagosomes or their direct fusion with autophagosomes/lysosomes (Levine et al., 2011).

Autophagy also has important functions in adaptive immunity where it participates in thymic T cell selection and the maintenance of lymphocytes, and is reportedly essential for major histocompatibility complex (MHC) class II antigen presentation (Lee et al., 2010; Mizushima and Levine, 2010). Interestingly, autophagy also suppresses interferon and interleukin cytokine production, which limits excessive activation of the immune and inflammatory responses. Mutations in autophagy-related genes are associated with common inflammatory diseases including Crohn's disease and lupus. Although the mechanisms are not known, a disease variant of *ATG16L1 (T300A)* associated with Crohn's disease and the several *ATG5* single-nucleotide polymorphisms (SNPs) associated with systemic lupus erythematosus (SLE) likely disrupt the balance between the pro- and anti-immune functions of autophagy (Levine et al., 2011).

1.3.3 Cell death – One of the most contentious aspects of autophagy is its role in cell death. Historically, cell death mechanisms have been classified into two morphologically-defined types: apoptosis and necrosis (Liu and Levine, 2015). More recently, some have argued that excessive autophagy can lead to cell death. Autophagic cell death was originally characterized as cell death

accompanied by extensive autophagic vacuolation. However, as the molecular understanding of autophagy has increased, the definition has been revised to include the requirement that autophagic cell death must be suppressed by genetic or chemical inhibition of autophagy (Galluzzi et al., 2012). This more stringent definition has introduced many questions as to whether autophagy is the actual executioner of cell death, or whether it is simply activated concomitantly as a survival response during cell death. Despite this, there are some examples of what has currently been defined as autophagic cell death, particularly during *Drosophila melanogaster* development or in cells deficient in apoptosis (Liu and Levine, 2015). Recently, a new distinct form of autophagic cell death was reported to be triggered by autophagy-inducing peptides, starvation and hypoxia-ischemia *in vitro* and *in vivo* (Liu et al., 2013b). This form of autophagic cell death, termed *autosis*, is dependent on Na^+,K^+-ATPase activity and shows unique morphological characteristics not observed in classical autophagic cell death or in apoptosis/necrosis (Liu and Levine, 2015).

Beyond its controversial role in autophagic cell death, autophagy has well-established molecular and functional mechanisms of crosstalk with apoptosis. In response to cell death stimuli, autophagy is often activated as a cytoprotective response and the inhibition of this stress-induced autophagy can promote further apoptosis (Boya et al., 2005; Galluzzi et al., 2012). Caspases also cleave a number of ATG proteins including Beclin 1, ATG4D, and ATG16L1, which likely suppresses the compensatory activation of autophagy during apoptosis (Betin

and Lane, 2009; Luo and Rubinsztein, 2010; Murthy et al., 2014). Cleavage of ATG5 by calpains, another family of cell death-associated proteases, reportedly generates a truncated fragment that triggers mitochondrial outer-membrane permeabilization (MOMP) and cell death (Yousefi et al., 2006). Numerous ATG proteins are cleaved by calpains *in vitro*, although the *in vivo* relevance of this is unknown (Norman et al., 2010). Other autophagy-related proteins apparently have direct roles in apoptosis, including BNIP3/BNIP3L and unconjugated ATG12 (Zhang and Ney, 2009; Radoshevich et al., 2010; Haller et al., 2014). Thus, depending on the context, autophagy seems function in both cell survival and cell death, which complicates its role in many human diseases such as cancer.

1.3.4 Tumorigenesis and tumor progression – Oncogene overexpression and activation are common hallmarks of cancer and have been shown to both positively and negatively regulate autophagy through highly complex and contextual mechanisms that are not well understood (Galluzzi et al., 2015). The homeostatic function of selective autophagy, which occurs at basal levels in all cell types, is critical for the suppression of malignant transformation and tumorigenesis. The first evidence of this was the finding that mice possessing a heterozygous deletion of *Becn1*, the gene encoding for Beclin 1, spontaneously developed a variety of malignancies in the blood, liver and lungs (Qu et al., 2003; Yue et al., 2003). Mosaic deletion of *Atg5* or liver specific deletion of *Atg7* also

resulted in the development of liver tumors in mice; however, these tumors remained benign and did not progress into carcinomas (Takamura et al., 2011). This was the first indication that stress-induced autophagy, which can be activated by stressors within the tumor microenvironment or during invasion and metastasis, may be required for tumor cell survival or progression. In both V-raf murine sarcoma viral oncogene homolog B (*BRAF*^{V600E}) and Kristen rat sarcoma viral oncogene homolog (*KRAS*^{G12D})-driven murine lung cancer models, knockout of *Atg7* or *Atg5* accelerated tumor initiation. However in both models, the acceleration in tumor formation was coupled with a reduction in tumor progression into malignancy, resulting in increased mouse survival (Strohecker et al., 2013; Rao et al., 2014). Similar results were found with *KRAS*^{G12D}-driven murine pancreatic cancer models (Rosenfeldt et al., 2013; Yang et al., 2014). Based on these mouse model findings, the current hypothesis is that autophagy plays a dual-role in tumorigenesis, where selective autophagy suppresses early stages of tumor initiation, while stress-induced autophagy promotes tumor survival and progression at later stages. However, deletion of *Atg5* or *Atg7* had completely opposite effects on pancreatic tumor progression depending on the status of *Trp53* (Rosenfeldt et al., 2013), which indicates that there are important contextual aspects that affect the function of autophagy in cancer.

There are several potential mechanisms for the tumor suppressive function(s) of autophagy. In addition to its controversial role in autophagic cell death, autophagy has been increasingly implicated in the initiation of oncogene-

induced senescence and cell death (Young et al., 2009; Liu et al., 2013a). Another potential tumor suppressive mechanism is the mitophagic removal of dysfunctional mitochondria that can produce ROS, since ROS damage DNA, increase genomic instability and promote malignant transformation (Lorin et al., 2013; Sabharwal and Schumacker, 2014). Autophagy also directly targets proteins that can promote oncogenesis including p62, mutant tumor protein p53 (p53), and the oncogenic fusion proteins: breakpoint cluster region–c-Abl oncogene 1-ABL proto-oncogene 1 (BCR–ABL1), and promyelocytic leuikemia–retinoic acid receptor, alpha (PML–RARA), which result from chromosomal translocations (Galluzzi et al., 2015). Finally, autophagy may function to suppress tumorigenesis through xenophagic elimination of potentially oncogenic bacteria and viruses and by the suppression of excessive or chronic inflammation, which are known to promote tumorigenesis (Hanahan and Weinberg, 2011) (Fig. 1.6).

In contrast, the stress-induced cell survival function of autophagy is thought to promote tumor progression once malignant transformation occurs. Conditions commonly found within the tumor microenvironment, such as hypoxia, low pH, and high levels of oxidative and metabolic stress are all known inducers of autophagy. In the absence of an autophagic response, these conditions can promote tumor cell death and limit tumor progression (Galluzzi et al., 2015). Autophagy also suppresses anoikis, which is cell death resulting from a loss of cell adhesion, which occurs during the epithelial-mesenchymal transition (EMT)

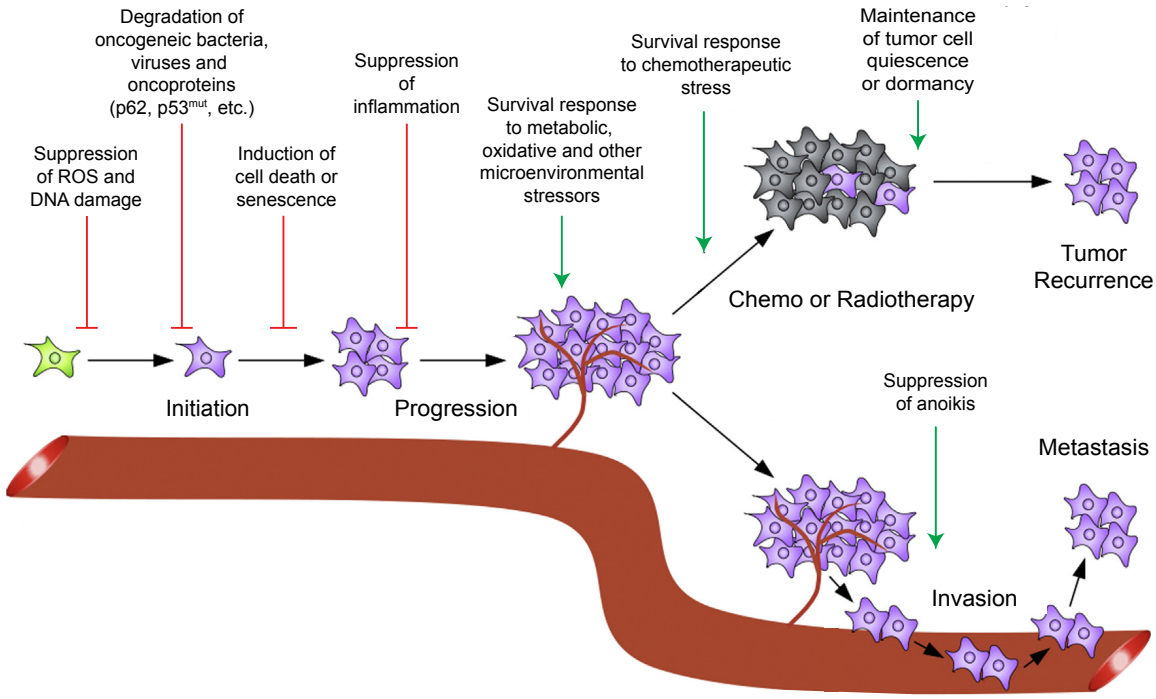

Figure 1.6 – Role of autophagy in tumor initiation, progression and therapy. Preclinical data suggest autophagy plays a highly contextual role in cancer depending on the tumor type, stage and genetic background. Autophagy is generally thought to suppress early tumorigenesis by eliminating sources of reactive oxygen species (ROS), such as damaged mitochondria, that can promote DNA damage and lead to malignant transformation. Autophagy can also directly eliminate oncogenic factors including p62, mutant p53, viruses, etc. Although not well understood, autophagy has been implicated in both cell death and oncogene-induced senescence, which may prevent the expansion of transformed cells. Autophagy also plays an important role in the suppression of chronic inflammation that can promote tumor growth and progression. Once a tumor is formed, however, it is thought that stress-induced autophagy becomes tumor promotive. The harsh conditions often found in the tumor microenvironment including low pH, low nutrient and oxygen levels, and high levels of ROS are all known to activate autophagy. Autophagy may also help cells survive detachment from the extracellular matrix (ECM) during invasion and metastasis. Chemotherapeutic agents elicit autophagy-dependent survival responses and autophagy may also help maintain dormant, quiescent tumor subpopulations in response to cancer therapies that can potentialy lead to tumor recurrence. These tumor promotive aspects make autophagy a highly attractive therapeutic target. Adapted from: Lorin et al. (2013). Semin Cancer Biol **23**(5): 361-379.

and is thought to precede tumor cell invasion and metastasis (Avivar-Valderas et al., 2013; Cai et al., 2014) (Fig. 1.6). Thus, since tumor invasion and metastasis are ultimately responsible for cancer mortality, the prosurvival function of autophagy has become a major point of interest for potential therapeutic intervention.

1.3.5 Cancer therapy – In addition to autophagy activation during invasion and metastasis, tumor cells treated with radiation and chemotherapeutic agents also activate autophagy as a cytoprotective response (Gewirtz, 2014). In contrast to its potential role in oncogene-induced senescence, autophagy may also play a role in maintaining tumor cell quiescence and dormancy (Lu et al., 2008). Interestingly, autophagy was recently found to sustain a dormant, cancer stem cell–like population upon oncogenic KRAS ablation in a murine pancreatic cancer model (Viale et al., 2014). This suggests that autophagy may be essential for the survival of chemoresistant tumor cells that are responsible for cancer recurrence (Fig. 1.6). These observations have become the basis for numerous ongoing clinical trials in which autophagy inhibitors (primarily hydroxychloroquine) have been used in an attempt to sensitize tumor cells to chemotherapies and reduce the incidence of tumor recurrence (Jiang and Mizushima, 2014).

Despite the promise of these current clinical trials, expectations are somewhat tempered due to a number of outstanding problems for which we currently lack understanding. At a basic level, it is not entirely clear which types

of tumors are susceptible to sensitization by autophagy inhibitors. One recent examination of breast cancer cells with different subtypes found that the transcription factor, signal transducer and activator of transcription 3 (STAT3), imparted sensitivity to autophagy inhibition (Maycotte et al., 2014). Identifying the specific tumor types most likely to be sensitized by autophagy inhibitors is a crucial task for the future. Hydroxychloroquine, a derivative of chloroquine, is a lysosomotropic agent that neutralizes the pH of the lysosome and inactivates the acid hydrolases responsible for lysosomal degradation, therefore blocking both autophagic and lysosomal degradation. A recent study suggests that the tumor suppressive effects of chloroquine are autophagy-independent, casting some doubt onto the efficacy of autophagy inhibition, per se, in combination with chemotherapy (Maes et al., 2014). Still, extensive preclinical data suggest that autophagy plays an important, though context-dependent role, in tumor formation, progression, and therapeutic responses. Our increased understanding of the mechanisms involved in autophagy will help in the design of more targeted and effective approaches to treating cancer.

Chapter 2: Materials and Methods

2.1 Expression constructs – The lentiviral FG9-Puro vector, as well as pRSV-REV, pRRE and pHCMV-G 3rd generation lentivirus packaging vectors were kindly provided by Dr. Casey Wright (University of Texas at Austin, Austin, TX). FG9-Puro-FLAG was designed by knocking out the XbaI site downstream of the multiple cloning site (MCS) by site-directed mutagenesis followed by oligo cloning a FLAG tag into the XbaI/BamHI sites just upstream of the MCS. Human *ATG5* cDNA was obtained by reverse transcriptase-PCR (RT-PCR) of mRNA isolated from PC-3 PCa cells. Murine *Atg5* cDNA was purchased from Addgene (#13095; Cambridge, MA). Both *hATG5* and *mAtg5* were then cloned into the BamHI/NotI sites of FG9-Puro-FLAG. Site directed mutagenesis was used to introduce the K130R mutation into both human and mouse versions.

The psPAX2 2nd generation lentivirus packaging vector was purchased from Addgene (#12260). ATG5 short hairpin RNA (shRNA) #1 (V3LHS_301134; sense 5´-CCA ACT TGT TTC ACG CTA T-3´); ATG5 shRNA #2 (V2LHS_67978; sense 5´-CCC ATC TTT CCT TAA CGA A-3´); and a non-silencing control (#RHS4346; sense 5´-CTC GCT TGG GCG AGA GTA A-3´) in the pGIPZ shRNA lentiviral vector were obtained from the shRNA and ORFeome Core Facility at the University of Texas MD Anderson Cancer Center.

ATG5 cDNA cloned into the pLOC lentiviral vector was also obtained from the shRNA and ORFeome Core Facility. ATG5 pLOC-STOP was created by

reintroduction of the endogenous stop codon in order to eliminate extra downstream nucleotides resulting from the “open” ORF configuration. K130R, all structure-directed, and most of the cancer-associated mutations were introduced by site-directed mutagenesis. For those mutations predicted to result in N-terminal deletions, only the portion of *ATG5* predicted to be translated was amplified by PCR and cloned into BamHI/NheI sites of pLOC. pLOC-HA was designed by amplifying *ATG5* by PCR with the HA-tag sequence contained within the reverse primer (forward: 5´-GGA GGA TCC ATG ACA GAT GAC AAA GAT GTG CTT-3´; reverse: 5´-ATA GCG CGC CTC AAG CAT AAT CTG GAA CAT CAT ATG GAT AGC TAG CAT CTG TTG GCT GTG-3´) and cloning it into the BamHI/AscI sites of pLOC. The predicted coding sequence of each *ATG5* splice variant was amplified by PCR and cloned into the BamHI/NheI sites of pLOC-HA.

Incomplete cDNAs for ATG16L1 (ORF50-54133 and HsCD00400231) were purchased from the CCSB Human ORFeome Collection (Boston, MA). The C-terminal portion of ATG16L1 from was amplified from ORF50-54133 template by PCR (forward: 5´-CCG GAA TTC CAG AGA CAG GCG TTC GAG GAG-3´; reverse: 5´-AAT GCG GCC GCG TAC TGT GCC CAC AGC ACA GC-3´) and cloned into the EcoRI/NotI sites of pGEX-4T-1 vector. Next, full-length ATG16L1 was assembled by PCR amplifying the N-terminus from HsCD00400231 (forward: 5´-CCG GAA TTC CAG AGA CAG GCG TTC GAG GAG-3´; reverse: 5´-AGA AGA TCT GAC TTT TCC AGC AAT TTG TTA TAC-3´) and cloning it into the EcoRI/BglII sites of the previously mentioned ATG16L1 C-terminal construct.

Once assembled in pGEX-4T-1, the internal BamHI site was removed by site directed mutagenesis and full-length ATG16L1, and ATG16L1 with an N-terminal deletion (Δ-39), were amplified by PCR and cloned into the BamHI/NheI sites of pLOC-HA.

2.2 Reagents and antibodies – TransIT®-2020 Transfection Reagent (#MIR5400) was purchased from Thermo Fisher Scientific (Waltham, MA). MG132 (#S2619) was purchased from Selleck Chemicals (Houston, TX). Bafilomycin A1 (Baf A1, #1334) was purchased from Tocris Bioscience (Bristol, UK). L-valine [^{14}C(U)] (#MC-277) was purchased from Moravek Biochemicals, (Brea, CA). Cold L-Valine (#V0500) and 3-methyladenine (3-MA; #M2981) were purchased from Sigma-Aldrich (St. Louis, MO).

Antibodies for β-actin (#4967), AMBRA1 (#12250), ATG3 (#3415), ATG5 (#2630, C-terminal, human-specific), ATG7 (#2631), ATG12 (D88H11, #4180), ATG13 (#6940), ATG16L1 (D6D5, #8089), ATG101 (#8764), Beclin 1 (#3738), LC3B (#2775), p62/SQSTM1 (#5114), TECPR1 (D6C10, #8097), and ULK1 (D8H5, #9084) were purchased from Cell Signaling Technology (Danvers, MA). N-terminal mouse-reactive ATG5 antibody (#NB110-53818) was purchased from Novus Biologicals (Littleton, CO). FIP200/RB1CC1 antibody was purchased from Proteintech Group (Chicago, IL). PIK3C3/Vps34 antibody (#38-2100) was purchased from Life Technologies (Grand Island, NY). β-Tubulin antibody (E7) was purchased from the Developmental Studies Hybridoma Bank (DSHB) (Iowa

City, IA). HA antibody (HA.11 Clone 16B12; #MMS-101P) was purchased from Covance (Princeton, NJ). FLAG antibody (M2; #F1804) was purchased from Sigma-Aldrich (St. Louis, MO).

2.3 Cell lines and culture conditions – DU145 PCa cells (HTB-81) were purchased from American Type Culture Collection (ATCC) (Manassas, VA). PC-3 and LNCaP PCa cells were kindly provided by Dr. Dean Tang (The University of Texas MD Anderson Cancer Center-Science Park, Smithville, TX). PCa cells were grown in RPMI-1640, supplemented with 10% fetal bovine serum (FBS), and 2mM L-glutamine. A549 lung cancer cells were kindly provided by Dr. Gerald Cohen (University of Liverpool, Liverpool, UK). A549 cells were grown in DMEM supplemented with 10% FBS and 4mM L-glutamine. *ATG16L1*$^{+/+}$ WT and *ATG16*$^{-/-}$ HCT116 colorectal cancer cells were kindly provided by Dr. David Boone (Indiana University School of Medicine-South Bend, South Bend, IN) (Messer et al., 2013). HCT116 cells were grown in McCoy's 5A media supplemented with 10% FBS and 2 mM L-glutamine. All cancer cells were maintained at 37°C in humidified air containing 5% CO_2 and routinely passaged every 3 days.

Atg5$^{+/+}$ WT and Atg5$^{-/-}$ mouse embryonic fibroblasts (MEFs) were kindly provided by Dr. Noboru Mizushima (University of Tokyo, Tokyo, JP) (Kuma et al., 2004). *Atg12*$^{+/+}$ and *Atg12*$^{-/-}$ MEFs were kindly provided by Dr. Jayanta Debnath (University of California-San Francisco, San Francisco, CA) (Malhotra et al.,

2015). *Atg16L1*$^{+/+}$ and *Atg16L1*$^{\Delta/\Delta}$ MEFs were kindly provided by Dr. Shizuo Akira (Osaka University, Osaka, JP)(Saitoh et al., 2008). These MEFs were grown in DMEM supplemented with 10% FBS and 4mM L-glutamine at 37°C in humidified air containing 5% CO_2 and were routinely passaged every 3 days. *Atg3*$^{+/+}$, *Atg3*$^{-/-}$, *Atg7*$^{+/+}$, and *Atg7*$^{-/-}$ MEFs were kindly provided by Dr. Masaaki Komatsu (Tokyo Metropolitan Institute of Medical Science, Tokyo, JP)(Komatsu et al., 2005; Sou et al., 2008). These MEFs were grown the same conditions as the others except they were maintained at 32.5°C.

2.4 Lentiviral transduction and stable cell line generation – Human embryonic kidney cells (HEK293T) were kindly provided by Dr. Casey Wright (University of Texas at Austin, Austin, TX). Cells were grown in DMEM media supplemented by 10% FBS and 4 mM L-glutamine 37°C in humidified air containing 5% CO_2 and were routinely passaged every 3 days. To start, $2.5x10^6$ low-passage number HEK293T cells were plated in a 10 cm plate. The next day, cells were transfected with a lentiviral vector along with packaging plasmids (15 µg total DNA with 45 µl TransIT-2020 transfection reagent) in a total of 7 mL of media. For 2nd generation lentiviral packaging, psPAX2 and pHCMV-G packaging vectors were used. For 3rd generation lentiviral packaging: pRSV-REV, pRRE and pHCMV-G packaging vectors were used. ~48 hours later the media was collected in a 10 mL syringe and 7 µL of sterile polybrene (5 µg/µL) was added and mixed. Collected media was filtered through a 0.45 µm PVDF

syringe filter into two wells of a 6-well plate. $3x10^5$ target cells in 1mL of culture media were then immediately added to each well and incubated until confluent. For pLOC or pGIPZ vectors, successful transduction was verified by GFP expression. For FG9 vectors, transduced cells were cultured in media containing 2 µg/µL puromycin dihydrochloride (#540411; EMD Millipore, Billerica, MA) for 7 days.

2.5 Western blot analysis – After various treatments, $1.5x10^6$ cells in a 6 cm plate were collected and lysed in 100 µL RIPA Buffer (50 mM Tris-HCl pH 7.4, 150 mM NaCl, 1% NP-40, 1% Na-deoxycholate, 0.1% SDS and proteasome inhibitors). Lysates were stored at -20°C until ready for use. For SDS-PAGE, lysates were sonicated, centrifuged and the soluble fraction was collected, quantified by Bradford assay and normalized to equal concentrations. 6X Laemmli buffer (375 mM Tris pH 6.8, 12% SDS, 50% glycerol, 10% β-mercaptoethanol, 0.06% bromophenol blue) added to the lysates and boiled for 5 min. 50 ug of total lysate was added to each lane of 10% or 15% polyacrylamide gels. SDS-PAGE was run at 125 V for 90 min prior to transfer onto nitrocellulose or PVDF membrane for 2 h at 90 V. Membranes were blocked in 5% non-fat milk in TBS-T (Tris-buffered saline + 0.1% Tween-20) for 1 h at room temperature. Membranes were washed twice in TBS-T for 5 min and incubated in primary antibody overnight with constant agitation. The next day membranes were washed twice with TBS-T and incubated in secondary antibody diluted 1:2000 in

5% milk in TBST-T for 1 h at room temperature. Blots were then washed twice with TBS-T and visualized on x-ray film using enhanced chemiluminescence (Perkin Elmer-Lighting Plus or Pierce ECL2).

2.6 Transmission electron microscopy – Cells were fixed in Karnovsky's fixative (0.2 M sodium cacodylate (Na-Caco), 2.5% glutaraldehyde, and 2% paraformaldehyde) for 1 h, post-fixed with osmium-ferrocyanide (2% OsO_4, 2% ferrocyanide in 0.2 M Na-Caco buffer) for 1-2 h, and then stained with 2% aqueous uranyl acetate for 1 h. Cells were then dehydrated stepwise and embedded in epoxy resin. Sectioning, imaging and data interpretation was performed by Dr. Dwight Romanovicz (University of Texas at Austin, Austin, TX) or Dr. David Dinsdale (University of Leicester, Leicester, UK).

2.7 Long-lived protein turnover assay – $0.5x10^6$-$1.0x10^6$ cells were plated in duplicate in 6-well plates for each time point, including time 0 h and cold controls. The next day the media was replaced with fresh media containing 0.2 μCi/mL L-valine [^{14}C(U)] (MC-277, Moravek Biochemicals, Brea, CA). Cold control cells received cold L-valine instead. Cells were incubated overnight then the hot media was removed and cells were washed 3X with Hank's buffered saline solution (HBSS). Cells were then incubated for 1 h with fresh media containing 10 mM cold L-valine. Time 0 h controls were then harvested and precipitated with 10% Trichloroacetic Acid (TCA). The cells were spun down and

the soluble fraction was removed and collected. The insoluble fraction was then dissolved in 1 mL 0.2 M NaOH. 100 µL of each fraction was added to 5mL of scintillation cocktail (Biocount cocktail, RPI Corp #111182) and measured for counts per minute (cpm) using a scintillation counter. The total cpms were calculated by multiplying the measured cpm by the 1:10 dilution factor. The two fractions were added together to calculate the *total radioactivity (T)*.

In the meantime, the rest of the cells were washed twice with HBSS and then either incubated with 2 mL of complete media containing 10 mM cold L-valine + dimethyl sulfoxide (DMSO), 10 mM cold-L-Valine + 3-MA (10 mM), HBSS + DMSO or HBSS + 3-MA (10 mM). At each time point 50 µL of media from each well was collected and TCA precipitated with 50 µL of 20% TCA. The cpm of the soluble fraction was then measured as stated previously and the total radioactivity released into the media *(M)* was calculated by multiplying the measured cpm by the 1:40 dilution factor. This was repeated at each time point. The *fraction of protein degradation* (*D*) was calculated as a function of the fraction of the total radioactivity released into the media. To calculate this, we took the corrected cpm from each time point *(M)* and divided it by the *total radioactivity* (*T*). To isolate degradation specifically related to autophagy from other forms of protein turnover, we subtracted the fraction of protein degradation in the presence of the autophagy inhibitor 3-MA ($D_{3\text{-}MA}$) from the fraction of protein degradation from DMSO treated cells (D_{DMSO}). The same calculations

were made for HBSS+DMSO and HBSS+3-MA. This results in the % of 3-MA sensitive protein degradation.

(M)/(T)=(D)

(D_{DMSO})-($D_{3\text{-}MA}$) x100 = % of 3-MA sensitive protein degradation

2.8 Reverse transcriptase-PCR and genomic PCR. mRNA was isolated from DU145 PCa cells using the Qiagen RNeasy Kit (#74104). cDNA was synthesized using 1 µg of mRNA template and the Promega Reverse Transcription System (#A3500) in 20 µL total volume. cDNA (2 µL)was then used as template to amplify ATG5 transcripts by PCR (forward: 5´-GGA GGA TCC ATG ACA GAT GAC AAA GAT GTG CTT-3´; reverse: 5´-GCT GCT AGC TCA ATC TGT TGG CTG TGG GAT G-3´). PCR products were separated on an agarose gel, excised and purified and then cloned into the pGEM-T easy vector (Promega, Madison, WI). Clones were sequenced and identified splice variants were then cloned into the BamHI/NheI enzyme sites of pLOC-HA.

Genomic DNA from DU145 PCa cells was isolated using the Promega Wizard® Genomic DNA Purification Kit (#A1120) and used as a template for PCR using primers flanking ATG5 exon 6 (forward: 5´-CAG AAA CTT CTA GAG GGA TAT TTA-3´; reverse: 5´-ACC GTT TAG TTA CTA TGC AGA CAA-3´). The PCR product was cloned into pGEM-T easy vector and several clones were sequenced to verify the genomic sequence.

2.9 Bioinformatic analyses – *ATG5* splice region and nonsynonymous coding sequence mutations identified in human tumor samples were compiled from the Catalogue of Somatic Mutations in Cancer (COSMIC: http://cancer.sanger.ac.uk/cosmic), the cBIOPortal for Cancer Genomics (http://www.cbioportal.org), and the International Cancer Genome Consortium (ICGC: https://icgc.org). Original sequencing and copy number information comes from ICGC, the Cancer Genome Atlas (TCGA: https://tcga-data.nci.nih.gov/tcga/) and other publically available tumor datasets. cBioPortal was also used to compare mutation and copy number alteration frequency in TCGA datasets. We used The Oncomine™ Platform (Life Technologies, Ann Arbor, MI) for analysis and visualization of copy number alterations and mRNA expression in multiple PCa datasets. Oncomine™ ranks genes based on the significance of copy number or mRNA expression alterations and performs student's t-tests across all data sets to determine statistical significance.

2.10 *In vitro* cell proliferation assay – DU145 PCa cells stably expressing an empty vector (EV) or FLAG-ATG5, were transduced with lentivirus expressing firefly luciferase fused to mCherry. Successful transduction of luciferase was verified by mCherry fluorescence. $1x10^4$ EV and FLAG-ATG5 expressing cells were plated in duplicate into 6-well plates. Once per day, cells were collected in a total volume of 1 mL and the number of cells in 100 µL was measured daily using flow cytometry (Accuri™ C6 Cytometer, BD Biosciences, San Jose, CA).

The total number of cells in each group was then calculated based on the 1:10 dilution factor.

2.11 PCa xenograft tumor model – The same cell lines described above were used for a PCa xenograft tumor model. For each group, $1x10^4$ cells in 50 µL of RPMI media containing 50% Matrigel™ Membrane Matrix (Corning, #356237) were subcutaneously injected into each dorsal flank of 5 female *NOD/SCID* mice aged between 6 and 8 weeks. Tumor growth was monitored weekly using the IVIS Spectrum *in vivo* imaging system. Mice were intraperitoneally injected with 100 µl of D-Luciferin (15 µg/µL; 50-853-139 Thermo Fisher Scientific, Waltham, MA) and measured for luminescence after 10-15 min with the IVIS Spectrum. Tumor growth was taken to be a function of the average radiance (photons/s/cm^2/sr). After 7 weeks, mice were sacrificed and the tumors were harvested, weighed and photographed. Tumor lysates were also prepared and immunoblotted for ATG5, ATG12, ATG16L1 and p62.

Chapter 3: Regulation of ATG12–ATG5-ATG16L1 complex formation

3.1 Introduction

Macroautophagy, herein referred to as autophagy, is the most extensively understood form of autophagy. It requires the formation of a double-membrane autophagosome, which envelops cytoplasmic material prior to fusing with the lysosome where the inner membrane and the sequestered cargo are degraded. Autophagosomes can non-selectively sequester bulk cytoplasmic cargo, although it is increasingly clear that soluble proteins, protein aggregates, invading pathogens and a wide variety of organelles can be selectively degraded as well (Okamoto, 2014).

Over thirty ATG genes have been identified, most of which are essential for the intricate process of autophagosome formation. The ULK1 complex controls the initiation of autophagosome formation by integrating upstream AMPK and mTORC1 nutrient-related signaling pathways (Russell et al., 2014). Active ULK1 phosphorylates several subunits of the Beclin 1-PIK3C3 complex, which promotes the activation of PIK3C3 lipid kinase activity and the translocation of the complex to autophagosome formation sites on the ER, via the accessory subunit ATG14 (Shibutani and Yoshimori, 2014). At the ER, active PIK3C3 phosphorylates the 3´-position of the inositol ring of phosphatidylinositol, forming

PI(3)P. PI(3)P is essential for formation of the omegasome that serves as a cradle for the double-membrane precursor of the autophagosome, known as the phagophore or isolation membrane (Shibutani and Yoshimori, 2014). The PI(3)P effector protein, WIPI2, was recently shown to recruit the ATG12–ATG5-ATG16L1 complex to the phagophore through an interaction with ATG16L1 (Dooley et al., 2014). FIP200, a scaffold protein of the ULK1 complex, interacts with ATG16L1 at an adjacent region and may also be involved in recruitment of the complex (Gammoh et al., 2013; Nishimura et al., 2013).

Formation of the ATG12–ATG5-ATG16L1 complex requires a ubiquitin-like (UBL) conjugation reaction involving the UBL protein, ATG12. Similar to ubiquitin conjugation, this reaction requires an E1-like activating enzyme (ATG7) and an E2-like conjugating enzyme (ATG10), which together mediate the covalent conjugation of the C-terminal glycine of ATG12 to Lys-130 of ATG5 (Mizushima et al., 1998b). There is no known E3-like enzyme that catalyzes the conjugation reaction per se and almost nothing is known about how the reaction is regulated (Fig. 1.5). Through its interaction with FIP200 and/or WIPI2, ATG16L1 is thought to localize the ATG12–ATG5 conjugate to the phagophore where it functions as an E3-like enzyme for another ubiquitin-like reaction involving LC3. LC3 is activated by ATG7 and transferred to the E2-like enzyme ATG3, which is then recruited to the phagophore by ATG12. ATG12–ATG5 binding to ATG3 induces a conformational change in ATG3 that triggers conjugation of LC3 to PE, which is essential for phagophore extension and

formation of the autophagosome (Noda et al., 2013; Otomo et al., 2013; Sakoh-Nakatogawa et al., 2013). PE-conjugated LC3 has a well-established role in the recruitment of cargo into the autophagosome (Rogov et al., 2014). It has also been shown to promote membrane fusion with the phagophore and may also serve as a membrane scaffold together with the ATG12–ATG5-ATG16L1 complex (Nakatogawa et al., 2007; Weidberg et al., 2011; Kaufmann et al., 2014).

ATG16L1, ATG16L2 and TECPR1 all interact with ATG5 in the same region and thus form mutually exclusive interactions with the ATG12–ATG5 conjugate (Kim et al., 2015). Despite sharing a domain structure with ATG16L1, ATG16L2 does not catalyze LC3 conjugation and its function is unknown (Ishibashi et al., 2011). TECPR1, on the other hand, has been implicated specifically in selective autophagy (Ogawa et al., 2011). Binding of ATG12–ATG5 to TECPR1 is also reported to promote its interaction with PI(3)P and the fusion of autophagosomes and lysosomes (Chen et al., 2012). Still, many open questions remain about the interplay between these different ATG5-interacting proteins.

There are numerous examples of ubiquitin conjugation regulating ATG proteins. Ubiquitination of Beclin 1, in particular, results in its activation or degradation depending on the type of polyubiquitin linkage (Reidick et al., 2014). Similarly, ULK1 is reportedly stabilized by Lys^{63}-polyubiquitination while also being a target of proteasomal degradation (Joo et al., 2011; Nazio et al., 2013).

An early finding suggested that cellular levels of ATG16L1 are maintained by the proteasome and this was also recently found to be true for free, unconjugated ATG12 (Fujita et al., 2009; Haller et al., 2014).

In this study, we have determined that DU145 PCa cells are deficient in autophagy due to an *ATG5* donor splice-site mutation that triggers aberrant splicing and loss of ATG5, ATG12 and ATG16L1. Re-expression of ATG5 in DU145 rescues the ubiquitination and proteasomal turnover of ATG12 and ATG16L1, formation of a functional ATG12–ATG5-ATG16L1 complex and autophagy. We have also determined that all known alternative ATG5 protein isoforms are rapidly ubiquitinated and degraded and are unable to interact with ATG16L1, which we have found is required to stabilize ATG5 and allow conjugation to ATG12. Thus, the competing conjugation reactions of ubiquitin and the ubiquitin-like protein, ATG12, control ATG5 stability and formation of the ATG12–ATG5-ATG16L1 complex. These findings highlight the importance of ubiquitination and proteasomal degradation in regulating the formation of the ATG12–ATG5-ATG16L1 complex and autophagy.

3.2 Results

3.2.1 DU145 prostate cancer cells are autophagy deficient due to absence of the ATG12–ATG5-ATG16L1 complex. We initially found DU145 prostate cancer (PCa) cells were unable to undergo LC3B lipidation, which is an essential

step in autophagosome formation. Bafilomycin A1 (Baf A1) alkalinizes the lysosome and blocks autophagic degradation of LC3 and other substrates, making it useful for examining autophagic flux. Baf A1 treatment resulted in the accumulation lipid-conjugated LC3B (LC3-II), an autophagosome marker, in LNCaP and PC-3 cells, indicating the treatment inhibited autophagic flux. Surprisingly, however, LC3-II remained undetectable in DU145 cells, suggesting that either the levels of basal autophagy were extremely low in this particular cell line or that a potential defect existed in the LC3 ubiquitin-like conjugation reaction (Fig. 3.1*A*).

To address these possibilities, we starved DU145 PCa cells and A549 lung cancer cells in nutrient-free media, which is known to induce robust autophagosome formation detectable by transmission electron microscopy (TEM) (Eskelinen, 2008). Autophagic vacuoles were readily detected in A549 cells after starvation; however, we did not find evidence of autophagosome formation in DU145 cells (Fig. 3.1*B)*. To further investigate whether the lack of observed autophagosomes corresponded with a block in actual autophagic protein degradation, we examined DU145 PCa cells and A549 lung cancer cells for the turnover of radioactively labeled long-lived proteins in response to starvation. Control and starved cells were simultaneously treated with or without the PI3K and autophagy inhibitor, 3-methyladenine (3-MA). 3-MA blocks PI(3)P formation and thus, prevents autophagosome formation. We calculated the difference in the amount of protein degradation between untreated and 3-MA-treated cells in

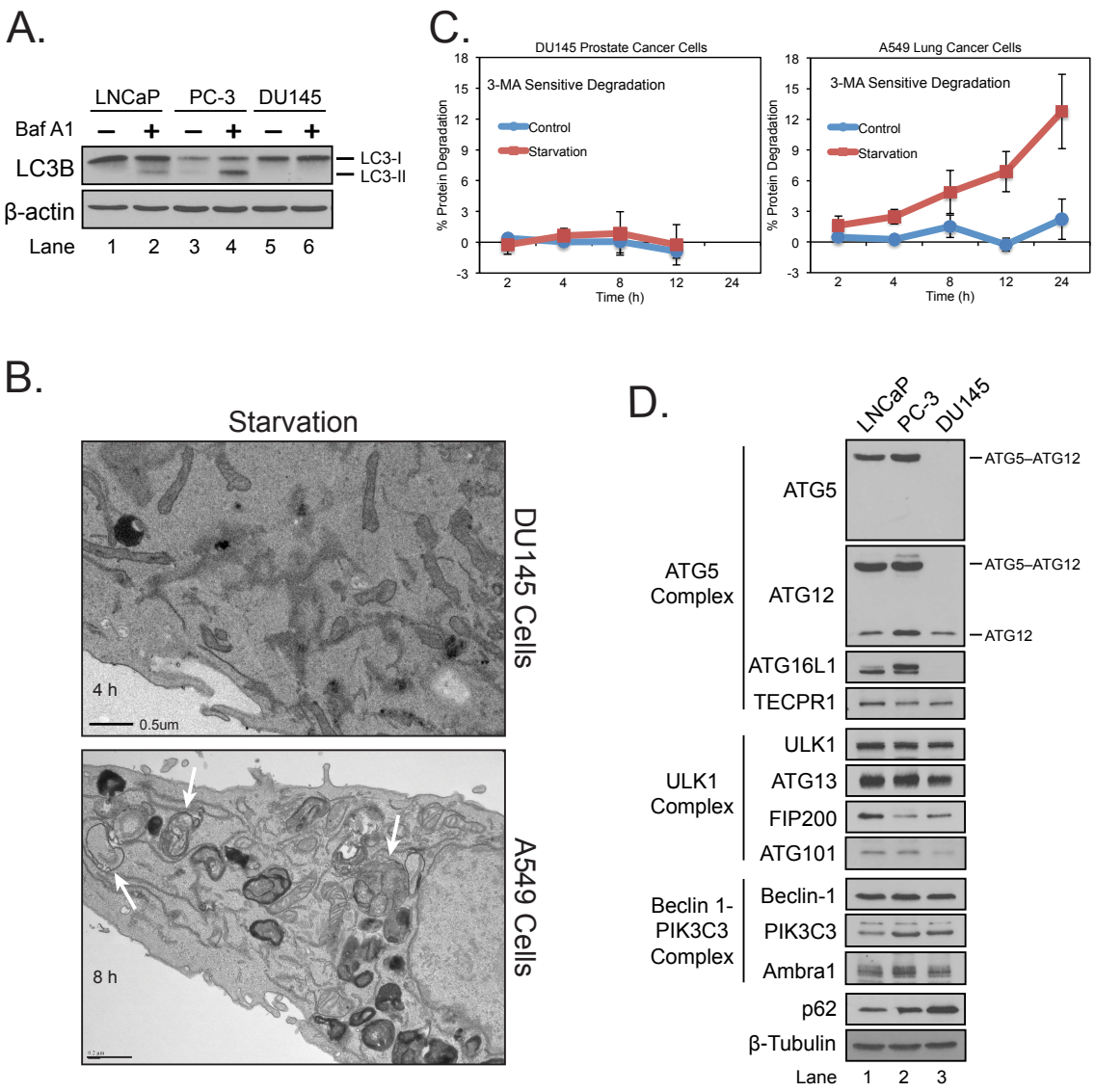

Figure 3.1 – DU145 PCa cells are autophagy-deficient due to absence of the ATG12–ATG5-ATG16L1 complex. (*A*) LNCaP, PC-3 and DU145 PCa cells were treated with DMSO or Bafilomycin A1 (Baf A1). Cell lysates were then prepared and immunobloted for LC3B and β-actin. LC3-I and LC3-II are the cytosolic and lipid-conjugated forms of LC3, respectively. (*B*) Transmission electron microscopy (TEM) was used to examine autophagosome formation in DU145 PCa cells and A549 cells after starvation. White arrows indicate autophagic vacuoles. (*C*) The 3-methyladenine (3-MA) sensitive degradation of radioactively labeled long-lived proteins in response to starvation was monitored in DU145 PCa cells and A549 lung cancer cells. DU145 cells did not survive beyond 12 h of complete starvation (data not shown). (*D*) Cell lysates of LNCaP, PC-3 and DU145 PCa were immunoblotted for ATG proteins.

order to isolate autophagy-specific degradation and exclude other potential forms of protein turnover. This approach yielded robust starvation-induced protein degradation in A549 cells that was completely absent in DU145 cells (Fig. 3.1*C*).

Together, these data confirmed that DU145 PCa cells were autophagy-deficient due to an apparent absence of LC3 lipid conjugation, which was essential for the formation of an autophagosome and for autophagic degradation. We then examined the levels of other ATG proteins in LNCaP, PC-3 and DU145 cells in an attempt to identify the mechanism behind the loss of LC3 conjugation (Fig. 3.1*D*). Strikingly, the levels of ATG5, the ATG12–ATG5 conjugate, and ATG16L1 were entirely absent in DU145 cells, while the levels of ULK1 and Beclin 1-PIK3C3 complex components were relatively comparable. Only unconjugated ATG12 was detectable in DU145 cells, albeit at lower levels. TECPR1, which interacts with the ATG5–ATG12 conjugate at the same region as ATG16L1, was not lost in DU145 cells, which indicated the loss is specific to the ATG12–ATG5-ATG16L1 complex. Since the ATG12–ATG5-ATG16L1 complex is essential for LC3 conjugation, its absence explained why LC3-II was not detected in response to Baf A1 treatment in DU145 cells (Fig. 3.1*A*). The absence of the ATG12–ATG5-ATG16L1 complex was directly correlated with a high level of the autophagy substrate, p62, in DU145 cells compared to LNCaP and PC-3 cells, which further indicated a block in autophagic flux (Fig. 3.1*D*).

3.2.2 ATG5, ATG12 and ATG16L1 are coordinately degraded by the proteasome when not associated with the ATG12–ATG5-ATG16L1 complex. The near total loss of ATG12 and the complete absence of ATG5 and ATG16L1 in DU145 PCa cells suggested that either DU145 cells had a simultaneous genetic deficiency in both *ATG5* and *ATG16L1* or the individual subunits of the ATG12–ATG5-ATG16L1 complex were coordinately downregulated. The simplest mechanism for the simultaneous loss of ATG5, ATG12 and ATG16L1 was proteasomal degradation of the entire complex.

To test this possibility, we treated LNCaP, PC-3 and DU145 cells with the reversible proteasome inhibitor, MG132. MG132 treatment significantly increased unconjugated ATG12 levels in both PC-3 and DU145 cells (Fig. 3.2*A*, lanes 4 and 6), which indicated that it was being continually expressed and degraded by the proteasome. Additionally, MG132 treatment partially rescued ATG16L1 levels in DU145 cells, but had no effect on ATG16L1 in LNCaP or PC-3 cells (Fig. 3.2*A*, lanes 2, 4, and 6). This suggested that either that proteasomal turnover of ATG16L1 occurs only in DU145 cells or that its degradation only occurs in the absence of the ATG12–ATG5 conjugate. Finally, MG132 did not rescue any detectable ATG5 in DU145 cells, which meant that these cells were potentially ATG5-deficient (Fig. 3.2*A*). If unconjugated ATG12 is continually degraded and ATG16L1 is degraded only in the absence of the ATG12–ATG5 conjugate, then a specific loss of ATG5 in DU145 cells would explain the proteasomal-dependent elimination of the remaining subunits of the complex.

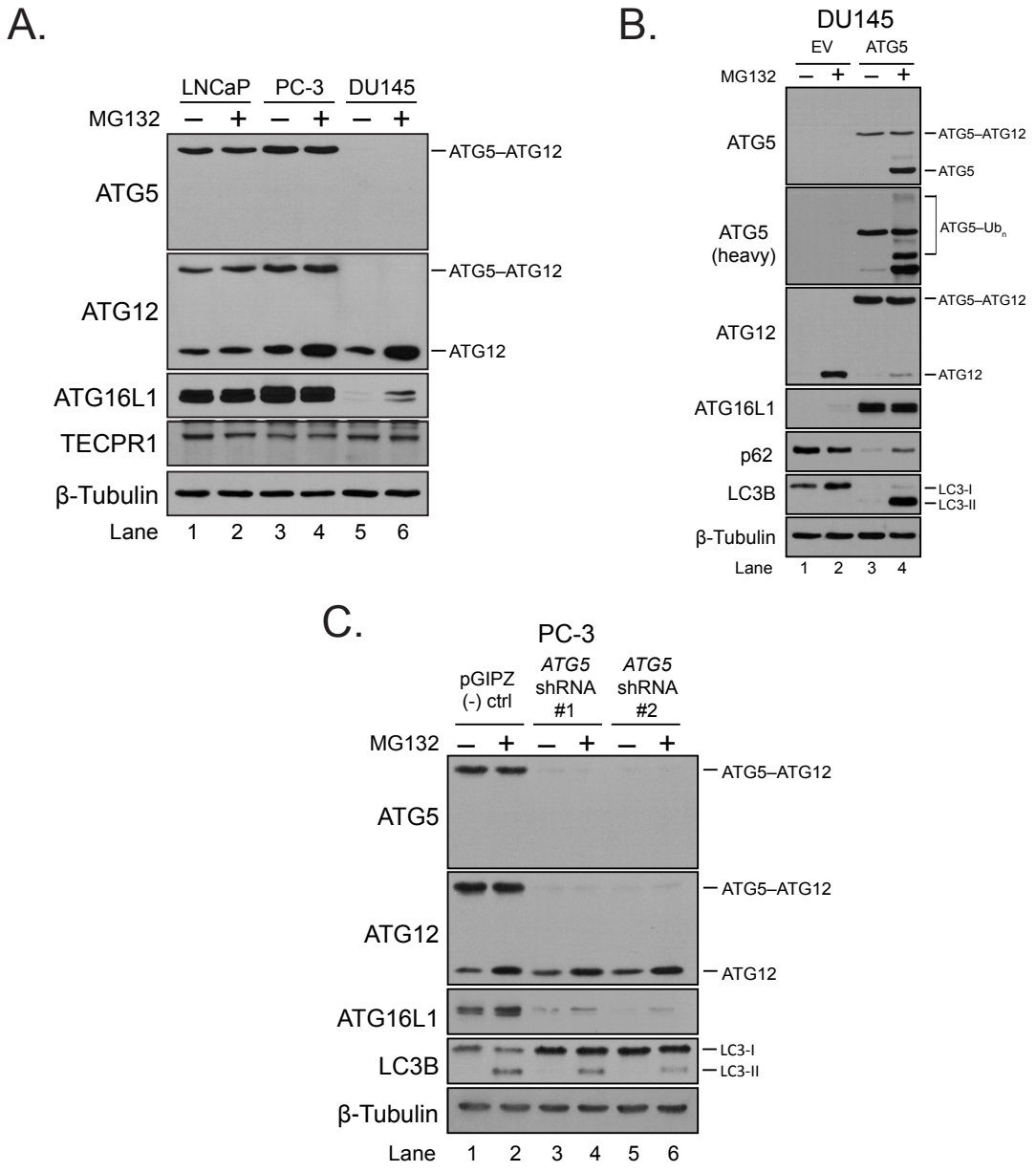

Figure 3.2 – ATG5, ATG12 and ATG16L1 are coordinately degraded by the proteasome when not associated with the ATG12–ATG5-ATG16L1 complex. (*A*) LNCaP, PC-3 and DU145 PCa cells were treated with DMSO or MG132. Cell lysates were then prepared and immunoblotted for ATG5 complex components. (*B*) DU145 cells stably expressing an empty vector or FLAG-ATG5 were treated with DMSO or MG132. Lysates were prepared and immunoblotted for ATG proteins. (*C*) PC-3 cells stably expressing a non-silencing control shRNA or an shRNA targeting *ATG5* were treated with DMSO or MG132. Lysates were prepared and analyzed by immunoblotting for ATG proteins.

To test this prediction, we stably expressed ATG5 in DU145 PCa cells. ATG5 expression in DU145 cells rescued both ATG12 conjugation and ATG16L1 levels. We confirmed that ATG5 expression rescued functional ATG12–ATG5-ATG16L1 complex formation by examining the levels of p62 (Fig. 3.2*B*, lanes 1 and 3) and lipid-conjugated LC3-II (Fig. 3.2*B*, lanes 2 and 4), both of which indicated a rescue of functional autophagy. Proteasome inhibition is known to robustly activate autophagy (Park and Cuervo, 2013), which explains why LC3 lipid conjugation was readily detected upon MG132 treatment in ATG5 expressing DU145 cells, but not in control cells (Fig. 3.2*B*, lanes 2 and 4).

MG132 treatment had no effect on the ATG12–ATG5 conjugate levels, but it did result in the drastic accumulation of unconjugated ATG5 along with a ladder of higher molecular weight species generally indicative of polyubiquitination (Fig. 3.2*B*, lane 4). This suggested that unconjugated ATG5 was continually ubiquitinated and degraded by the proteasome similar to unconjugated ATG12. The more obviously apparent polyubiquitination of ATG5 was likely due to the rate of expression of exogenous ATG5 compared to that of endogenous ATG12. Together these data suggest that unconjugated ATG5 and ATG12 are continually degraded by the proteasome even with intact ATG12–ATG5 conjugate present, while ATG16L1 appears to be degraded only in the absence of the ATG12-ATG5 conjugate. This model can explain why, the DU145 ATG5-deficiency resulted in the proteasomal degradation of ATG12 and ATG16L1.

To determine if ubiquitination and proteasomal regulation of ATG12 and ATG16L1 occurs in other cell types, we used RNA interference to knockdown *ATG5* in PC-3 PCa cells (Fig. 3.2*C*). Stable knockdown of *ATG5* using two different shRNAs resulted in a drastic reduction in the total amount of ATG12, both conjugated and unconjugated, as well as reduced ATG16L1 levels (Fig. 3.2*C*, lanes 1, 3 and 5). MG132 treatment partially rescued ATG16L1 and unconjugated ATG12 levels (Fig. 3.2*C*, lanes 4 and 6), which confirmed that loss of ATG5 triggers proteasomal degradation of ATG12 and ATG16L1 in other cell types. Since MG132 treatment was limited to 8 h to avoid excessive toxicity, the modest effect on the accumulation of ATG16L1 was most likely due to low basal rate of ATG16L1 expression in these cells.

3.2.3 ATG5 and ATG16L1 partially stabilize one another independently of ATG12, although a fully assembled ATG12–ATG5-ATG16L1 complex is required for maximum stability of ATG12, ATG5 and ATG16L1. We have determined that loss of ATG5 resulted in the complete proteasomal degradation of ATG12 and ATG16L1 in multiple cell types. In ATG5 re-expressing DU145 cells, MG132 treatment increased levels of unconjugated ATG12 and ATG5 while the ATG12–ATG5 conjugate remained unaffected. This suggested the ATG12–ATG5 conjugate was stable and that unconjugated ATG12 and ATG5 were inherently unstable. Unlike ATG12 or ATG5, ATG16L1 did not undergo proteasomal degradation in the presence of the ATG5-ATG12 conjugate, which

suggested its stability is dependent on the fully assembled ATG12–ATG5-ATG16L1 complex. Although the current model for ATG12–ATG5-ATG16L1 complex formation suggests that ATG12 conjugation to ATG5 occurs prior to its interaction with ATG16L1 (Fig. 1.5, p.29), it remained possible that ATG16L1 stability was dependent upon ATG5 expression alone and not on formation of the ATG12–ATG5 conjugate.

To distinguish between these possibilities we needed a way to uncouple ATG5 expression from conjugation to ATG12. To do this, we stably expressed a mutant version of ATG5 that cannot undergo conjugation due to mutation of the target Lys-130. This K130R mutation completely blocked ATG12 conjugation and formation of a functional complex as determined by p62 degradation (Fig. 3.3*A*, lanes 3 and 5) and LC3 lipidation (Fig. 3.3*A*, lanes 4 and 6). Despite the complete block in ATG12 conjugation, which was predicted to be required for ATG5 stability, the unconjugated ATG5 (K130R) was incompletely degraded and remained stably expressed, albeit at lower levels than wild-type ATG5. The mutant also rescued ATG16L1 levels, but to a lesser extent than wild-type ATG5 (Fig. 3.3*C*, lanes 3 and 5). This suggested that ATG5 may partially rescue ATG16L1 from proteasomal degradation, independent of ATG12 conjugation.

Since unconjugated, wild-type ATG5 is readily degraded by the proteasome (Fig. 3.3*A* lanes, 3 and 4), the partial stability of ATG5 (K130R) could be because Lys-130 is an important residue for ubiquitination or proteasome turnover. Another possibility is that unconjugated ATG5 and

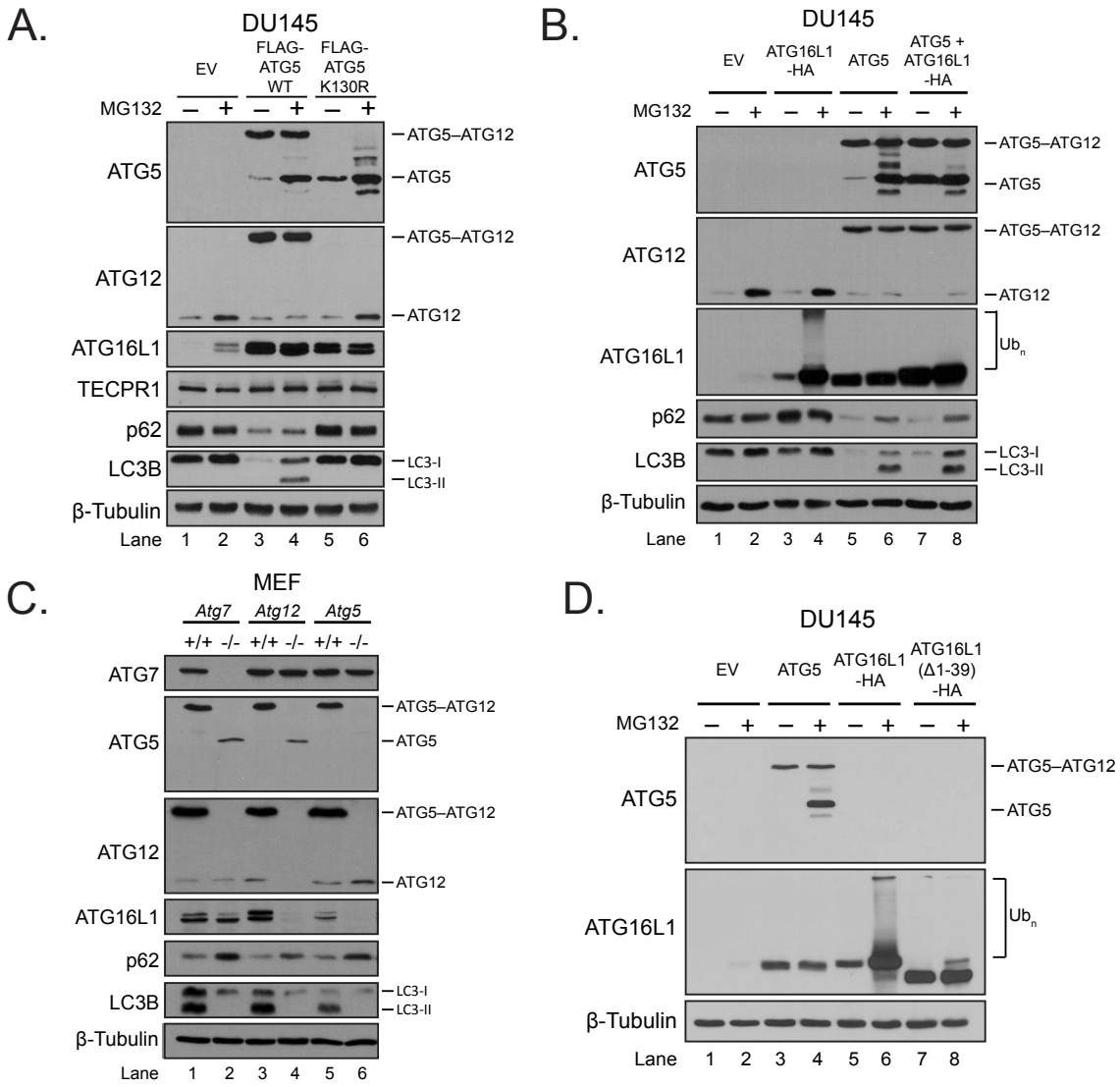

Figure 3.3 – ATG5 and ATG16L1 partially stabilize one another independently of ATG12, although the fully assembled ATG12–ATG5-ATG16L1 complex is required for maximum stability. (*A*) DU145 cells stably expressing an empty vector, wild-type FLAG-ATG5 (WT) or FLAG-ATG5 (K130R) were treated with DMSO or MG132. Lysates were prepared and immunoblotted for ATG proteins. (*B*) DU145 cells stably expressing an empty vector, ATG5, ATG16L1-HA or both ATG5 and ATG16L1-HA together were treated with DMSO or MG132. Cell lysates were prepared and immunoblotted for ATG proteins. (*C*) Lysates prepared from *Atg7*, *Atg12*, and *Atg5* wild type ($^{+/+}$) and knockout ($^{-/-}$) MEFs were immunoblotted for ATG proteins. (*D*) DU145 cells stably expressing an empty vector (EV), wild-type ATG5, C-terminally HA-tagged wild-type ATG16L1 or N-terminally deleted ATG16L1 (Δ1-39) were treated with DMSO or MG132. Lysates were prepared and immunoblotted for ATG5, ATG16L1 and α-Tubulin. ubiquitination and proteasomal degradation.

ATG16L1 interact independently of ATG12 and partially stabilize one another. Treatment of ATG5 (K130R) expressing DU145 cells with MG132 had no obvious effect on ATG16L1, but still resulted in the accumulation of unconjugated ATG5 along with laddering typical of polyubiquitination (Fig. 3.3*A*, lane 6). While this did not completely rule out that K130 was an important site for ubiquitination and turnover, it did show that K130 was clearly not the only available ubiquitination target on ATG5.

The fact that MG132 treatment caused the accumulation of polyubiquitinated ATG5 (K130R), but had no obvious effect on ATG16L1 could be related to their relative expression levels. ATG5 (K130R) was expressed at a much higher level than endogenous ATG16L1; which, assuming a 1:1 stoichiometry, would result in excess unbound ATG5 that could then be ubiquitinated and degraded. Therefore, while overexpression of ATG5 (K130R) may have driven the equilibrium towards mutual interaction and artificially stabilized both proteins, the excess ATG5 (K130R) not bound to ATG16L1 was still capable of being ubiquitinated and degraded. Similarly, it is likely that unconjugated wild-type ATG5 was turned over because it was also expressed in excess and the endogenous ATG16L1 was likely fully saturated with the ATG5-ATG12 conjugate (Fig. 3.3*A*, lane 3 and 4).

Co-expressing exogenous wild-type ATG5 and ATG16L1 at similar levels in DU145 cells resulted in the stabilization of both ATG16L1 and unconjugated ATG5 compared to the levels upon expression of each protein alone (Fig. 3.3*B*,

lanes 3, 5 and 7). MG132 treatment of ATG16L1 or ATG5 expressing DU145 cells resulted in a drastic accumulation of polyubiquitinated ATG16L1 and unconjugated ATG5, which confirmed these proteins are highly unstable when expressed in excess (Fig. 3.3*B*, lanes 4 and 6). However, co-expression of ATG5 and ATG16L1 largely reduced, or even completely eliminated, the ubiquitination and proteasomal degradation of each protein (Fig. 3.3*B*, lane 8). This strongly indicates that these proteins were capable of stabilizing one another by preventing ubiquitination and proteasomal degradation. Co-expression did not result in any increase in the amount of ATG12–ATG5 conjugate, which is likely because all available ATG12 had already undergone conjugation with ATG5 expression alone (Fig. 3.3*B*, lanes 5 and 7).

To examine the stability of ATG16L1 and unconjugated ATG5 at endogenous levels in a non-overexpression system, we used mouse embryonic fibroblasts (MEFs) containing genetic deletions of *Atg5*, *Atg12* or *Atg7*, the latter of which encodes for an E1-like enzyme essential for Atg12 conjugation (Fig. 3.3*C*). As expected, inactivation of ATG12 conjugation, through genetic deletion of *Atg7* or *Atg12,* completely blocked formation of the ATG12–ATG5 conjugate, although to our surprise, this did not coincide with a dramatic increase in the amount of unconjugated ATG5. Instead, a low level of unconjugated ATG5 was detected, which corresponded with a significant decrease in ATG16L1 levels (Fig. 3.3*C*, lanes 1-4). This indicated that, at endogenous expression levels, the ATG5-ATG16L1 interaction only provides slight, partial protection from

proteasomal turnover. If an equilibrium exists between the stabilizing ATG5-ATG16L1 interaction and dissociation that leads to proteasomal turnover of ATG5 and ATG16L1, then the removal of the unbound subunits from the equilibrium would shift the equilibrium more towards dissociation and turnover (Fig. 3.4). This could explain why endogenous ATG5 and ATG16L1 only partially protected one another from proteasomal degradation.

Since co-expression of ATG5 and ATG16L1 resulted in reciprocal protection from ubiquitination and turnover, we suspected the binding sites through which these proteins interacted were shared by the unknown E3 ligases that mediated their ubiquitination, thereby shielding them. Indeed, ATG16L1 binds to ATG5 solely through its N-terminus (Otomo et al., 2013); therefore, this region may also recruit E3 ligases responsible for ATG16L1 ubiquitination and turnover. To test this hypothesis, we stably expressed wild-type ATG16L1 and a N-terminal deleted version of ATG16L1 (Δ1-39) in DU145 cells (Fig. 3.3*D*). Interestingly, this N-terminal deletion almost entirely blocked its ubiquitination and turnover. This suggested that individual ATG5-ATG16L1 binding surfaces also recruit unknown E3 ligases that mediate their ubiquitination and turnover (Fig 3.3*D*).

In summary, these data indicate that: (1) the DU145 autophagic defect is due to the specific absence of ATG5 expression and the subsequent proteasomal degradation of ATG12 and ATG16L1; (2) the ATG12–ATG5 conjugate is stable, while both unconjugated ATG5 and ATG12 are inherently

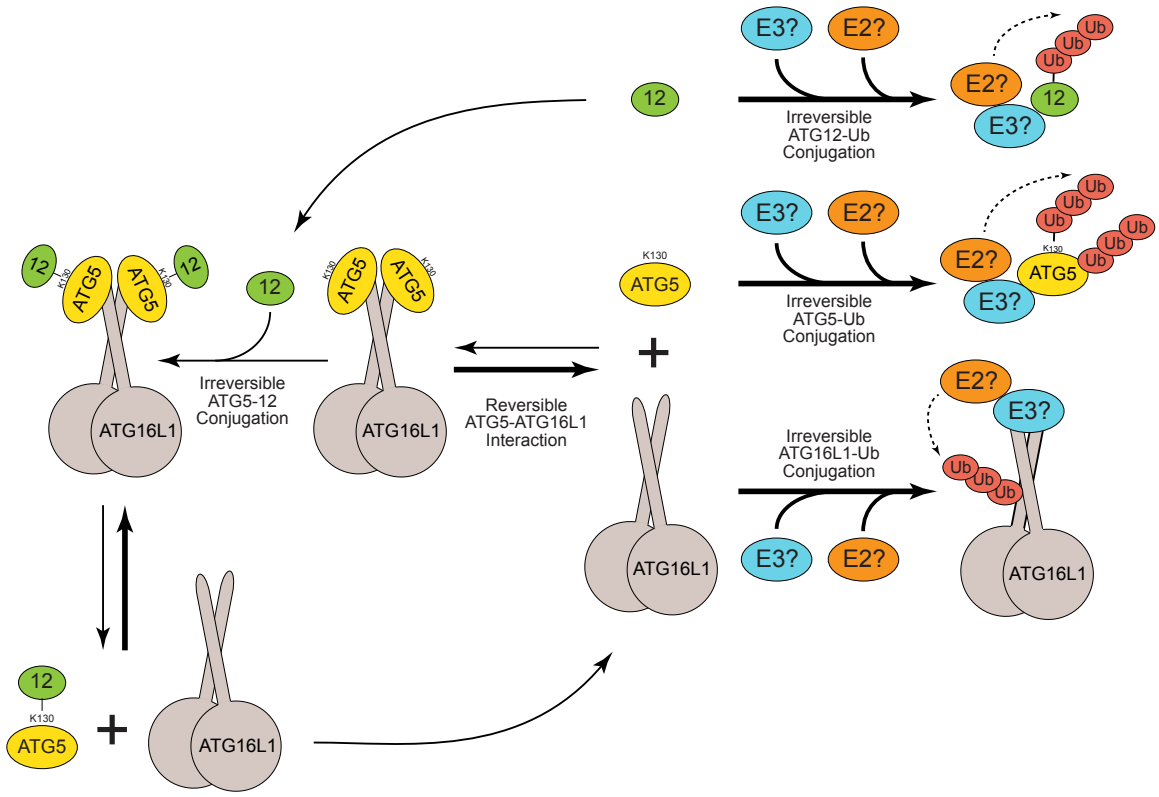

Figure 3.4 – Proposed model for ATG12–ATG5-ATG16L1 complex assembly. ATG16L1 and unconjugated ATG12 and ATG5 are rapidly ubiquitinated by unknown E3 ligases, which promotes their proteasomal degradation. ATG5 and ATG16L1 form a mutually protective interaction by shielding E3 ligase recruitment sites. This stabilizes the ATG5-ATG16L1 intermediate and allows ATG12 conjugation to ATG5 to occur, thus stabilizing ATG12 and the ATG5-ATG16L1 interaction.

unstable and are continually ubiquitinated and degraded by the proteasome; and (3) ATG5 and ATG16L1 can, at least partially, protect one another from ubiquitination and proteasomal turnover, independent of ATG12 conjugation.

Therefore, we propose a model in which the reversible interaction between ATG16L1 and ATG5 prevents recruitment of E3 ligases that mediates ubiquitination and degradation of each protein. This stabilizes the intermediate and allows ATG12 conjugation to occur and form a stable ATG12–ATG5-ATG16L1 complex (Fig. 3.4). This model is a significant deviation from the current model suggesting ATG12–ATG5 conjugation occurs prior to its association with ATG16L1 (Fig. 1.5, p.29). Based on this proposed model, one would predict that ATG16L1, or another protein capable of stabilizing ATG5, is essential for ATG12 conjugation to ATG5. In the next few sections of this chapter, we will prove that is indeed the case.

3.2.4 A splice donor-site mutation within intron 6 causes aberrant *ATG5* mRNA splicing and skipping of exon 6 in DU145 PCa cells. Having shown that DU145 PCa cells do not express ATG5, which results in the proteasomal degradation of ATG12 and ATG16L1 as well as the coordinated downregulation of FIP200 and ATG13, we set out to identify the mechanism for the loss of ATG5 expression. Given the possibilities that DU145 cells were genetically deficient in *ATG5* or simply transcriptionally repressed *ATG5* expression, we decided to examine *ATG5* mRNA expression levels. We isolated mRNA from DU145 PCa

cells and performed RT-PCR to amplify *ATG5* transcripts (Fig. 3.5*A*). Surprisingly, the *ATG5* mRNA was readily detected; however, we did note more than one band that was suggestive of *ATG5* alternative mRNA splicing. All visible bands were isolated, cloned and sequenced, revealing that two novel, alternative splice variants were expressed in DU145 cells, while full length ATG5 was absent. One variant contained an exon 6 deletion and the other was missing exons 3 and 6. We presumed these splice variants were not translated into functional ATG5 proteins and thus, DU145 PCa cells were ATG5-deficient due to alternative mRNA splicing of *ATG5*.

Unfortunately, during our more in-depth investigation into this finding, this novel alternative splicing and loss of ATG5 expression was discovered and published by another group (Ouyang et al., 2013). However, why DU145 PCa cells were ATG5-deficient was not investigated. Therefore, many interesting mechanistic questions remained unanswered. Since both novel splice variants identified in DU145 cells contained deletions of exon 6, we suspected there might be a genetic alteration in this region that might be disrupting normal *ATG5* splicing. Using DU145 genomic DNA as template, we PCR amplified the region surrounding exon 6, cloned and sequenced several of the resulting clones. As predicted, we identified a mutation (c.573+1G>A) at the most 5′ nucleotide of intron 6, which is the location of the highly conserved GT splice donor consensus sequence (Fig 3.5*B*). Mutation of the splice donor site of intron 6 is predicted to prevent nucleophilic attack by the 2′ hydroxyl group of the conserved branch-site

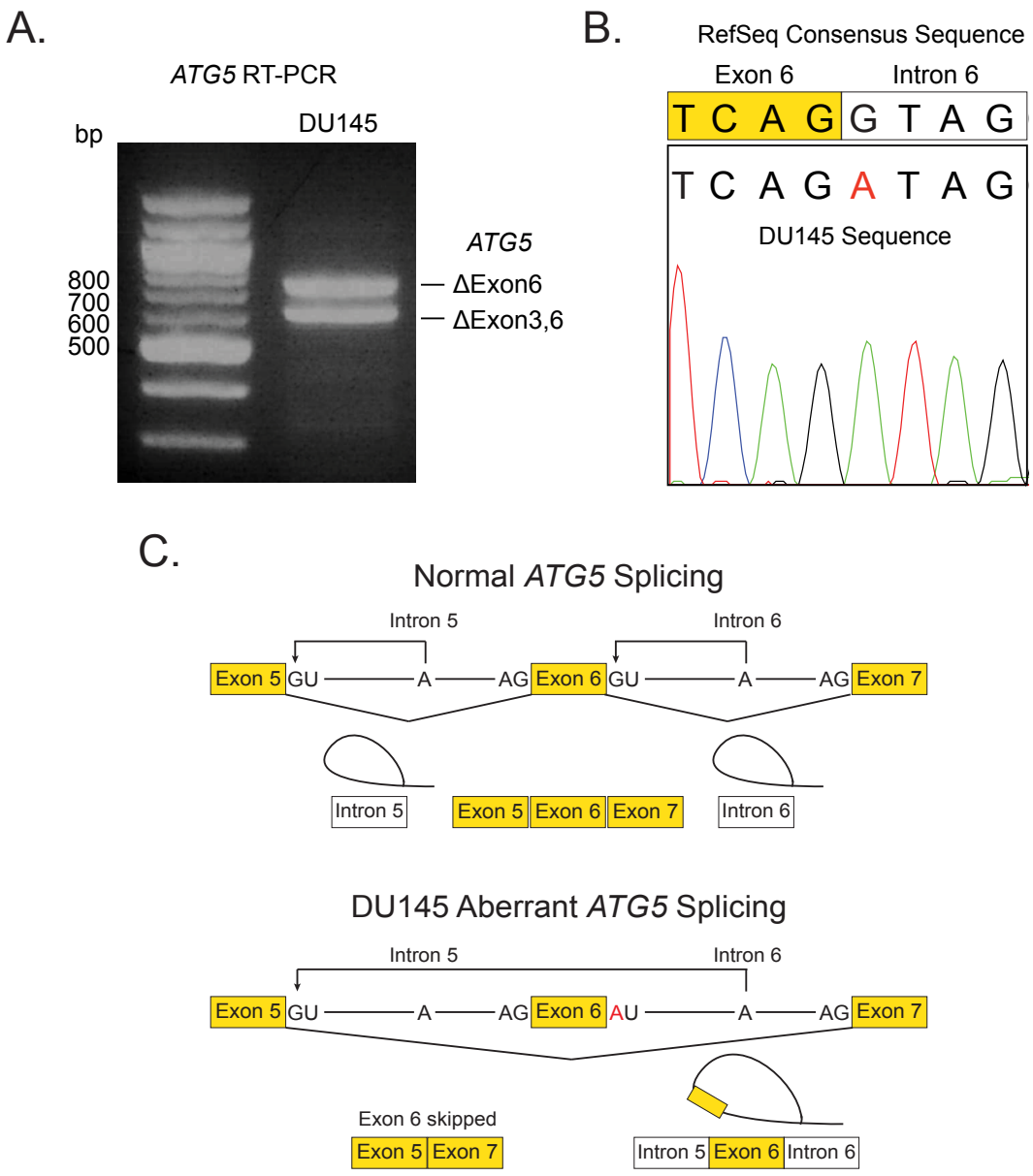

Figure 3.5 – A splice donor-site mutation within intron 6 of *ATG5* causes aberrant mRNA splicing and skipping of exon 6 in DU145 PCa cells. (*A*) RT-PCR for *ATG5* using mRNA isolated from DU145 PCa cells. The identified splice variants are indicated. (*B*) Sequencing chromatogram of the PCR amplified exon 6–intron 6 boundary of DU145 PCa cells. The DU145 genomic sequence is compared to the NCBI RefSeq consensus sequence. (*C*) Diagram of normal *ATG5* splicing and the proposed mechanism of exon 6 skipping caused by the DU145 donor splice-site mutation.

adenosine residue within intron 6 (Patel and Steitz, 2003). Instead, attack should occur at the next upstream splice donor site located at the 5´ end of intron 5, resulting in the "skipping" of exon 6 by aberrant removal of exon 6 along with introns 5 and 6 (Fig. 3.5*C*).

After identifying the splice-site mutation, we consulted the COSMIC Cell Line Project database (cancer.sanger.ac.uk) to verify if genome sequencing had identified this same mutation in DU145 cells (Forbes et al., 2011). The c.573+1G>A mutation was listed in the database and was classified as homozygous and unverified in DU145 cells. Therefore, we propose that this mutation is the sole cause of *ATG5* alternative splicing and the autophagy deficiency in DU145 prostate cancer cells and is not an artifact of PCR or sequencing.

3.2.5 All alternative ATG5 protein isoforms are non-functional due to rapid ubiquitination and proteasomal degradation. *ATG5* spans approximately 141 kb on the minus strand of chromosome 6 and comprises a total of 8 exons (Fig. 3.6*A*). Including our recently identified DU145 *ATG5* splice variants, seven potentially coding *ATG5* splice variants have been identified to date, according to Aceview and National Center for Biotechnology Information (NCBI) RefSeq databases (Thierry-Mieg and Thierry-Mieg, 2006; Pruitt et al., 2014) (Fig. 3.6*A*). All alternative *ATG5* splice variants, with the exception of variant 2 (v2), contain alternative translational start sites and/or premature stop codons and, thus, are

potential targets of nonsense-mediated mRNA decay (NMD) that may preclude expression of the encoded alternative ATG5 protein isoforms. Splice variants 6 and 7 (v6 and v7), which we identified in DU145 cells, are designated as targets for NMD by the NCBI RefSeq database, although this has not been empirically verified.

We did not detect any alternative ATG5 protein isoforms in LNCaP, PC-3 or DU145 cells even after 8 h of MG132 treatment (Fig. 3.2*C*). This could be indicative of NMD targeting of the *ATG5* splice variants; however, the fact that full-length ATG5, which is readily expressed in LNCaP and PC-3 cells, also did not accumulate after MG132 treatment suggests endogenous ATG5 expression rates are simply not high enough to detect the rapidly degraded unconjugated forms of ATG5 within the allowable 8 h of proteasome inhibition. All *ATG5* splice variants, including full-length *ATG5*, contain an upstream open reading frame (uORF) in 5′ untranslated region (UTR) of exon 2, which precedes the translational start site (Fig. 3.6*A*). uORFs have been correlated with translational repression of downstream ORFs (Barbosa et al., 2013), meaning they could be responsible for the low rate of ATG5 expression. However, the specific effects of uORFs and NMD are not well understood, and it is difficult to predict exactly how they might regulate expression of full-length ATG5 or its alternative protein isoforms.

In order to overcome the inability to detect endogenous, unconjugated ATG5 protein isoforms, we exogenously expressed HA-tagged versions in

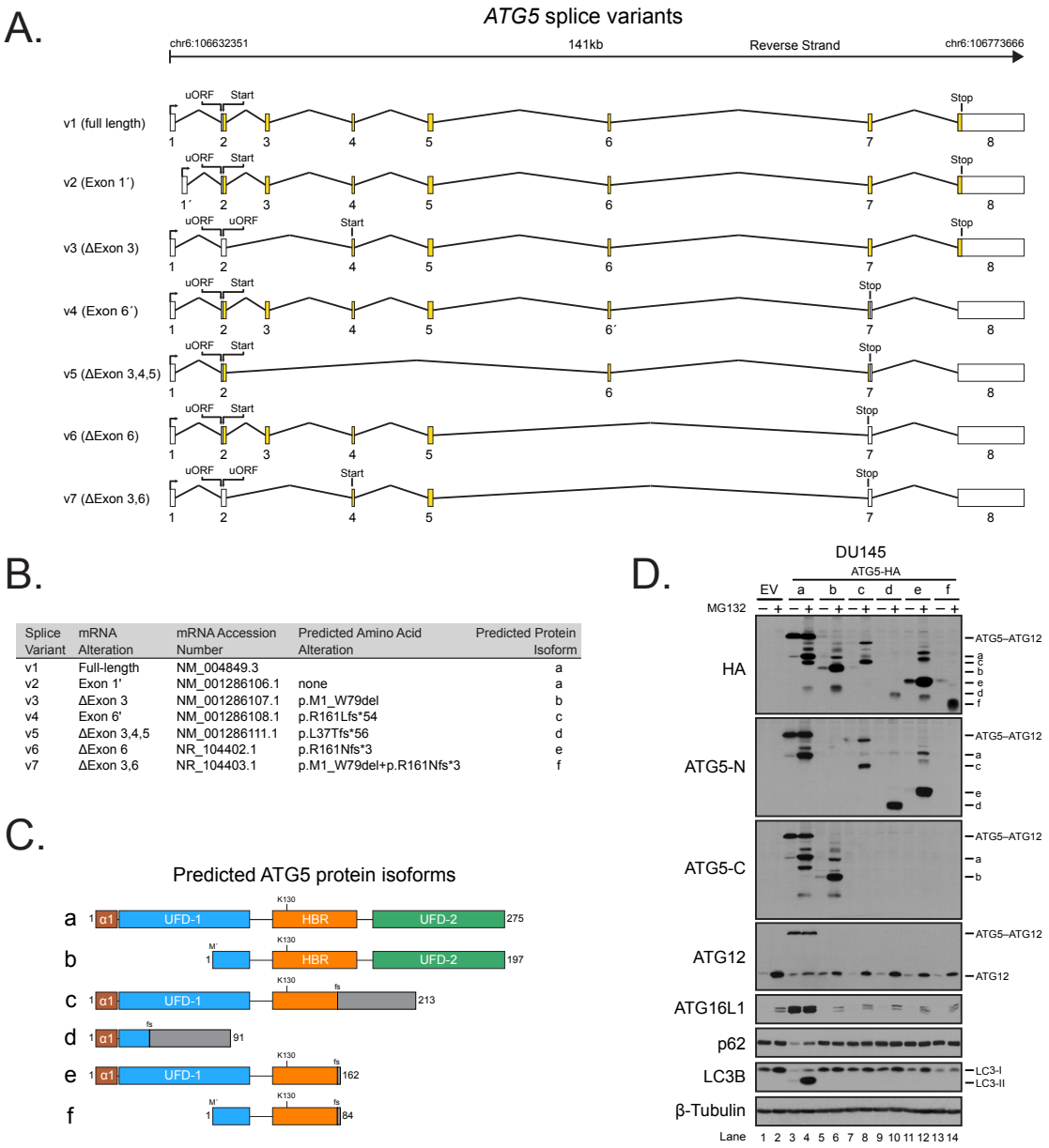

Figure 3.6 – All known alternative ATG5 protein isoforms are non-functional due to rapid ubiquitination and proteasomal degradation. (*A*) Diagram of all known *ATG5* alternative splice variants. (*B*) Table listing mRNA accession numbers of all known *ATG5* splice variants and the predicted amino acid alterations of their encoded isoforms. (*C*) Diagram of ATG5 domain structure and predicted ATG5 protein isoforms. Full-length ATG5 consists of an N-terminal α-helix (α1), two ubiquitin-like fold domains (UFD-1 and UFD-2) and a helix-bundle region (HBR) that contains the site of ATG12 conjugation (Lys-130). (*D*) DU145 cells stably expressing an empty vector or C-terminal HA-tagged ATG5 isoforms a-f were treated with MG132. Lysates were prepared and immunoblotted for HA, N and C-terminal ATG5 and autophagy-related proteins.

DU145 cells to determine if any of the predicted alternative ATG5 protein isoforms were capable of conjugating to ATG12 and forming a functional ATG12-–ATG5-ATG16L1 complex. The predicted amino acid alteration for each splice variant is listed in Fig. 3.6*B* and diagrammed in Fig. 3.6*C*. Full-length ATG5 contains an N-terminal α-helix domain (α1), followed by two ubiquitin-fold domains (UFD-1 and UFD-2) that flank a helix bundle region (HBR) containing Lys-130, which is the site of ATG12 conjugation (Fig. 3.6*C*). Splice variant 2 contains an alternative exon 1, which affects only the 5´ UTR and is still predicted to encode for full-length ATG5. Splice variants 3 and 7, encoding isoforms b and f respectively, have predicted alternative translational start sites that create N-terminal deletions. Splice variant 7 (encoding isoform f), in addition to variants 5 and 6 (encoding isoforms d and e, respectively) are missing one or more exons, creating frameshifts and introducing premature stop codons that are predicted to cause C-terminal truncations. Splice variant 4 contains an alternative exon 6, likely resulting from cryptic splicing, which also introduces a frameshift and premature stop codon predicted to encode for a severely truncated ATG5 isoform d (Fig. 3.6*B* and 3.6*C*).

Stable expression of all ATG5 protein isoforms clearly revealed that only full-length ATG5 expression rescued ATG12 and ATG16L1 turnover (Fig. 3.6*D*). Rescue of p62 degradation and LC3 lipid-conjugation was also only seen for full-length ATG5 and not for any of the other ATG5 isoforms (Fig. 3.6*D*). All the alternative ATG5 protein isoforms were nearly undetectable in cells not treated

with MG132, suggesting they may be degraded by the proteasome. Indeed, in the presence of MG132, the levels of unconjugated ATG5, including full-length and all alternative isoforms, were dramatically increased, along with a laddering of higher molecular weight bands indicative of polyubiquitination.

In summary, while we cannot rule out the possibilities that endogenous *ATG5* splice variants are translationally repressed by uORFs or are targeted by the NMD pathway, these data demonstrate that regardless of expression, all alternative ATG5 isoforms are inherently unstable and are unable to conjugate to ATG12 and form a functional complex. Thus, alternative splicing of *ATG5* is a highly selective mechanism capable of regulating autophagosome formation and autophagy. DU145 PCa cells happen to possess a genetic mutation that completely disables autophagy by irreversibly inducing aberrant *ATG5* splicing.

3.2.6 Binding to ATG16L1 is essential for ATG5 stability and conjugation to ATG12. All but one of the alternative ATG5 isoforms retained the majority of the helix bundle region (HBR) and the Lys-130 site of ATG12 conjugation. Therefore, it was not immediately apparent why these isoforms were targeted by ubiquitin conjugation instead of ATG12 conjugation. All the alternative isoforms had deletions of the N and/or C-termini, which are more likely to affect interaction with ATG16L1, rather than with ATG12, based on the ATG12–ATG5-ATG16L1 crystal structure (Otomo et al., 2013). Since we had previously determined that that unconjugated ATG5 and ATG16L1 could partially protect one another from

proteasomal degradation (Fig. 3.3), we hypothesized that the alternative ATG5 protein isoforms might be susceptible to ubiquitination and proteasomal degradation due to an inability to bind ATG16L1, which consequently prevents ATG12 conjugation.

To test this prediction, we used the ATG12–ATG5-ATG16L1 crystal structure and a yeast Atg5-Atg16L1 peptide affinity study as guides for selecting ATG5 residues that might be involved in ATG16L1 binding (Otomo et al., 2013; Zhao et al., 2013). We then mutated ATG5 N- and C-terminal residues located around the ATG16L1 binding interface by site-directed mutagenesis (Fig. 3.7*A*). Having generated multiple mutants, across all ATG5 domains, that could potentially disrupt its interaction with ATG16L1, we then stably expressed them in DU145 cells. Interestingly, several of the mutants did not conjugate to ATG12 and did not rescue ATG12 or ATG16L1 levels. These mutants were only detectable in unconjugated and polyubiquitin-conjugated forms after MG132 treatment, which indicated that they were ubiquitinated and degraded instead of conjugated to ATG12 (Fig. 3.7*A*).

These results confirmed that specific disruption of the ATG5-ATG16L1 interaction leads to the proteasomal turnover of both ATG5 and ATG16L1, thereby preventing its conjugation to ATG12, which is also subsequently degraded. Notably, the most effective mutations to the ATG12–ATG5-ATG16L1 complex mapped to the critical ATG16L1 binding interface at the boundary of the α1-helix and the two UFD domains, comprising both the N and the C-termini (Fig.

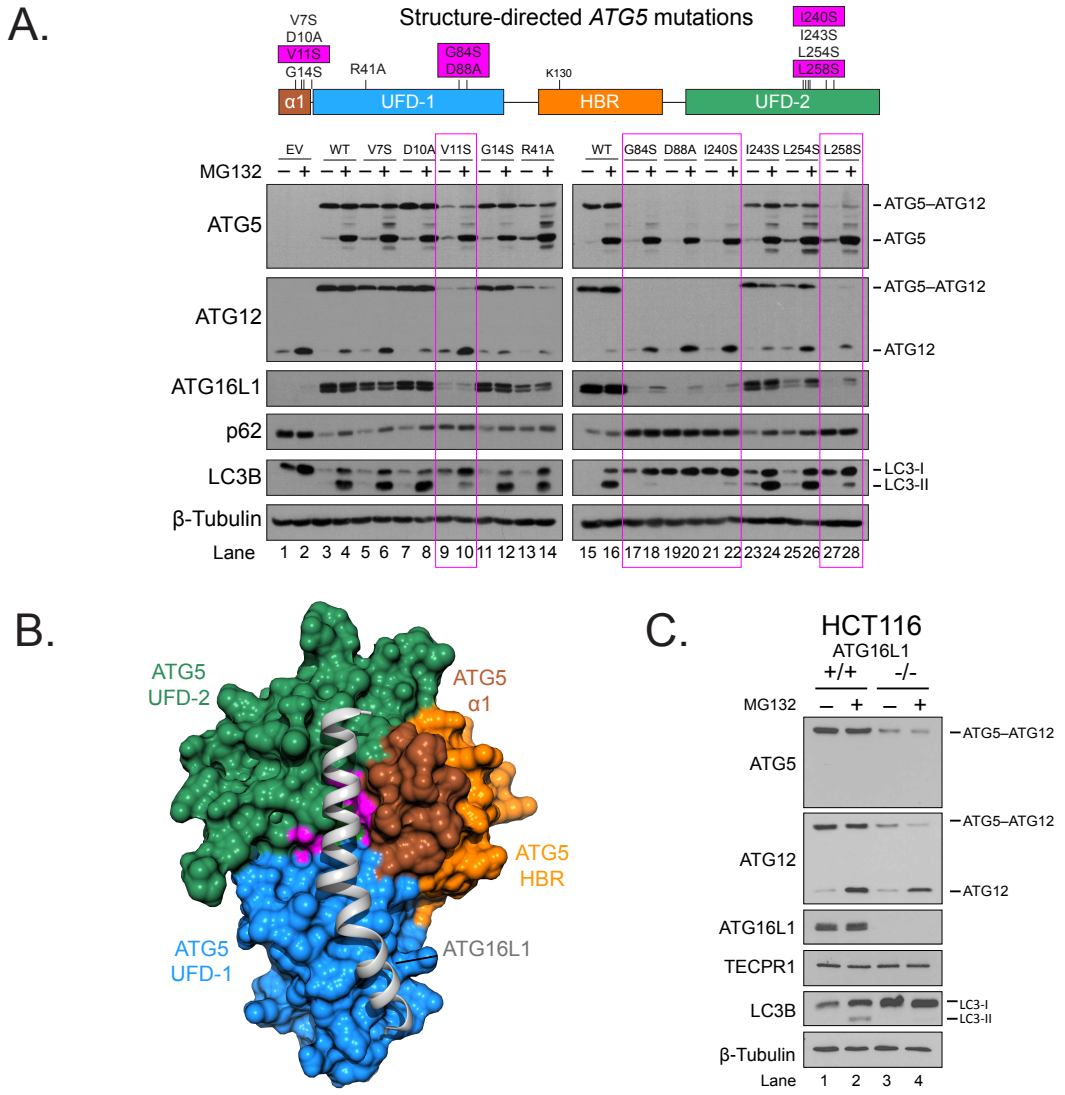

Figure 3.7 – ATG16L1 binding is essential for ATG5 stability and conjugation to ATG12. (*A*) Based on the crystal structure of the ATG12–ATG5-ATG16L1 complex, N and C-terminal ATG5 residues along the ATG16L1 binding interface were altered by site-directed mutagenesis. The diagram shows the location of the mutations within the domain structure of ATG5. DU145 PCa cells, stably expressing an empty vector (EV), wild-type (WT) ATG5 or mutant ATG5, were treated with DMSO or MG132. Lysates were prepared and immunoblotted for ATG proteins. Mutations that dramatically disrupted ATG12 conjugation are highlighted in magenta. (*B*) Surface rendering of the ATG12–ATG5 in complex with an N-terminal fragment of ATG16L1. ATG5 domain colors correspond to the illustration in (*A*). ATG16L1 N-terminal fragment (grey) is rendered as a ribbon to allow visualization of the critical residues at the ATG5-ATG16L1 binding interface (magenta). ATG12 is conjugated on the other side of ATG5, opposite the ATG16L1 interface, and is therefore not visible. (*C*) *ATG16L1*$^{+/+}$ and *ATG16L1*$^{-/-}$ HCT116 colorectal cancer cells lines were treated with DMSO or MG132. Lysates were prepared and immunoblotted for autophagy-related proteins.

3.7*B*). This explains why the ATG5 alternative isoforms, containing either N or C-terminal deletions, fail to conjugate to ATG12, as they are unable to form the requisite interaction with ATG16L1 and instead rapidly undergo ubiquitination and proteasomal degradation.

To confirm ATG12 conjugation was ATG16L1-dependent, we obtained *ATG16L1*-deficient HCT116 colorectal cancer cells and tested them for ATG12 conjugation. ATG12–ATG5 conjugate levels were reduced compared to wild-type cells, indicating that the ATG12 conjugation reaction is impaired in the absence of ATG16L1 (Fig. 3.7*C*). However, ATG12 conjugation in the ATG16L1-deficient cells was not completely abolished and still resulted in detectable levels of ATG12–ATG5 conjugate. Despite the presence of detectable ATG12–ATG5 conjugate, LC3-lipid conjugation was still inactive in ATG16L1-/- (Fig. 3.7C, lanes 2 and 4). This finding suggested that ATG16L1 is essential for the catalyzing LC3 conjugation to PE, but is not absolutely essential for ATG12 conjugation to ATG5.

ATG5 can interact with ATG16L2 and TECPR1, both of which bind ATG5 in the same region as ATG16L1 and form distinct complexes with ATG12–ATG5 (Kim et al., 2015). Despite the interactions with ATG12–ATG5, neither protein is involved catalyzing the LC3 lipid conjugation (Ishibashi et al., 2011; Ogawa et al., 2011; Chen et al., 2012). Therefore, at least in this cell type, it suggests ATG16L1 is the dominant factor in stabilizing ATG5 and mediating ATG12 conjugation, although there is likely some level of compensation by ATG16L2

and/or TECPR1. The ATG5 mutations likely disrupt interaction with all three proteins and, thus, have a more profound effect on ATG12 conjugation than simply knocking out ATG16L1 alone.

3.2.7 ULK1 complex components are coordinately regulated with the ATG12–ATG5-ATG16L1 complex in different cell types. We have characterized, in depth, how subunits in the ATG12–ATG5-ATG16L1 complex are dependent upon one another for stability. Interestingly, recent findings in MEFs indicate that FIP200 interacts directly with ATG16L1 and that the levels of ULK1 complex components are also reduced in *Atg5*$^{-/-}$ and *Atg16*$^{\Delta/\Delta}$ cells (Nishimura et al., 2013). This suggests that assembly of the ATG12–ATG5-ATG16L1 complex might also affect other protein complexes including the ULK1 complex.

We therefore examined the expression levels of both the ATG12–ATG5-ATG16L1 complex as well as the ULK1 complex in previously untested wild-type and knockout *Atg7* and *Atg3* MEFs. ATG3 is the E2-like enzyme responsible for LC3 conjugation. We compared those MEFs to the previously reported *Atg5*$^{+/+}$, *Atg5*$^{-/-}$ *Atg16L1*$^{+/+}$ and *Atg16*$^{\Delta/\Delta}$ MEFs (Nishimura et al., 2013) (Fig. 3.8*A*). As reported by Nishimura et al., we confirmed that ULK1, ATG13 and FIP200 levels are all reduced in *Atg5*$^{-/-}$ and *Atg16*$^{\Delta/\Delta}$ MEFs compared to their corresponding wild-type controls. We also determined that *Atg7*$^{-/-}$ MEFs also had reduced ULK1 complex levels, suggesting that ULK1 complex formation or stability is dependent

upon the fully assembled ATG12–ATG5-ATG16L1 complex. The reduced levels of ULK1 complex subunits directly correlates with the loss of ATG16L1, which given its known interaction with FIP200, might mean it functions to stabilize the ULK1 complex.

Surprisingly, *Atg3*$^{-/-}$ MEFs also had reduced levels of both the ATG12–ATG5-ATG16L1 complex and the ULK1 complex when compared to wild-type *Atg3*$^{+/+}$ MEFs (Fig. 3.8*A*, lanes 3 and 4). While ATG12 conjugation did occur in these cells, the levels of the ATG12–ATG5 conjugate were reduced and this corresponded to a significant reduction in the level of ATG16L1. This was a very unexpected result as ATG3 is thought to act downstream of the ULK1 complex and ATG12 conjugation. ATG3 is known to interact with ATG12 (Noda et al., 2013; Otomo et al., 2013; Sakoh-Nakatogawa et al., 2013); however, there is no obvious explanation for why the loss of an E2-like enzyme would affect the stability of two distinct upstream protein complexes (Fig. 1.5, p.29).

To confirm the coordinated regulation between the ATG12–ATG5-ATG16L1 and ULK1 complexes, we examined the levels of ULK1 complex components in *Atg5*$^{-/-}$ MEFs in which murine *ATG5* (mATG5) was stably re-expressed. As expected, ATG5 rescued formation of the functional ATG12–ATG5-ATG16L1 complex, as determined by the levels of ATG16L1, the ATG12-ATG5 conjugate, LC3-II and p62 (Fig. 3.8*B*). Similar to earlier findings, TECPR1 levels remained unaffected by ATG5 expression; however, mATG5 expression did increase the levels of ULK1, ATG13 and FIP200 (Fig. 3.8*B*). To test if

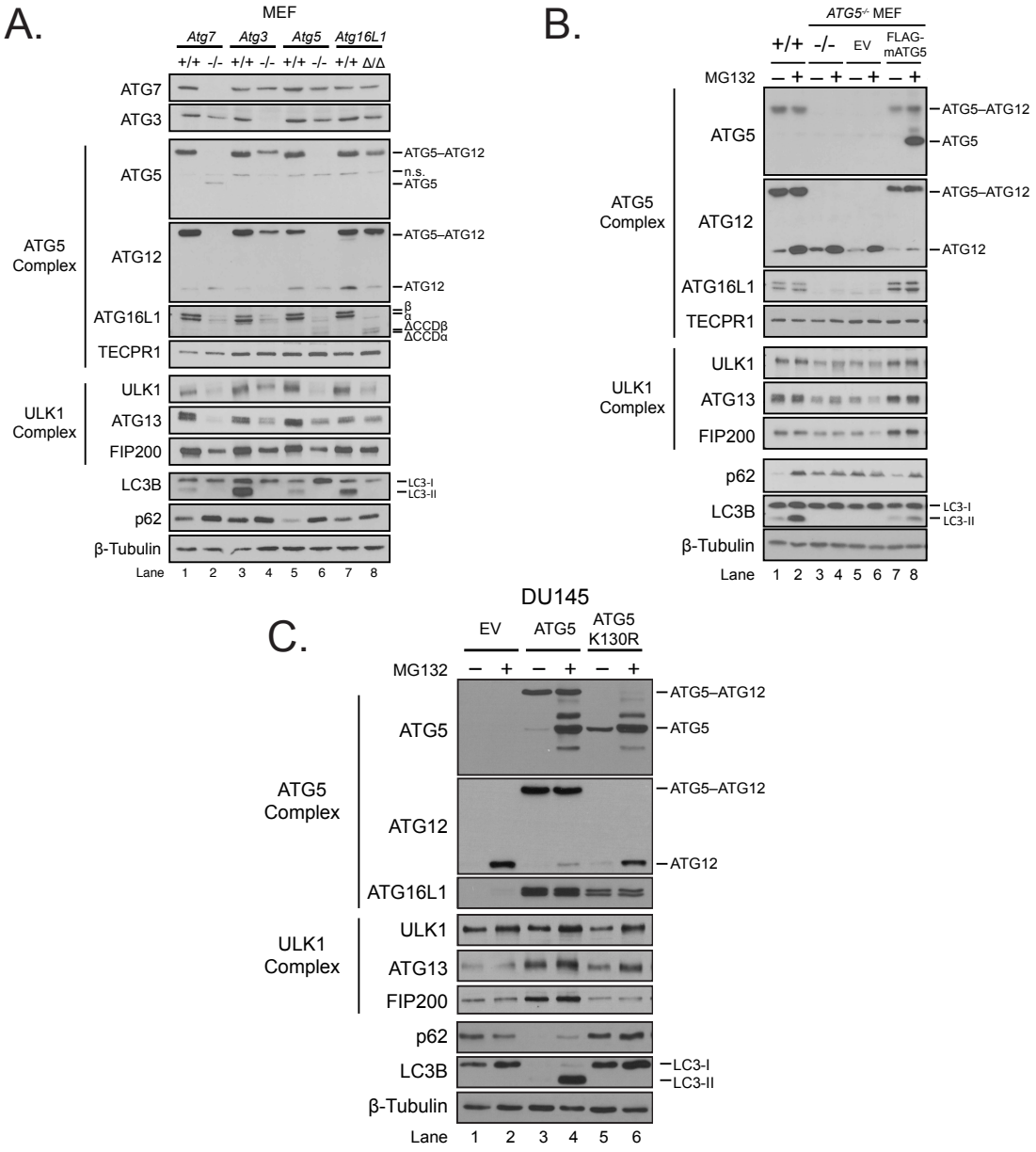

Figure 3.8 – ULK1 complex components are coordinately regulated with the ATG12–ATG5-ATG16L1 complex in different cell types. (*A*) Lysates were prepared from *Atg7*, *Atg3*, or *Atg5* wild type ($^{+/+}$) and knockout ($^{-/-}$) MEFs, in addition to *Atg16L1*$^{+/+}$ and *Atg16L1*$^{\Delta/\Delta}$ MEFs, which lack the coiled-coil domain. Lysates were prepared and immunoblotted for ATG proteins. (*B*) *Atg5*$^{+/+}$ wild type and *Atg5*$^{-/-}$ MEFs, stably expressing an empty vector (EV) or FLAG-tagged murine ATG5 (FLAG-mATG5), were treated with DMSO or MG132. Lysates were prepared and analyzed by immunoblotting for ATG proteins. (*C*) DU145 PCa cells, stably expressing an empty vector (EV), wild-type ATG5 or ATG5 (K130R), were treated with DMSO or MG132. Cell lysates were then prepared and immunoblotted for ATG proteins.

expression of ATG5 protected the ULK1 complex subunits from proteasomal degradation, we treated the cells with MG132. Unexpectedly, this did not result in obvious accumulation of any of the ULK1 complex components. Nishimura et al. reported that mRNA levels of ULK1 complex components are unaffected by ATG5 expression, indicating ULK1 complex downregulation is unlikely to be caused by transcriptional suppression (Nishimura et al., 2013). Therefore it's possible that either the expression rate for these proteins is too low to affect accumulation within 8 h of proteasome inhibition or there is a proteasome-independent mechanism for ULK1 complex regulation.

Having observed a dramatic loss in ULK1 complex subunits in the absence of the ATG12–ATG5-ATG16L1 complex in MEFs, we wondered if the effect was cell-type specific since previously we did not observe drastically different levels of ULK1 complex subunits in DU145 cells when compared to other PCa cells (Fig. 3.1D). To verify that the coordinated regulation between the ULK1 and ATG12–ATG5-ATG16L1 complexes occurs in other cell types, we examined DU145 PCa cells stably expressing ATG5 (Fig. 3.8*C*). ATG5 expression increased the levels of ATG13 and FIP200, although it did not significantly affect ULK1 levels. Therefore, there is clearly a significant level of crosstalk between these two complexes; however, there are also cell type differences with regards to the stability of ATG12-ATG5-ATG16L1 and ULK1 complex components in MEFs and DU145 cells. The ULK1 complex is thought to be involved in recruitment of the ATG12–ATG5-ATG16L1 complex to the

isolation membrane (Nishimura et al., 2013), although its unclear how this might relate to the stabilities of each complex.

3.3 Discussion

Our initial observation that DU145 PCa cells did not undergo LC3 lipidation led to our discovery that a splice donor-site mutation results in aberrant splicing of *ATG5* and the inactivation of autophagy. To our knowledge, this is the first mutation identified in a cancer cell line or tumor sample that has been proven to completely inactivate autophagy. Having made this discovery, an obvious question is whether *ATG5* genetic mutations occur in primary human tumor samples and inactivate autophagy through similar mechanisms. This question will be addressed in the next chapter.

We also determined that the DU145 splice donor-site mutation irreversibly activated a highly specific mechanism for toggling autophagy on and off through alternative splicing of *ATG5*. *ATG5* is an immensely important gene for regulating autophagy and there are no other genes that functionally compensate for it (Feng et al., 2014). Its inactivation also leads to the coordinated downregulation of numerous other autophagy-related proteins including ATG12, ATG16L1 and ULK1 complex proteins. Since autophagy appears to function both as a tumor suppressor and a tumor promoter depending on the stage and context (Galluzzi et al., 2015), *ATG5* splicing may serve as an important,

reversible modulator of autophagy during tumorigenesis and progression. It is imperative that we further investigate how *ATG5* splicing is regulated and determine if tumor cells are capable of switching autophagy on and off at different stages of tumorigenesis via *ATG5* splicing. If certain kinases control *ATG5* splicing, they would make intriguing therapeutic targets that could selectively activate or inactivate autophagy to enhance the efficacy of chemotherapy. In a similar vein, we have successfully characterized the binding region most critical for ATG5-ATG16L1 interaction, *in vivo*, which could be used to develop small molecule or peptides inhibitors that disrupt this interaction and inhibit autophagy with high selectivity, which currently available inhibitors do not provide.

Our findings in DU145 cells reveal that they are an excellent tool for investigating the, as yet, undefined mechanisms that regulate ATG12–ATG5-ATG16L1 complex formation. Proteasomal degradation of ATG16L1 and ATG12 has been previously reported (Fujita et al., 2009; Haller et al., 2014), but not, to our knowledge, for ATG5. Additionally, we are the first group to clearly describe the coordinated and rapid ubiquitination and proteasomal degradation of ATG12–ATG5-ATG16L1 complex subunits, as well as the importance of the ATG5-ATG16L1 interaction for facilitating ATG12 conjugation.

These novel findings introduce many new intriguing questions regarding the assembly and regulation of the ATG12-ATG5-ATG16L1 complex. Given that rapid ubiquitination and degradation essentially eliminates all free, unbound

forms of ATG5, ATG12 and ATG16L1 and that ATG16L2 and TECPR1 also compete for available ATG5, it is rather incredible that functional ATG12–ATG5-ATG16L1 complexes are formed in the cell at all. There may well be unidentified factors that prevent proteasomal degradation and mediate assembly of the complex. Regardless, once formed, the complex appears to be very stable, suggesting that its formation and/or disassembly is unlikely to occur in rapid response to an autophagy stimulus. Thus, it seems more likely that a pool of ATG12–ATG5-ATG16L1 complex is maintained in the cell where its activity, rather than its formation, is specifically modulated in response to an autophagy stimulus, perhaps through interaction with WIPI2 or the ULK1 complex.

The extensive degradation of free, unbound ATG5, ATG12 and ATG16L1 may indicate that having substantial levels of these subunits may be deleterious to the cell. ATG12 has been reported to function in mitochondrial homeostasis and apoptosis, independently of ATG5 (Radoshevich et al., 2010; Haller et al., 2014). Thus, other non-autophagic functions for free ATG12, ATG5 or ATG16L1 may be normally repressed by rapid proteasomal turnover. The same might be true for ULK1 complex subunits, given that it is also downregulated in response to loss of the ATG12–ATG5-ATG16L1 complex. FIP200, also known as RB1CC1, interacts with a variety of non-autophagy-related proteins and functions as a signaling node for many different signaling pathways (Gan and Guan, 2008). Thus, our ability to regulate formation of the ATG12–ATG5-ATG16L1 complex

should allow us to isolate unique and novel functions of ATG12-ATG5-ATG16L1 and ULK1 complex subunits.

Chapter 4: Downregulation of *ATG5* in Prostate Cancer

4.1 Introduction

Advances in next-generation sequencing (NGS) have revolutionized the fields of clinical diagnostics and cancer biology by revealing recurrent genetic alterations that can be used to guide personalized treatment of cancer patients. While, historically, cancers were thought to be driven by the accumulation of single mutations over time, it is increasingly clear that large-scale chromosomal alterations are not only frequent, but are important drivers of tumor progression, particularly for prostate cancer (PCa) (Williams et al., 2014). The discovery of the transmembrane protease, serine 2 – E twenty-six transcription factor family (TMPRSS2–ETS) gene fusions in PCa, which occur in roughly 50% of advanced prostate tumors, made it the first solid cancer found to have recurring large-scale chromosomal rearrangements (Tomlins et al., 2005). Recently, complex chromosomal rearrangement events, known as chromoplexy, were shown to frequently occur in PCa and are thought to drive genetic alterations, prostate tumor evolution and progression. This process involves coordinated structural rearrangements across multiple chromosomes, which can create oncogenic gene fusions and disrupt numerous tumor suppressor genes in one single rearrangement event (Baca et al., 2013).

Copy number analysis, using comparative genomic hybridization (CGH), has identified frequently occurring chromosomal alterations in tumors affecting loci containing genes traditionally implicated in PCa, such as 8q [v-myc avian myelocytomatosis viral oncogene homolog (*MYC*)], 10q [phosphatase and tensin homolog (*PTEN*)], 12p [cyclin-dependent kinase inhibitor 1B (*CDKN1B/p27*)], 13q [retinoblastoma 1 (*RB1*)] and 17q (*TP53*), in addition to several other regions with no well-established driver gene (Taylor et al., 2010). Still, the clinical relevance of many of these structural alterations is unknown. The total copy number alteration burden was recently shown to predict the likelihood of biochemical relapse of intermediate-risk Gleason 7 grade tumors (Hieronymus et al., 2014). Distinguishing indolent from highly aggressive clones within this intermediate risk tumor population is critical for mitigating overtreatment of prostate cancers that would normally pose little risk to patient quality of life for many years.

Interestingly, deletions of chromosomal locus 6q21, which contains *ATG5*, occurs in 47% of total PCa samples and 74% of advanced PCa cancers, making it one of the most frequently altered regions in PCa (Williams et al., 2014). Additionally, a subtype of PCa defined by mutations in speckle-type POZ protein (*SPOP*), was found to be almost exclusively enriched for deletions of 6q21 loci (Barbieri et al., 2012). Despite this, *ATG5* has been completely overlooked as a putative prostate tumor suppressor gene and the role of autophagy in PCa is unknown.

The earliest genetic evidence implicating autophagy in tumorigenesis came from a pair of studies that concluded Beclin 1 was a haploinsufficient tumor suppressor based on the finding that *Becn1*$^{+/-}$ mice spontaneously developed lymphomas, lung and liver cancers with high frequency (Qu et al., 2003; Yue et al., 2003). However, Beclin 1 has since been shown to prevent the ubiquitination and proteasomal degradation of the tumor suppressor, p53, while also promoting proteasomal degradation of the anti-apoptotic Bcl-2 family member, Mcl-1 (Liu et al., 2011; Elgendy et al., 2014). Loss of either of these functions could contribute to tumorigenesis in *Becn1*$^{+/-}$ mice, raising doubts as to whether the Beclin 1 tumor suppressive function is actually dependent upon its role in autophagy.

Other autophagy-specific mouse models, including the mosaic deletion of *Atg5* or liver-specific deletion of *Atg7*, also result in the spontaneous development of liver tumors, although the tumors remain benign and do not progress to malignancy (Takamura et al., 2011). This was the first indication that autophagy may play opposing roles in tumor initiation and progression. Knockout of *Atg5* or *Atg7* in established mouse models of cancer, including *BRAF*^{V600E} and *KRAS*^{G12D}-driven lung cancer models, increased tumor initiation while also increasing overall mouse survival by suppressing tumor progression (Strohecker et al., 2013; Rao et al., 2014). Similar results were observed in *KRAS*^{G12D}-driven pancreatic cancer models (Rosenfeldt et al., 2013; Yang et al., 2014). The current hypothesis, based on these data, is that autophagy

suppresses tumor initiation, while also playing an essential role in tumor progression after a tumor is established.

The seemingly opposing roles of autophagy in tumorigenesis and progression are thought to be due to the different functions of homeostatic and stress-induced autophagy. Autophagy is known to maintain homeostasis by eliminating damaged mitochondria and other deleterious elements that generate ROS and can damage DNA or promote inflammation. Thus, autophagy suppresses conditions known to promote cellular transformation and tumor initiation (Sabharwal and Schumacker, 2014). On the other hand, autophagy can be induced in tumor cells as a survival response to stressors found in the tumor microenvironment, during invasion and metastasis or even during tumor therapy (Galluzzi et al., 2015). This potential aspect has made autophagy a therapeutic target of great interest.

However, the role of autophagy in tumor progression appears to be highly context-specific. In the mouse *KRAS*^{G12D}-driven pancreatic cancer model, the tumor suppressive effect of *Atg5* or *Atg7* deletion was completely reversed and actually promoted tumor progression when *Trp53* was also deleted (Rosenfeldt et al., 2013). Additionally, this current model is not extensively supported by human cancer data. *BECN1* is reportedly monoallelically deleted in numerous malignancies, including breast and ovarian cancer; however, recent analysis shows this is likely due to its proximity to the well-established tumor suppressor gene, breast cancer 1, early onset (*BRCA1*), at chromosome locus 17q21

(Laddha et al., 2014). Another study indicates that *ATG5* is downregulated in human melanoma samples, which was shown to prevent oncogene-induced senescence in cultured melanocytes (Liu et al., 2013a). Thus, while numerous mouse models have implicated autophagy as a suppressor of tumor initiation and a promoter of tumor progression, this may only be true in specific tissues or in specific genetic backgrounds.

In this study, we have characterized the effects of somatic *ATG5* mutations identified in many human cancer cell types and the mechanisms for how they inactivate *ATG5* gene function. We have also determined that the frequent genetic deletions of 6q21 found in prostate tumors coincide with a specific decrease in *ATG5* mRNA expression that does not occur for neighboring genes. In fact, we have discovered *ATG5* is more significantly downregulated than many well-established PCa tumor suppressor genes, such as *PTEN* and *RB1*. Additionally, *ATG5* mRNA is further downregulated in PCa metastases compared to primary tumors, which implicates *ATG5* as a tumor suppressor even at later, more advanced stages of PCa. We confirmed a tumor suppressive function for *ATG5* in a PCa xenograft model in which rescue of *ATG5* in *ATG5*-deficient DU145 PCa cells significantly reduced the rate of tumor growth. Together, these data indicate that *ATG5* is inactivated in human tumors and strongly suggests it is a tumor suppressor at both early and late stages of prostate tumorigenesis.

4.2 Results

4.2.1 Human tumor samples contain *ATG5* splice region mutations that may cause exon skipping and result in the proteasomal degradation of ATG5, ATG12 and ATG16L1.

Having identified the splice donor site mutation (c.573+1G>A) that inactivates autophagy in DU145 PCa cells, we used publically available catalogs of genetic information collected from human tumor samples to determine if similar *ATG5* splice-site mutations have been identified in other tumors. We compiled a list of all somatic *ATG5* splice-region and nonsynonymous coding sequence mutations from: the Catalogue of Somatic Mutations in Cancer (COSMIC: http://cancer.sanger.ac.uk/cosmic), the cBioPortal for Cancer Genomics (http://www.cbioportal.org) and the International Cancer Genome Consortium (ICGC: https://icgc.org) (Table 4.1). These databases compile sequencing information originally from the Cancer Genome Atlas (TCGA: https://tcga-data.nci.nih.gov/tcga/), ICGC and other publically available tumor sequencing datasets. As of this writing, five *ATG5* splice-region mutations have been identified, in addition to the c.573+1G>A mutation in intron 6 that we identified in DU145 PCa cells.

One of the splice region mutations (c.236+1G>C), found in a hepatic tumor sample (Kan et al., 2013), occurs in the consensus splice donor site at the 5′ end of intron 3 (Table 4.1). This mutation is analogous to the c.573+1G>C mutation within intron 6 that results in skipping of exon 6 and the inactivation of

Table 4.1 – Somatic *ATG5* splice region and nonsynonymous coding sequence mutations identified in human tumor samples.

Mutation Type	Mutation (CDS)	Predicted Amino Acid Alteration	Tumor type	Sequencing Source	Tumor Sample Count	Functional Classification
Splice Region						
	c.109-3C>G	p.?	Hepatic	ICGC - Japan	1	*
	c.236+1G>C	p.M1_W79del	Hepatic	Kan et al., *Genome Research,* 2013	1	Amorph*
	c.237-3delT	p.?	Colorectal	TCGA	1	*
	c.573+1G>A	p.R161Nfs*2	Prostate metastasis (DU145 cell line)	Current publication	1	Amorph
	c.573+8A>G	p.?	Hepatic	ICGC - Japan	1	*
	c.691+9A>G	p.?	Hepatic	ICGC - Japan	1	*
Nonsense						
	c.25C>T	p.R9*; p.M1_V59del	Brain	TCGA	2	Amorph
	c.43C>T	p.R15*; p.M1_V59del	Prostate & Brain	TCGA	2	Amorph
	c.157A>T	p.K53*	Hepatic	TCGA	1	Amporh*
	c.169C>T	p.Q57*	Squamous cell carcinoma	Pickering et al., *Clin Cancer Res*, 2014	1	Amorph*
	c.430G>T	p.E144*	Colorectal	TCGA	1	Amorph
	c.535G>T	p.E179*	Colorectal	Seshagiri et al., *Nature*, 2012	1	Amorph
Deletion						
	c.28_31delGATG	p.M1_V11del	Hepatic	ICGC - Japan	1	Amorph
	c.36_38delGTT	p.W12_F13delinsC	Hepatic	ICGC - Japan	1	Amorph
	c.704delA	p.K235Rfs*4	Gastric & colorectal	TCGA & Kang et al., *J. Pathology*, 2009	4	Amorph
Missense						
	c.16G>T	p.D6Y	Colorectal	TCGA	1	
	c.172A>G	p.K58E	Colorectal	TCGA	1	
	c.173A>G	p.K58R	Colorectal	TCGA	5	
	c.173A>T	p.K58M	Colorectal	Sjöblom et al., *Science*, 2006	1	
	c.197G>A	p.S66N	Uterine	TCGA	1	
	c.245C>T	p.P82L	Melenoma	TCGA	1	Hypomorph
	c.272C>T	p.A91V	Hepatic	ICGC - Japan	1	*
	c.286C>G	p.L96V	Breast	TCGA	1	
	c.315G>T	p.K105N	Uterine	TCGA	1	
	c.317G>T	p.S106I	Uterine	TCGA	1	
	c.334C>T	p.L112F	Hepatic	An et al., *Pathol Res Pract*, 2011	1	
	c.346_347CC>TT	p.P116L	Squamous cell carcinoma	Pickering et al., *Clin Cancer Res*, 2014	1	*
	c.397G>A	p.D133N	Cervical	TCGA	1	*
	c.449A>G	p.H150R	Colorectal (HCT15 cell line)	Mouradov et al., *Cancer Res*, 2014	1	*
	c.462G>T	p.W154C	Thyroid	ICGC - Saudi Arabia	1	
	c.463A>G	p.M155V	Brain	TCGA	1	
	c.547C>T	p.R183C	Melanoma	TCGA	1	
	c.556C>T	p.P186S	Melanoma	TCGA	1	Hypomorph
	c.577A>T	p.T193S	Breast	TCGA	1	
	c.580A>T	p.T194S	Breast	TCGA	1	
	c.611G>A	p.R204H	Gastric & colorectal (SW48 cell line)	Wang et al., *Nature Genetics*, 2014; Mouradov et al., Cancer Res, 2014	2	*
	c.622G>A	p.A208T	Uterine	TCGA	1	
	c.674C>T	p.S225F	Bladder	TCGA	1	
	c.688G>A	p.E230K	Colorectal	TCGA	1	
	c.705G>T	p.K235N	Colorectal (HCC_2998 cell line)	NCI-60	1	
	c.721C>T	p.H241Y	Gastric	An et al., *Pathol Res Pract*, 2011	1	Amorph
	c.724G>A	p.G242R	Pancreatic	ICGC - Australia	1	Amorph
	c.770A>G	p.H257R	Hepatic	TCGA	1	*
	c.775A>C	p.S259R	Hepatic	TCGA	1	*
	c.782C>T	p.P261L	Gastric	TCGA	1	Hypomorph
	c.793C>A	p.L265I	Colorectal	TCGA	1	Hypomorph
						not tested*

ATG5 in DU145 PCa cells. Although we have not directly tested the effects of the c.236+1G>C mutation, given its location at the splice donor site of intron 3, it may result in a similar skipping of exon 3. While this could result in NMD or another form of translational repression, we have already confirmed that the N-terminally deleted form of ATG5 predicted to result from the removal of exon 3 does not interact with ATG16L1 and is rapidly ubiquitinated and degraded (Fig. 3.6, p.76). Since any alteration of splicing would disrupt either the N or C-terminus of ATG5 and would cause the complete proteasomal degradation of ATG5, ATG12 and ATG16L1, we therefore predict that this mutation is likely a null or amorphic mutation.

Another *ATG5* splice region mutation was identified in a colorectal tumor sample sequenced by TCGA, while the remaining splice-region mutations were identified in hepatic tumors sequenced by the ICGC in Japan (Table 4.1). However, unlike c.236+1G>C or c.573+1>C mutations, these mutations do not occur directly in the nearly invariable consensus splice donor or acceptor sites, which are limited to the two nucleotides at the 5′ and 3′ ends of each intron, respectively (Patel and Steitz, 2003). However, two of them (c.109-3C>G and c.237-3delT) do occur at conserved splice acceptor regions, which can cover as many as 25 nucleotides at the 3′ end of introns (Caminsky et al., 2014). Without direct experimental evidence, it is difficult to conclusively determine whether these splice-region mutations affect *ATG5* splicing. If they do disrupt splicing, this would cause either N or C-terminal deletions of ATG5, which we have shown

can prevent stabilization by ATG16L1 and lead to complete proteasomal turnover of ATG5, ATG12 and ATG16L1 (Fig. 3.6, p.76). So while we have not directly tested the effects of these splice region mutations on *ATG5* splicing, any mutation that does inactivate an *ATG5* splice donor or acceptor site would completely disrupt *ATG5* gene function and autophagy.

4.2.2 All cancer-associated *ATG5* nonsense and deletion mutations result in proteasomal degradation of ATG5, ATG12 and ATG16L1 and the inactivation of autophagy. A number of *ATG5* nonsense and deletion mutations have been identified across diverse tumor types, including prostate cancer. The two most 5′ nonsense mutations, c.25C>T and c.43C>T, are predicted to introduce small uORFs that may still allow translation initiation to occur at a nearby downstream methionine, which would result in an N-terminally deleted version of ATG5 (p.M1_V59del). The remaining nonsense mutations are predicted to result in C-terminal truncations of varying lengths (Table 4.1 and Fig. 4.1*A*).

Two deletion mutations were identified in hepatic tumors by the ICGC in Japan. The c.28_31delGATG mutation introduces a novel translation initiation site predicted to encode for an ATG5 protein containing a small N-terminal deletion of 10 amino acids (p.M1_V11del). The c.26_28delGTT mutation is predicted to cause a small insertion/deletion in which Trp-12 and Phe-13 are replaced with a cysteine (p.W12_F13delinsC). Finally, the c.704delA mutation is

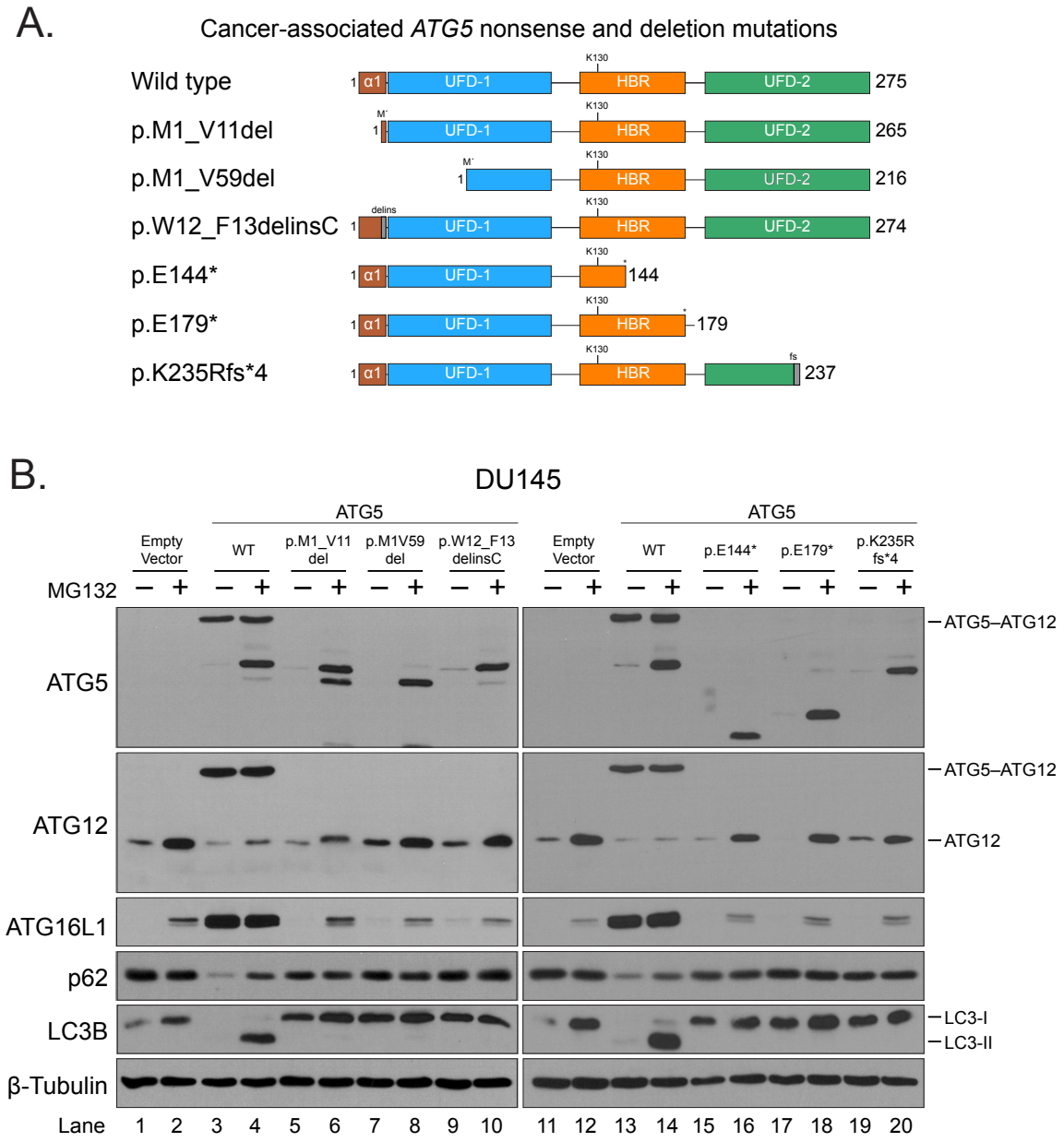

Figure 4.1 – All *ATG5* nonsense and deletion mutations identified in human tumor samples are amporphic mutations. (*A*) Diagram of *ATG5* nonsense and deletion mutations identified in human tumor samples. p.M1_V11del and p.M1_V59del are N-terminal deletions predicted to result from alternative translation initiation, which cirumvents the 5´ nonsense mutations that introduce short uORFs. (*B*) DU145 PCa cells, stably expressing an empty vector (EV), wild-type (WT) ATG5 or various mutant ATG5s, were treated with DMSO or MG132. Lysates were prepared and immunoblotted for ATG proteins.

predicted to introduce a frameshift and premature stop codon leading to C-terminal truncation of ATG5 (p.K235Rfs*4) (Table 4.1 and Fig.4.1*A*). This mutation is notable because it has been identified in four gastric and colorectal tumor samples (Kang et al., 2009)(Table 4.1). It occurs at a site containing seven consecutive adenine nucleotides, which suggests the deletion may be a result of microsatellite instability (MSI) (Kang et al., 2009).

We have previously shown that removal of either the N or C-terminus from ATG5 by alternative splicing prevented its interaction with and stabilization by ATG16L1. This resulted in proteasomal turnover of ATG5 and prevented conjugation to ATG12 (Fig. 3.6, p.76). However, many of these nonsense and deletion mutations affect very small portions of the N or C-terminus, so it was unclear if these small deletions were sufficient to impact the ATG16L1 interaction (Fig. 4.1*A*). To experimentally test the effects of these mutations we stably expressed the predicted ATG5 proteins encoded by each mutation in DU145 PCa cells and examined their abilities to conjugate to ATG12 and form a functional ATG12–ATG5-ATG16L1 complex (Fig. 4.1*B*). Strikingly, every nonsense and deletion mutant failed to conjugate with ATG12 and was completely degraded by the proteasome, as determined by rescue with MG132. Even p.W12_F13delinsC, which affects only two residues within the N-terminal α1-helix domain, was rapidly degraded Turnover of the ATG5 mutants coincided with the proteasomal degradation of ATG12 and ATG16L1 and the complete

inactivation of autophagy as determined LC3 lipid-conjugation and p62 degradation (Fig. 4.1*B*).

These data confirm that all of the cancer-derived *ATG5* nonsense and deletion mutations identified to date, are amorphic or null mutations (Table 4.1). Moreover, we have convincingly shown that fully intact ATG5 N and C-termini are absolutely essential for conjugation to ATG12. Even very small perturbations in these regions disrupt the stabilizing interaction with ATG16L1 and lead to ubiquitination and complete turnover of the complex subunits.

4.2.3 Several cancer-associated *ATG5* missense mutations disrupt ATG12 conjugation and formation of the ATG12–ATG5-ATG16L1 complex. The majority of *ATG5* mutations identified in various tumor samples are missense mutations (Table 4.1). Generally, at first glance, they do not cluster to specific regions of ATG5 and can be found across all domains, implying that many could be passenger mutations that have no effect on ATG5 function (Fig. 4.2*A*). However, we have previously identified specific residues in the N-terminal α1-helix domain and both UFDs that are essential for ATG5 stability and conjugation to ATG12 (Fig. 3.7, p.80); therefore, it is difficult to predict the effects of many of these mutations with any certainty.

To experimentally test the effects of these *ATG5* missense mutations in cells, we stably expressed each of them, individually, in DU145 cells in order to determine their abilities to form functional ATG12–ATG5-ATG16L1 complexes

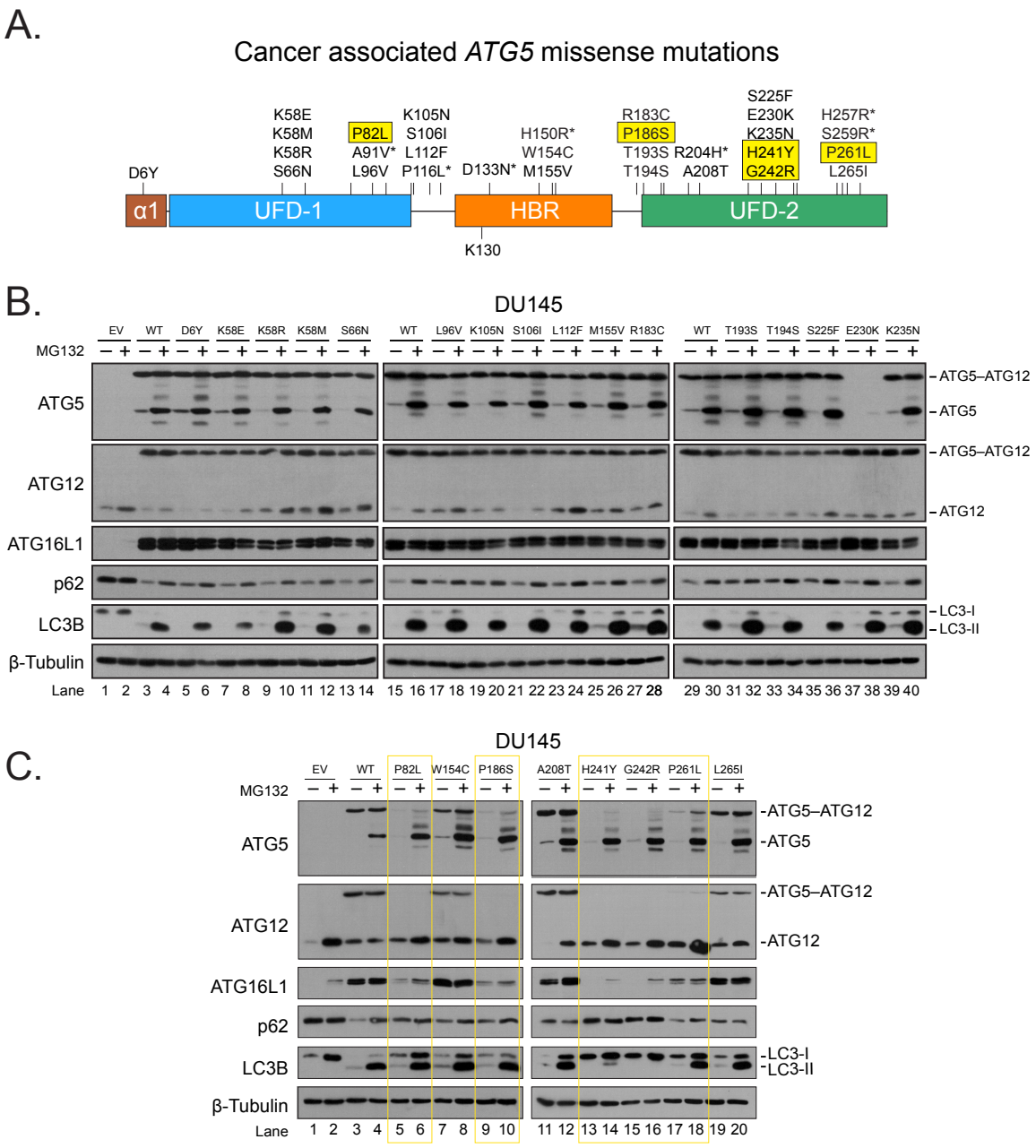

Figure 4.2 – Several *ATG5* missense mutations identified in human tumor samples are amorphic or hypomorphic mutations. (*A*) *ATG5* missense mutations identified in human tumor samples are indicated on the ATG5 domain structure diagram. Highlighted in yellow are those that dramatically reduce or eliminate ATG12 conjugation. (*B* and *C*) DU145 PCa cells expressing an empty vector (EV), wild-type (WT) ATG5 or mutant ATG5 were treated with DMSO or MG132. Lysates were prepared and immunoblotted for ATG proteins. The E230K mutation disrupts ATG5 antibody recognition; however, ATG12 conjugation is still readily detected with the ATG12 antibody.

(Fig. 4.2*B* and 4.2*C*). Many of the missense mutations had no discernable effect on ATG12 conjugation or complex formation (Fig. 4.2*B*). However, several mutations, marked in yellow, dramatically reduced or completely blocked ATG12 conjugation and formation of a functional complex based on p62 degradation and LC3 lipidation (Fig. 4.2*C*). Interestingly, the two mutations that completely disrupted all ATG12–ATG5-ATG16L1 complex activity, as determined by LC3 conjugation, mapped to same region we had previously identified as being critical for ATG16L1 interaction using structure-directed mutations (colored in magenta) (Fig. 4.3*A*). Therefore, its highly likely these mutations disrupt ATG5 interaction with ATG16L1, resulting in ATG5 ubiquitination and turnover, rather than conjugation to ATG12. The remaining three mutations with significant effects on ATG12 conjugation affected proline residues located towards the core of the protein and not directly on the surface within the previously characterized ATG16L1-binding region (Fig. 4.3*A*). Their surprisingly drastic effect on ATG12 conjugation may be due to an induced conformational change that disrupts the sensitive ATG16L1-binding residues at the N or C-terminus. Interestingly, the three proline mutations nearly, but not completely, eliminated ATG12 conjugation, yet following treatment with MG132, they had little impact on LC3 conjugation compared to wild-type ATG5 (Fig. 4.2*C*, lanes 4, 6, 10 and 18). This may indicate very little ATG12–ATG5-ATG16L1 complex is needed to efficiently catalyze LC3 conjugation, which has been observed in other systems (Hosokawa et al., 2006).

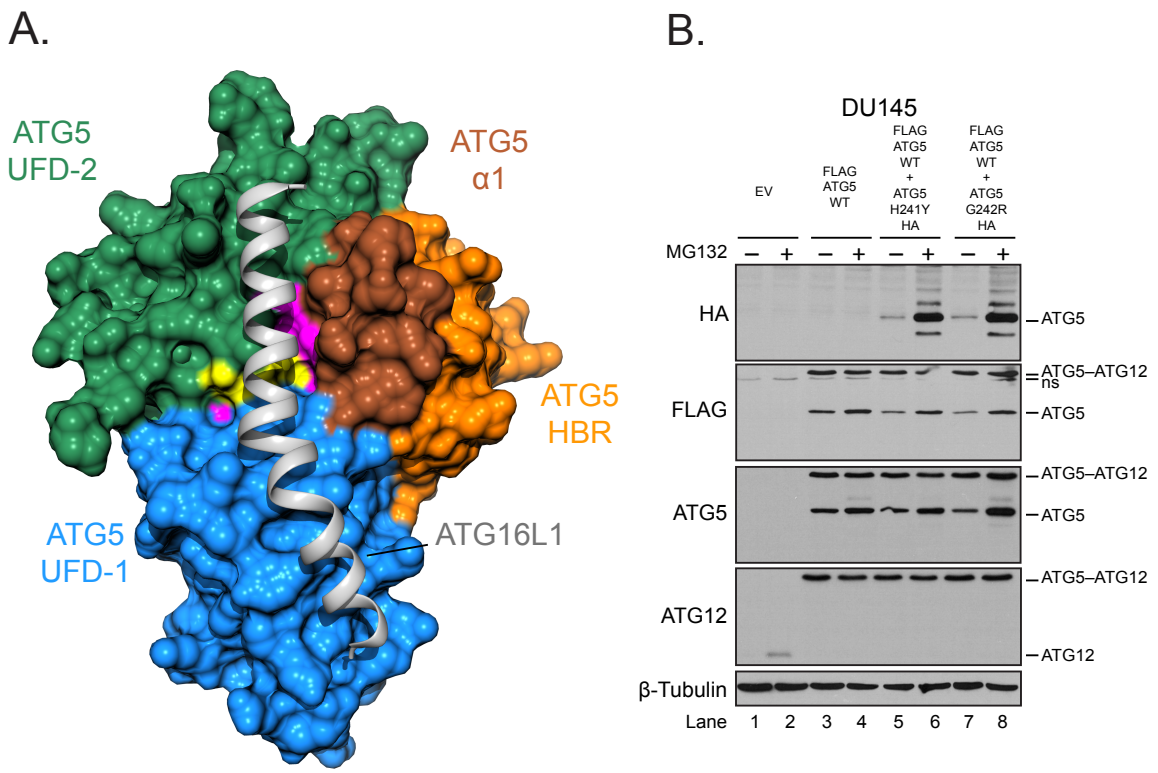

Figure 4.3 – Cancer-associated *ATG5* missense mutations that impact ATG12–ATG5-ATG16L1 complex formation and autophagy map to a distinct region of ATG5, but do not act as dominant negatives. (*A*) Mutated residues that severely compromise ATG12 conjugation are colored in yellow on the surface rendering of the ATG12–ATG5 in complex with an N-terminal fragment of ATG16L1. Cancer-associated *ATG5* mutations map to the same region we have shown to be critical for ATG16L1 binding based on structure-directed mutations (colored in magenta) (Fig. 3.7). (*B*) DU145 cells stably expressing an empty vector (EV), FLAG-tagged wild-type ATG5 (WT) or FLAG-tagged ATG5 (WT) plus either HA-tagged ATG5 (H241Y) or (G242R) were treated with DMSO or MG132. Lysates were prepared and immunoblotted for HA, FLAG, ATG5, ATG12 and β-Tubulin.

To determine if these *ATG5* mutations exhibited any dominant-negative effects, we stably co-expressed FLAG-tagged wild-type (WT) ATG5 with HA-tagged H241Y or G242R mutants to see if expression of either mutant had any effect on wild-type ATG5 or formation of the ATG12–ATG5-ATG16L1 complex (Fig. 4.3*B*). FLAG-tagged wild-type ATG5 readily formed an ATG12–ATG5 conjugate, even in the presence of the HA-tagged mutant versions of ATG5. As before, the HA-tagged ATG5 mutants failed to conjugate with ATG12 and instead were ubiquitinated and degraded by the proteasome (Fig. 4.3*B*). Therefore, we can classify the *ATG5* mutations that disrupt ATG12 conjugation as amorphic or hypomorphic as they do not exhibit any apparent dominant negative functions (Table 4.1).

Together, we have characterized nearly all of the *ATG5* mutations found in human tumors. We have classified many of the mutations as amorphic or hypomorphic due to their disruption of the ATG16L1 interaction, which prevents ATG12 conjugation and results in proteasomal degradation of ATG5, ATG12 and ATG16L1. The ratio of tumors with amorphic and hypomorphic *ATG5* mutations, which impact ATG12–ATG5-ATG16L1 complex formation, compared to those with seemingly innocuous *ATG5* mutations suggests that many of the mutations are, in fact, not simple passenger mutations. Moreover, we cannot rule out the possibility that other *ATG5* mutations may impact functions of ATG5 that are unrelated to autophagy. Thus, genetic mutation may be one mechanism for selectively inactivating *ATG5* tumor suppressive function in human cancers.

4.2.4 The 6q21 chromosomal locus containing *ATG5* is frequently deleted in human PCa. Although the ratio of *ATG5* amorphic and hypomorphic mutations to the those with no obvious effect on ATG12 conjugation suggests that *ATG5* is a tumor suppressor, the relatively low number of overall tumors containing *ATG5* mutations might suggest that *ATG5* is not a particularly important tumor suppressor. However, genetic mutation is only one of several mechanisms for inactivating gene function. Advances in genomic sequencing and techniques, such as CGH, have facilitated high-throughput examination of copy number variation and large chromosomal rearrangements. It is now clear that copy number variation occurs far more frequently than other types of mutations, with as much as 12% of the entire genome affected (Redon et al., 2006).

We used the cBioPortal for Cancer Genomics to examine the frequency of *ATG5* coding sequence mutations and copy number alterations in different TCGA cancer datasets (Fig. 4.4*A* and 4.4*B*). Depending on the dataset and cancer type, *ATG5* coding sequence mutations occur in up to ~1.5% of TCGA-sequenced tumors. In striking contrast, a deep loss of *ATG5*, which is thought to be indicative of a homozygous deletion, occurs in as high as 16% of TCGA-examined tumors. Deletion of *ATG5* is particularly prominent in diffuse large B-cell lymphoma (DLBC) and PCa TCGA datasets (Fig 4.4*B*).

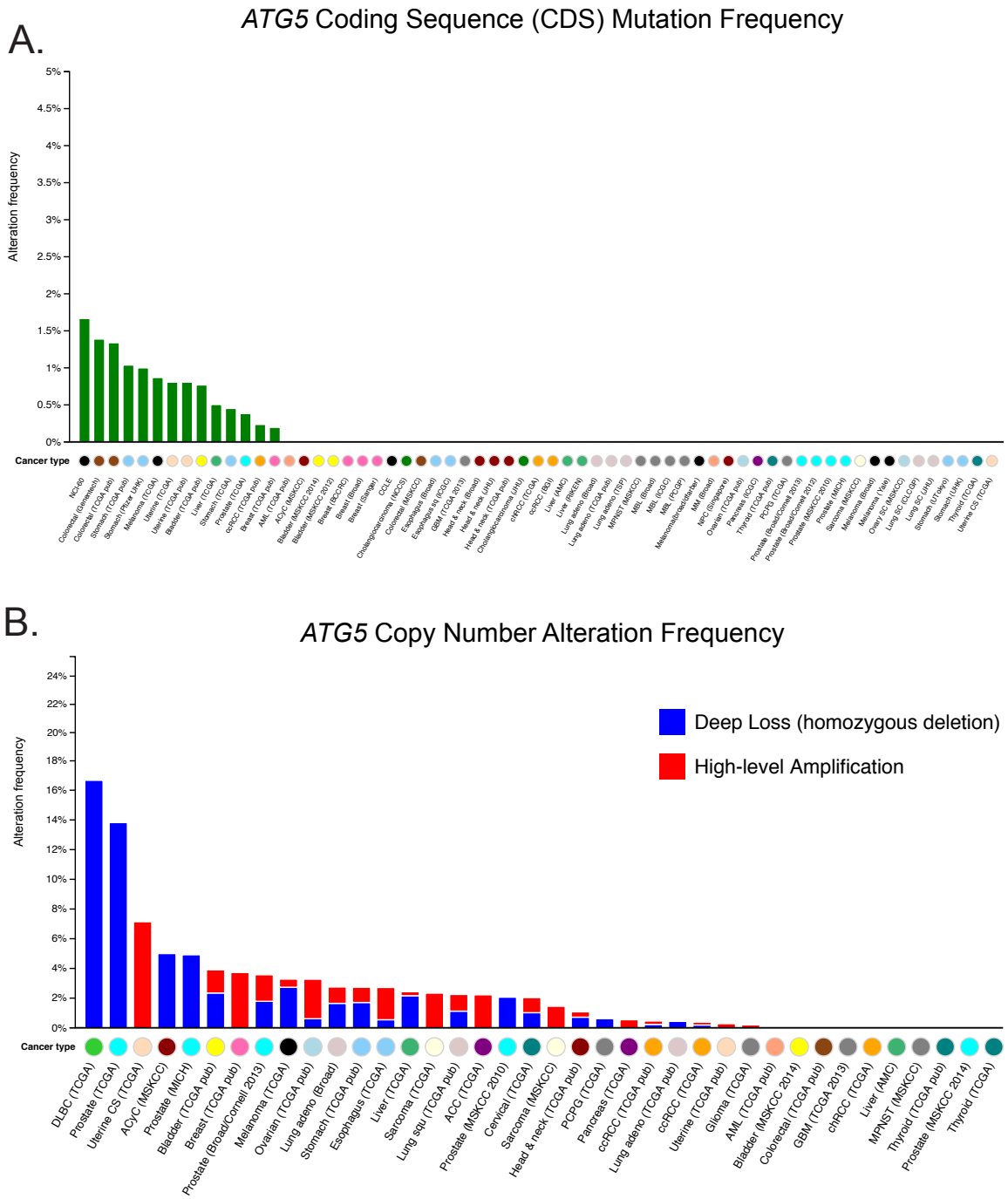

Figure 4.4 – *ATG5* is frequently deleted human prostate cancer. (*A*) Frequency of *ATG5* coding sequence (CDS) mutations in different tumor datasets. (*B*) Frequency of *ATG5* copy number alterations across different tumor datasets. A deep loss is thought to correspond to a homozygous deletion. Data accessed through cBioPortal (Cerami et al., *Cancer Discovery*, 2012).

ATG5 is located on chromosome 6 at the q21 locus (Fig. 4.5*A*). There is a long-standing association of 6q21 deletions with many types of hematological malignancies, including leukemias, lymphomas and myelomas (Kamada et al., 1992; Cigudosa et al., 1998). Only recently have chromosomal deletions been discovered in solid cancers, but it is now clear that 6q21 deletions are one of the most frequent alterations in PCa and occur in at least one allele in ~41% of primary PCa and ~74% of advanced PCa (Williams et al., 2014). Given our discovery and characterization of the *ATG5* mutation that inactivates autophagy in DU145 PCa cells and nothing is known about the specific role of autophagy in PCa, we decided to focus specifically on *ATG5* expression in PCa.

The main challenge in determining the specific effects of chromosomal alterations is they generally affect a large amount of genetic information, sometimes as much as entire chromosome arms, leading to the deletion/amplification of many passenger genes along with the driver gene(s) that directly affect tumorigenesis. Deletions of 6q21 have been specifically associated with the most commonly mutated gene in PCa, *SPOP*, for reasons that are unclear (Barbieri et al., 2012). We used cBioPortal to examine the TCGA prostate cancer dataset for *SPOP* mutations and genetic alterations of 6q21 genes previously implicated as tumor suppressor genes for other cancer types (Fig. 4.5A and 4.5*B*). Deep losses (or homozygous deletions) of *ATG5* and neighboring genes occur in roughly 14% of PCa tumors in this TCGA dataset, many of which occur independent of *SPOP* mutations (Fig. 4.5*B*)

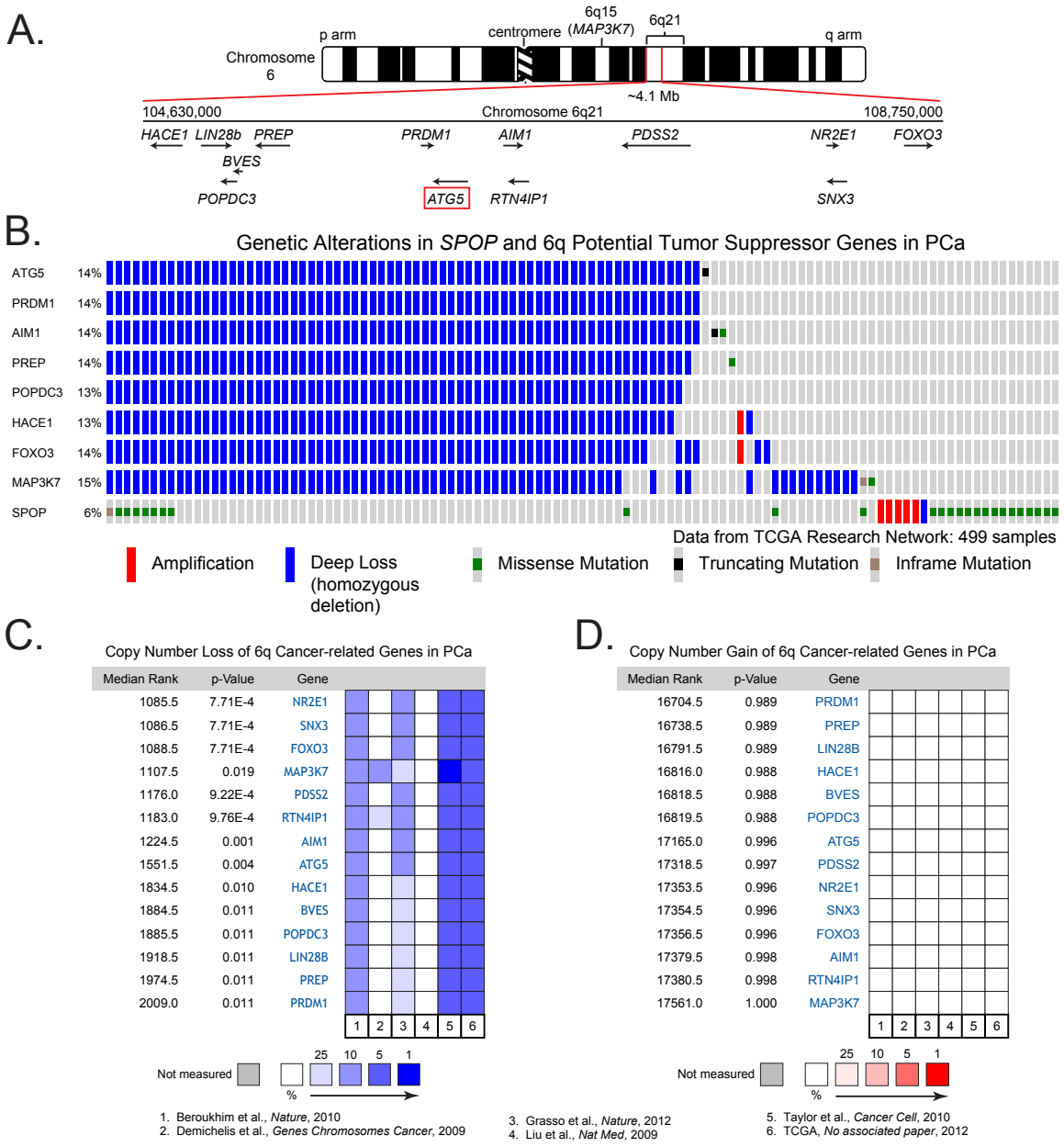

Figure 4.5 – *ATG5* deletions in PCa also encompass many neighboring 6q genes. (*A*) Diagram of the chromsome 6q21 locus. *ATG5* and other neighboring potential tumor suppressor genes are indicated. (*B*) Mutation and CNA of the TCGA prostate cancer dataset for *SPOP* and associated 6q potential tumor suppressor genes. Each column represents a single tumor sample. A deep loss is thought to correspond to a homozygous deletion. TCGA data accessed through cBioPortal (Cerami et al., *Cancer Discovery*, 2012). Copy number loss (*C*) and gain (*D*) of *ATG5* and other PCa-related genes across 6 PCa tumor datasets. The Oncomine™ Platform (Life Technologies, Ann Arbor, MI) was used for analysis and visualization.

With each column representing a single tumor sample, it is clear that the genes in 6q21 are most often co-deleted (Fig. 4.5*B*), which suggests the deletions affect the entire 6q21 locus. We compared the 6q21 genes to mitogen-activated protein kinase kinase kinase 7 (*MAP3K7/TAK1*), which is located relatively close by at 6q15 and has been directly implicated as a tumor suppressor gene in PCa (Wu et al., 2012; Rodrigues et al., 2015) (Fig. 4.5*A*). *MAP3K7* is also co-deleted with the 6q21 genes (Fig. 4.5*B*), indicating that deletions in this TCGA PCa dataset affect 6q21 along with a large portion of the q arm of chromosome 6. We used The Oncomine™ Platform (Life Technologies, Ann Arbor, MI) for analysis and visualization of copy number loss and gain across 6 available PCa datasets to confirm the results from the TCGA dataset (Fig. 4.5*C* and 4.5*D*). Oncomine™ ranks the genes based on the significance of their copy number loss or gain in prostate tumor samples compared to control normal tissue. It also calculates a p-value to indicate the statistical significance when comparing multiple datasets.

Oncomine™ analysis indicates *MAP3K7* and the potential tumor suppressor genes in 6q21 are all significantly deleted when compared across all available PCa datasets (Fig. 4.5*C*). This confirms 6q deletions occur frequently in PCa, but they affect many potential tumor suppressor genes, any of which could be driver genes.

4.2.5 *ATG5* mRNA expression is specifically downregulated in PCa. Since the 6q21 deletions in PCa affect a large number of genes, we next examined mRNA expression of these potential driver genes within the deleted region. Similar to before, we used The Oncomine™ Platform to examine mRNA under and overexpression of *ATG5* and other potential tumor suppressor genes located at 6q21, in addition to *MAP3K7*, across 15 PCa datasets (Fig. 4.6). Surprisingly, despite the frequency of 6q21 deletions (Fig. 4.5*B* and 4.5C), mRNA expression of the majority of genes within the locus were either not significantly affected or actually overexpressed, when comparing all available PCa datasets (Fig 4.6*B* and 4.6*C*). Of the genes analyzed, only *MAP3K7*, *ATG5* and blood vessel epicardial substance (*BVES*) were significantly underexpressed across all PCa datasets, although several datasets did not measure *BVES* expression (Fig. 4.6*B*). This indicates that either the remaining genes are not expressed at all in normal prostate or that hemizygous deletions of 6q21, which occur in the majority of PCa tumors, are insufficient to significantly suppress mRNA expression. The overexpression of popeye domain containing 3 (*POPDC3*) and prolyl endopeptidase (*PREP*) in prostate tumors indicates the remaining intact allele is more than capable of compensating for a hemizygous deletion. However, this does not occur for *MAP3K7* or *ATG5* (Fig. 4.6C), which indicates that there could be other mechanisms for selectively downregulating these genes beyond simple genetic deletions.

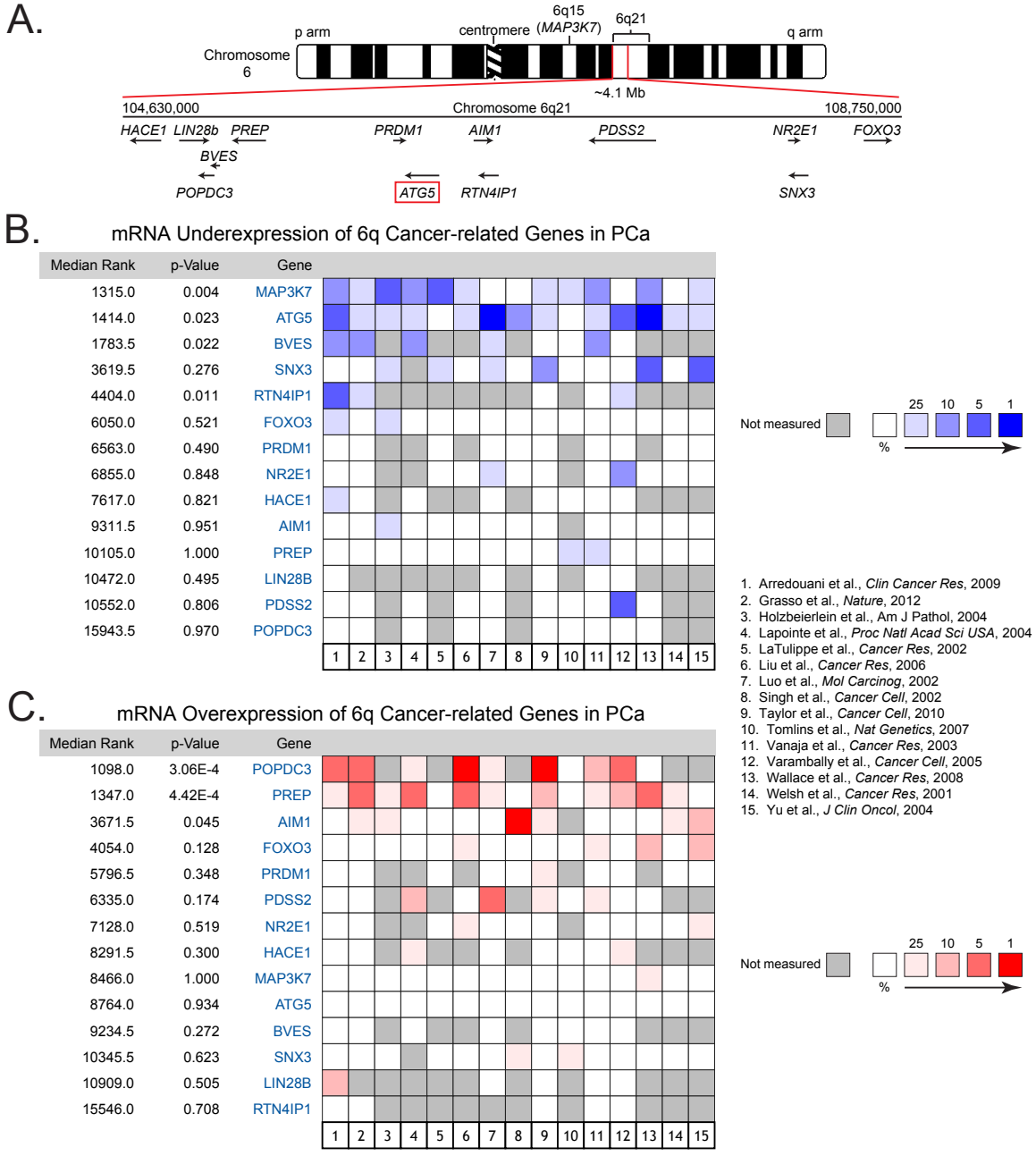

Figure 4.6 – *ATG5* mRNA expression is specifically downregulated in PCa. (*A*) Diagram of the chromsome 6q21 locus. *ATG5* and other neighboring potential tumor suppressor genes are indicated. (*B*) mRNA underexpression rankings of *ATG5* and other 6q potential tumor suppressor genes across 15 prostate tumor datasets. (*C*) mRNA overexpression rankings of *ATG5* and other 6q potential tumor suppressor genes across 15 prostate tumor datasets. The Oncomine™ Platform (Life Technologies, Ann Arbor, MI) was used for analysis and visualization.

One mechanism could be transcriptional repression of *ATG5*, which was shown to occur in human melanomas and was thought to result from *ATG5* promoter hypermethylation (Liu et al., 2013a). Therefore, in addition to the frequent genetic deletions, *ATG5* and *MAP3K7* may be epigenetically downregulated in PCa through a similar transcriptional mechanism. The fact that the mRNA expression levels of the majority of the analyzed genes remain unchanged in PCa, despite the high frequency of copy number loss, highlights the potential tumor suppressive functions of those genes that are selectively downregulated through other mechanisms, such as *ATG5* and *MAP3K7*.

4.2.6 *ATG5* is more significantly underexpressed in human PCa than many well-established PCa tumor suppressor genes. The frequency of *ATG5* deletion and the corresponding selective underexpression of *ATG5* mRNA in PCa, combined with our demonstrated effects of *ATG5* nonsense, deletion and missense mutations, strongly implicates *ATG5* as a tumor suppressor gene. We also used The Oncomine™ Platform to compare *ATG5* copy number and mRNA expression with other well-established PCa tumor suppressor genes (Fig. 4.7). In agreement with other meta-analyses of PCa (Williams et al., 2014), 6q deletions encompassing *ATG5* and *MAP3K7* are some of the most frequent alterations in PCa along with deletions of the PCa-related tumor suppressors: NK3 homeobox 1 (*NKX3-1*), *TP53*, *RB1*, *PTEN* and *CDKN1B* (p27) (Fig. 4.7*A*). Shockingly, however, the frequent genetic deletions did not strongly correlate

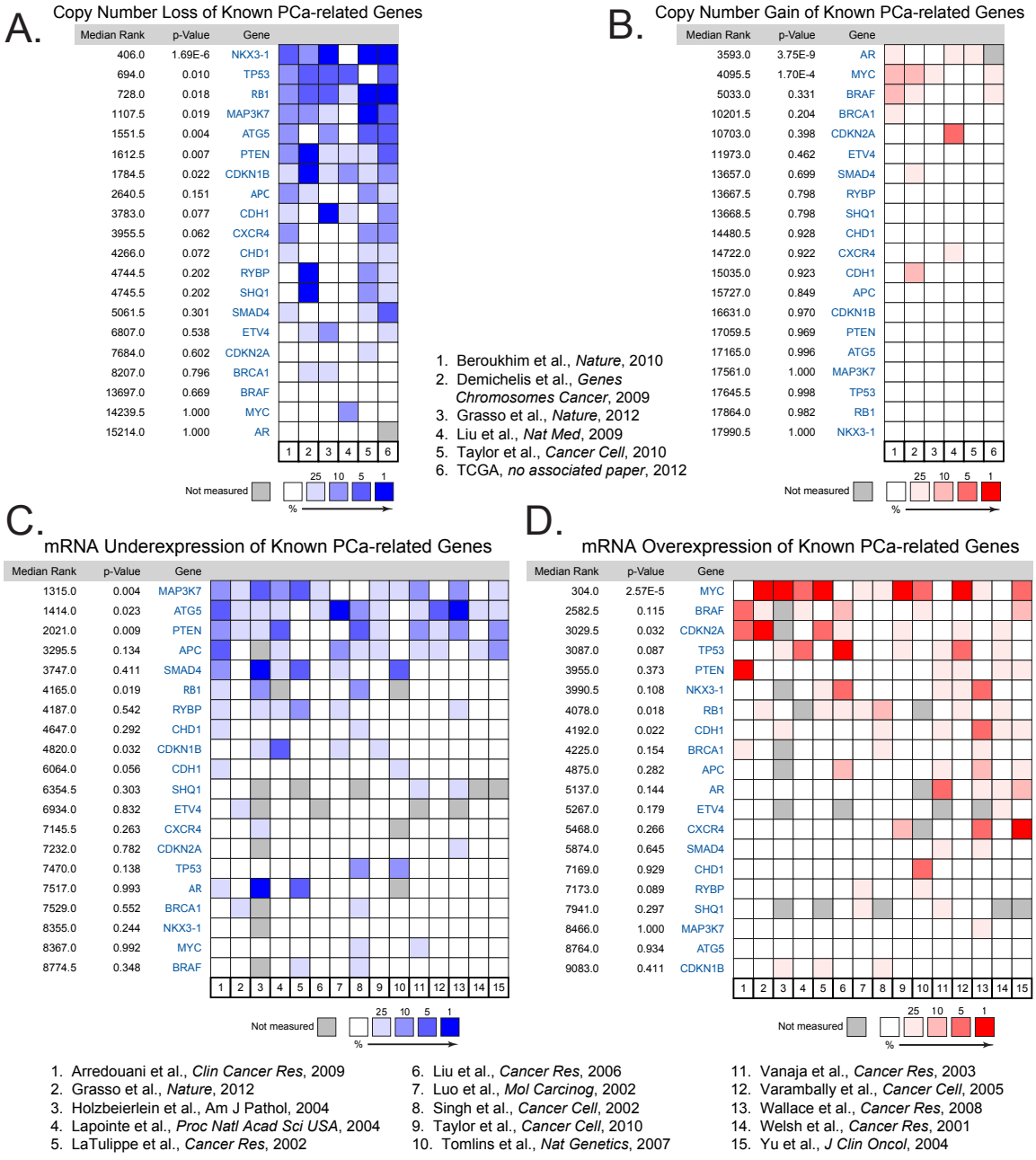

Figure 4.7 – *ATG5* is strongly underexpressed even compared to known PCa-related tumor suppressor genes. (*A*) Copy number loss of *ATG5* and other PCa-related genes across 6 PCa tumor datasets. (*B*) Copy number gain of *ATG5* and other PCa-related genes across 6 PCa tumor datasets. (*C*) mRNA underexpression rankings of *ATG5* and other known PCa-related genes across 15 prostate tumor datasets. (*D*) mRNA overrexpression rankings of *ATG5* and other known PCa-related genes across 15 prostate tumor datasets. The Oncomine™ Platform (Life Technologies, Ann Arbor, MI) was used for analysis and visualization.

with the mRNA underexpression data for many of these supposedly well-established PCa tumor suppressor genes, again likely indicating compensation from the remaining allele (Fig. 4.7*C*). *MAP3K7* and *ATG5* were the most significantly underexpressed genes out of all the analyzed PCa-related genes, followed by *PTEN* and *RB1*. This was a very unexpected finding and further stressed the likely importance of both *MAP3K7* and *ATG5* in the suppression of PCa.

4.2.7 *ATG5* and downstream *ATG* genes are significantly underexpressed in human PCa. The frequency of *ATG5* deletion and the degree to which it is underexpressed compared to other established tumor suppressor genes strongly suggests it functions as a tumor suppressor. Still, it was not clear if this putative tumor suppressor function was related to autophagy. To partially address this question, we examined other autophagy-related (ATG) genes that have been implicated as

tumor suppressors, including *BECN1* (Beclin 1), UV radiation resistance associated gene (*UVRAG*), and SH3-domain GRB2-like endophilin B1 (*SH3GLB1/Bif-1*) (Qu et al., 2003; Yue et al., 2003; Liang et al., 2006; Takahashi et al., 2007). Using the cBioPortal to analyze the TCGA PCa dataset for mutation and copy number alterations of *ATG5*, *BECN1*, *UVRAG* and *SH3GLB1* indicated that in PCa, *ATG5* is far more frequently deleted than the other proposed autophagy-related tumor suppressor genes (Fig. 4.8*A*).

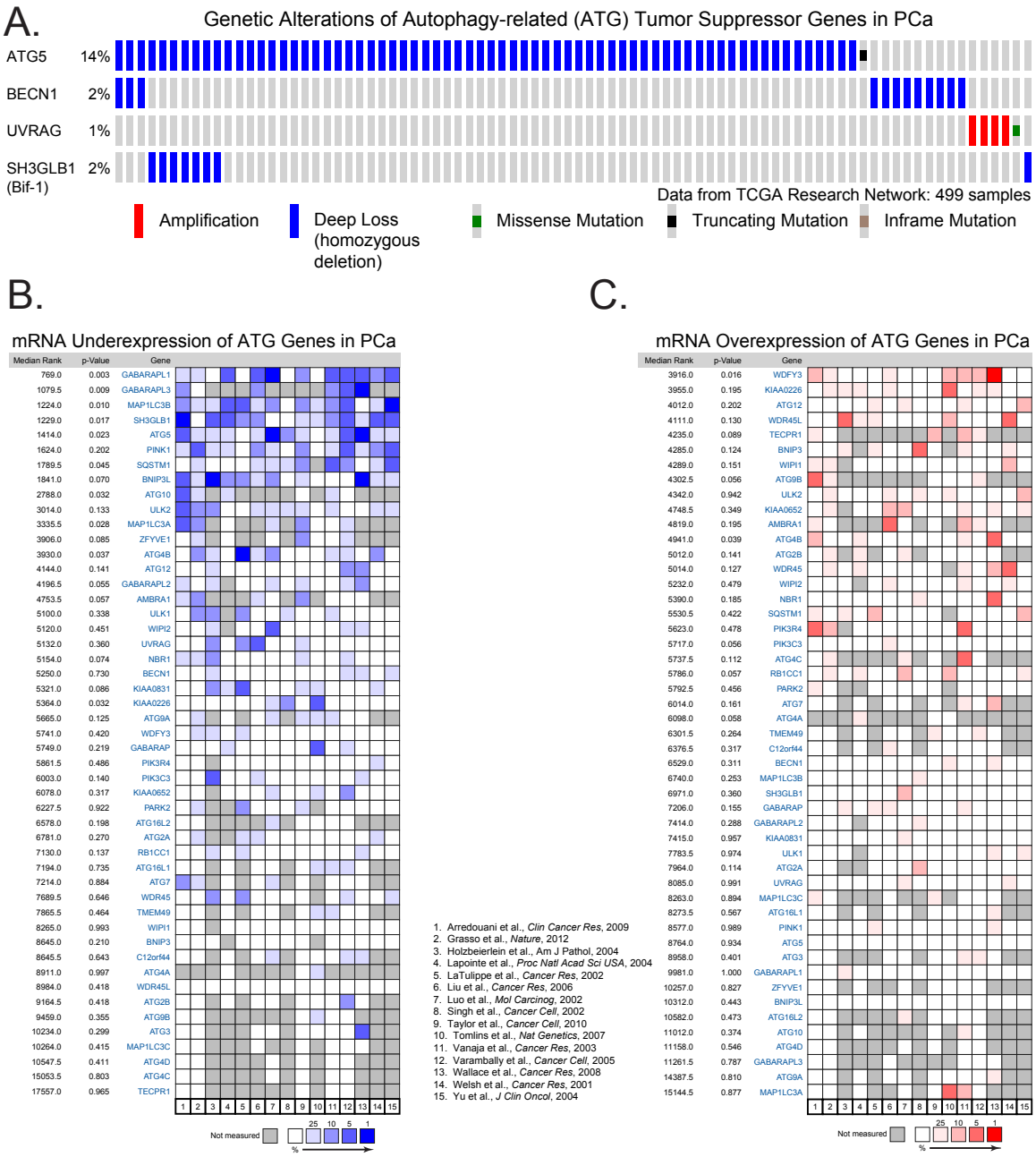

Figure 4.8 – *ATG5* and LC3 family members are selectively downregulated in PCa. (*A*) Mutation and CNA of TCGA prostate cancer dataset for autophagy-related (ATG) genes. Each column represents a single tumor sample. A deep loss is thought to correspond to a homozygous deletion. TCGA data accessed through cBioPortal (Cerami et al., *Cancer Discovery*, 2012). (*B*) mRNA underexpression and (*C*) overexpression rankings of *ATG5* and other ATG genes across 15 prostate tumor datasets. The Oncomine™ Platform (Life Technologies, Ann Arbor, MI) was used for analysis and visualization.

To determine if copy number correlated with mRNA expression, we examined under and overexpression of *ATG5* and all other autophagy-related genes in PCa (Fig. 4.8*B* and 4.8*C*). *SH3GLB1* (Bif-1) is significantly underexpressed, which given the relative infrequency of its genetic deletion, is likely due to epigenetic repression or some other mechanism (Fig. 4.8*B*). However, SH3GLB1 also stimulates BCL2-associaed X protein (BAX) and promotes apoptosis (Etxebarria et al., 2009), which means its underexpression may not be specifically related to its function in autophagy. Interestingly, a few other autophagy-related genes were significantly downregulated in PCa, almost all of which are LC3 family members (*GABARAPL1*, *GABARAPL3*, *MAP1LC3B*, *MAP1LC3A*). The ATG12–ATG5-ATG16L1 complex is believed to catalyze the lipid conjugation of all LC3 family members, which means these strongly underexpressed genes function directly downstream of *ATG5*, which is also strongly underexpressed (Fig. 4.8*B*).

The fact that several genes in the same pathway are significantly underexpressed and only a single autophagy-related gene was mildly overexpressed (Fig. 4.8B and 4.8*C*), suggests autophagy plays a role in prostate tumor suppression. In the previous chapter, we demonstrated that there is no genetic redundancy for *ATG5* function and that its absence leads to the loss of several other ATG proteins, including ATG12, ATG16L1 and ULK1 complex subunits. This suggests *ATG5* may be preferentially and specifically targeted by

several different mechanisms, all of which inactivate autophagy and its potential tumor suppressive function.

4.2.8 *ATG5* is even further underexpressed in PCa metastases. We have shown that *ATG5* is more strongly underexpressed than many well-established tumor suppressor genes in primary prostate tumors. However, characterization of advanced prostate cancers and metastases indicates that genetic alterations of these well-established genes is predominantly a late event in prostate tumor progression and is not often seen in earlier stage primary tumors (Taylor et al., 2010; Baca et al., 2013). The accumulation of these later stage lesions, including amplification of androgen receptor (*AR*) and deletion of *PTEN,* are strongly associated with poor clinical outcomes (Barbieri and Tomlins, 2014). Therefore, the extent of deletion and underexpression of *ATG5* in primary prostate tumors may be overstating its importance for PCa progression and, ultimately, for patient survival.

To determine if *ATG5* is similarly underexpressed in PCa metastases, we used The Oncomine™ Platform to examine mRNA under and overexpression for *ATG5* and other known PCa tumor suppressor genes in 11 publicly available datasets that compare PCa metastases to primary tumors (Fig. 4.9*A* and 4.9*B*). As expected, *PTEN* is the most significantly underexpressed gene out of the analyzed genes, while *AR* is the second most significantly overexpressed. SMAD family member 4 (*SMAD4*) is also strongly underexpressed in human PCa

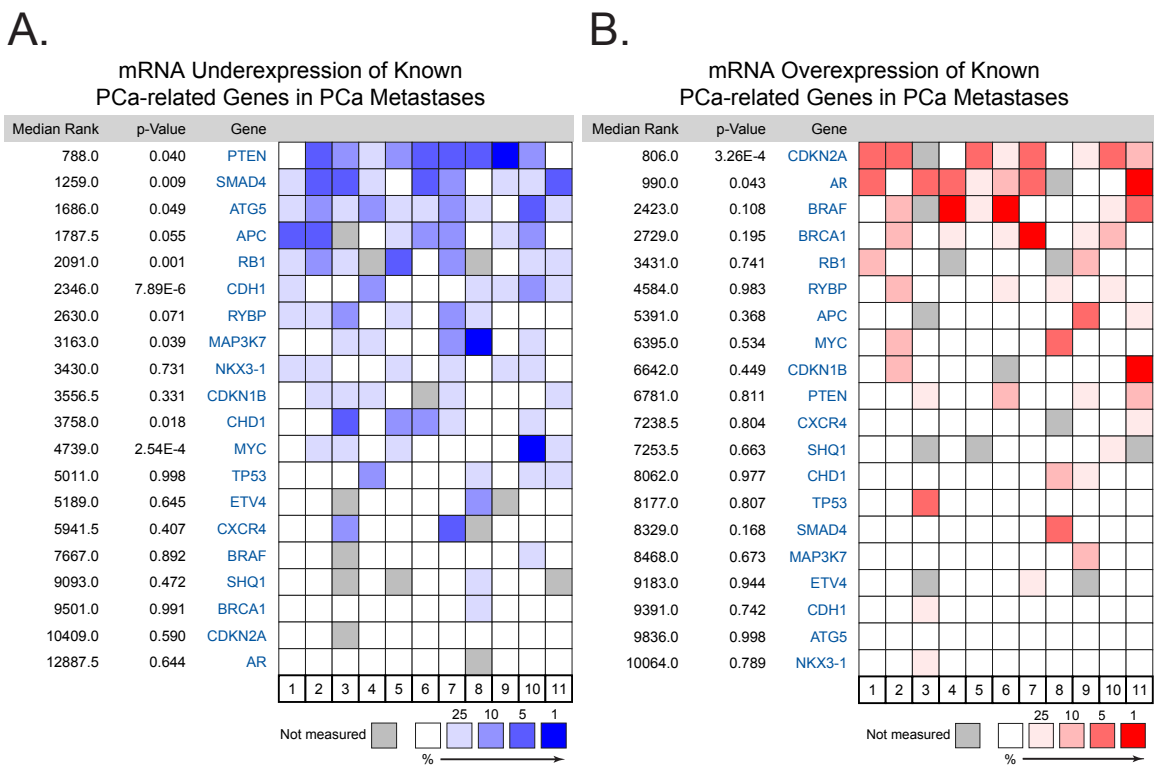

1. Chandran et al., *BMC Cancer*, 2007
2. Grasso et al., *Nature*, 2012
3. Holzbeierlein et al., *Am J Pathol*, 2004
4. Lapointe et al., *Proc Natl Acad Sci USA*, 2004
5. LaTulippe et al., *Cancer Res*, 2002
6. Tamura et al., *Cancer Res*, 2007
7. Taylor et al., *Cancer Cell*, 2010
8. Tomlins et al., *Nat Genet*, 2007
9. Vanaja et al., *Cancer Res*, 2003
10. Varambally, *Cancer Cell*, 2005
11. Yu et al., *J Clin Oncol*, 2004

Figure 4.9 – *ATG5* is further downregulated in PCa metastases compared to primary tumors. (*A*) mRNA underexpression rankings of *ATG5* and other known PCa-related genes across 11 prostate metastasis datasets. (*B*) mRNA overrexpression rankings of *ATG5* and other known PCa-related genes across 11 prostate metastasis datasets. The Oncomine™ Platform (Life Technologies, Ann Arbor, MI) was used for analysis and visualization.

metastases (Fig. 4.9*A*), which is consistent with the finding that genetic deletion of *Smad4* in a *Pten*-null mouse prostate induced invasive and metastatic PCa with 100% penetrance (Ding et al., 2011). Encouragingly, *ATG5* is similarly underexpressed in PCa metastases (Fig. 4.9*A*). This suggests *ATG5* functions as a tumor suppressor in both early and late stages of PCa.

4.2.9 *ATG5* suppresses DU145 PCa xenograft tumor growth. The human copy number and mRNA expression data, together with our characterization of *ATG5* mutations, all strongly suggested that *ATG5* is a prostate tumor suppressor gene that functions both early and late in tumor progression. However, we had not directly tested its function in any type of cancer model. To experimentally confirm its tumor suppressive function, we injected ATG5-deficient DU145 PCa cells and those re-expressing ATG5 into *NOD/SCID* immunocompromised mice. These mice have the severe combined immunodeficiency (*scid*) mutation in the protein kinase, DNA-activated, catalytic polypeptide (*Prkdc*) gene on an inbred non-obese diabetic (NOD) background. The $Prkdc^{scid}$ impairs B-, T- and natural killer cell function allowing xenotransplation.

DU145 cells have several advantages that make them an ideal model for examining the tumor suppressive function of ATG5. Firstly, we have confirmed DU145 cells are completely deficient in ATG5. This is an important aspect since it appears that very low amounts of the ATG12–ATG5 conjugate are sufficient to

promote some LC3 lipid conjugation in response to prolonged proteasome inhibition (Fig. 4.3*B*, lanes 5 and 6). Indeed, even an excellent *ATG5* knockdown did not completely prevent LC3 lipidation in PC-3 PCa cells (Fig. 3.2*C*, p.62). Secondly, we have determined that re-expression of *ATG5* is sufficient to fully rescue functional ATG12–ATG5-ATG16L1 complex formation and autophagy as determined by LC3 lipidation and p62 degradation (Fig. 3.3*A*, p.66). Finally, even though *ATG5* is technically being "overexpressed" in DU145 cells, we have already demonstrated that the levels of unconjugated ATG5 and the ATG12–ATG5-ATG16L1 complex are strictly dependent upon the expression levels of endogenous ATG12 and ATG16L1 (Fig. 3.3*B*, p.66). Therefore, the complex levels are self-regulated to near-endogenous levels and are not overexpressed, permitting the examination of "physiological" levels of ATG5 expression.

We first stably infected DU145 PCa cells expressing an empty vector (EV) or FLAG-ATG5 with a lentivirus containing firefly luciferase. Luciferase expression allowed us to use the IVIS Spectrum *in vivo* imaging system to track tumor growth as a function of luciferase activity. We initially tested whether ATG5 expression affected normal growth of these cells in culture, but did not find any difference in proliferation rates (Fig. 4.10*A*). We then injected DU145 or DU145 FLAG-ATG5 cells subcutaneously into the flanks of *NOD/SCID* mice and monitored tumor growth weekly by measuring luciferase activity with the IVIS Spectrum. Remarkably, stable expression of FLAG-ATG5 drastically suppressed DU145 xenograft tumor growth (Fig. 4.10*B*). After seven weeks, the mice were

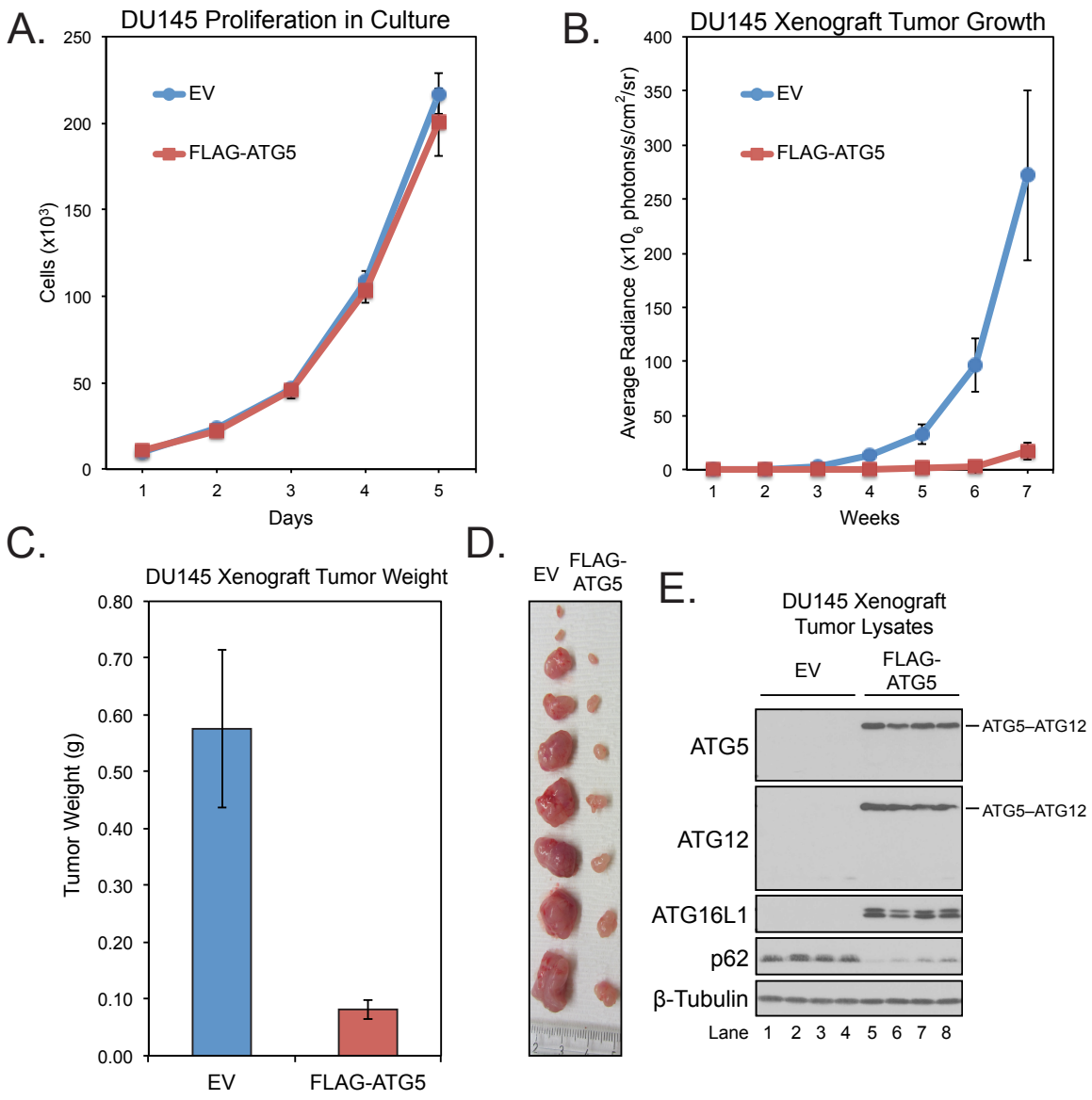

Figure 4.10 – Rescue of ATG5 in DU145 PCa cells did not affect proliferation in culture, but dramatically suppressed xenograft tumor growth. (*A*) 1x10⁴ DU145 PCa cells, stably expressing firefly luciferase and an empty vector (EV) or FLAG-ATG5, were plated in duplicate into 6-well plates. Total cell numbers were quantified daily by flow cytometry for 5 days. (*B*) 1x10⁴ DU145 PCa cells stably expressing firefly luciferase and an empty vector (EV) or FLAG-ATG5 were injected subcutaneously into the flanks of NOD/SCID mice. Xenograft tumor growth was determined by weekly measurements of luciferase activity using the IVIS Spectrum *in vivo* imaging system. Mice were sacrificed and the tumors from empty vector (EV) and FLAG-ATG5-expressing DU145 xenografts were harvested, (*C*) weighed, and (*D*) photographed. (*E*) Lysates were prepared from EV (lanes 1-4) and FLAG-ATG5 expressing tumors (lanes 5-8) and immunoblotted for the ATG12–ATG5-ATG16L1 complex and p62.

sacrificed and the xenograft tumors were harvested, weighed and imaged, which confirmed the IVIS luciferase activity data (Fig. 4.10*C* and 4.10*D*). We prepared protein lysates from the harvested tumors and immunoblotted them for the ATG5, ATG12 and ATG16L1 to confirm the tumors expressed the ATG12–ATG5-ATG16L1 complex (Fig. 4.10*E*). ATG5-expressing tumors had significantly lower levels of p62, which indicated that autophagy was activated and fully functional (Fig. 4.10*E*). While this result doesn't prove that autophagy, per se, suppressed tumor growth, it clearly indicates that ATG5 has tumor suppressive activity in this PCa xenograft model. This result, together with the human mutation, copy number and mRNA expression data, strongly suggests that *ATG5* is a powerful PCa tumor suppressor gene that is suppressed or inactivated through a variety of mechanisms in human cancer.

4.3 Discussion

Based on our initial discovery of a splice donor-site mutation that caused aberrant splicing and inactivation of *ATG5* in DU145 PCa cells, we set out to determine if *ATG5* functioned as a tumor suppressor gene in human cancer. Other ATG5 splice region mutations have been identified in human tumor samples that may disrupt normal splicing and lead to proteasomal degradation of ATG5, ATG12, and ATG16L1. Additionally, we have characterized *ATG5* nonsense, deletion and missense mutations, and determined many of them

prevent ATG12 conjugation and completely or partially inactivate ATG5. Like *ATG5* alternative splicing, the *ATG5* nonsense and deletion mutations affect the N- and C-termini, both of which are essential for the ATG16L1 interaction that stabilizes ATG5 and promotes ATG12 conjugation. Similarly, we have identified several *ATG5* missense mutations, some of which are located directly at the ATG16L1 binding interface, and others that are found more in the core of the protein and may disrupt ATG16L1 interaction by inducing conformational changes that affect either the N- and/or C-terminus. Thus, the unique biology of ATG5 and the mechanism for ATG12–ATG5-ATG16L1 complex assembly is such that a variety of different types of mutations all have the same functional effect and result in proteasomal degradation of ATG5, ATG12 and ATG16L1.

Even though the amorphic *ATG5* mutations that prevent ATG12 conjugation affect the ATG16L1 binding region, the absence of ATG16L1 does not entirely preclude ATG12 conjugation (Fig. 3.7*C*, p.80). This suggests the mutations do more than simply disrupt ATG16L1 binding. Since other proteins, including ATG16L2 and TECPR1, bind ATG5 in the same region as ATG16L1 (Kim et al., 2015), these proteins may also stabilize ATG5 and promote ATG12 conjugation. More investigation is needed to determine how these *ATG5* mutations affect the functions of ATG16L2 and TECPR1.

The ratio of amorphic or null *ATG5* mutations to those mutations that have no apparent functional effect, suggests that inactivating *ATG5* mutations may provide selective advantage, rather than simply existing as passenger mutations.

However, the frequency of *ATG5* mutations in human cancer is not particularly high, which means *ATG5* might also be inactivated through other mechanisms. The frequency of chromosomal deletions and rearrangements is now known to be far higher than single mutations, particularly in PCa (Redon et al., 2006). We have confirmed previous reports indicating that prostate tumors frequently contain genetic deletions at the 6q21 locus on chromosome 6, which contains *ATG5*. Surprisingly, this did not seem to affect the mRNA expression levels of many genes within the 6q21 locus, which could be due to compensation from the remaining allele. This suggested that additional mechanisms, possibly epigenetic, exist for suppressing *ATG5* expression in PCa. Promoter hypermethylation was proposed to suppress *ATG5* expression in human melanomas (Liu et al., 2013a). It remains to be seen whether this is also true in human PCa.

Surprisingly, *ATG5* is more significantly underexpressed in PCa than many well-established tumor suppressor genes. Since many genetic alterations, including *AR* amplification and *PTEN* deletion, occur almost exclusively in advanced prostate cancers (Taylor et al., 2010), we also examined *ATG5* expression in datasets comparing PCa metastases to primary tumors. *ATG5* was also significantly underexpressed in metastases, which strongly suggests that *ATG5* is an important tumor suppressor in late stage PCa. This is supported by the fact that the DU145 PCa cell line, which we have characterized as ATG5-deficient, was originally isolated from a brain metastasis.

However, this important finding does not directly agree with data from experimental mouse models of cancer, which suggest autophagy is required for tumor progression. This may be because *ATG5* functions uniquely as a tumor suppressor in PCa, while promoting growth of other cancer types, or it could simply be that the genetically engineered mouse models that have been used to study the effects of autophagy do not genetically approximate aggressive human PCa. Autophagy has been reported to suppress tumor progression in mouse models of lung and pancreatic cancer driven by activating mutations in *KRAS* or *BRAF*. Tumor cells with these mutations have high levels autophagy, which was shown to be essential for tumor cell growth *in vitro* and *in vivo* (Yang et al., 2011). However, unlike pancreatic and lung cancers, *RAS/RAF* mutations are rare in PCa (Grasso et al., 2012). Therefore, *ATG5* may behave differently in human PCa compared to mouse models of *RAS/RAF*-driven lung or pancreatic cancers due to differences in genetic backgrounds.

These seemingly opposing findings stress the need for examining the role(s) of ATG5 in models of human PCa. We compared ATG5-deficient DU145 PCa cells to those re-expressing ATG5 in a xenograft cancer model. We have fully characterized DU145 cells as being completely deficient in ATG5, which allowed us to cleanly assess its potential tumor suppressor function. Expression of ATG5 in DU145 PCa cells dramatically suppressed xenograft tumor growth. We confirmed ATG5-expressing tumors had functional ATG12–ATG5-ATG16L1 complexes and autophagy based on p62 degradation. These results support the

mutational, copy number and expression data and confirm that ATG5 functions as a PCa tumor suppressor. Follow up experiments are needed to determine the precise mechanism of tumor suppression and if it is entirely due to autophagy. The fact that several LC3 family member genes that function immediately downstream of ATG5 are also strongly underexpressed suggests that autophagy plays a role in ATG5 tumor suppression. Since ATG5 expression had no effect on proliferation in culture, but dramatically affected xenograft growth, it suggests that stressors in the tumor microenvironment may play a critical factor. Possible mechanisms for *ATG5* tumor suppression will be discussed more thoroughly in the final chapter.

Chapter 5: Conclusions and Future Directions

Our discovery and characterization of a splice donor-site mutation that causes aberrant splicing of *ATG5* in DU145 PCa cells is, to our knowledge, the first example of a genetic alteration in a human tumor or cancer cell line that has been proven to completely inactivate autophagy. This discovery provided insight into previously unknown mechanisms of ATG12–ATG5-ATG16L1 complex formation and turnover. This finding also implicated *ATG5* as a tumor suppressor gene, which we have confirmed in a human PCa xenograft model. The tumor suppressive function of *ATG5* was additionally supported by extensive mutation, copy number alteration and mRNA expression data from human tumor samples. Together, these results indicate that *ATG5* is a highly relevant PCa tumor suppressor that is tightly regulated through a variety of genetic, epigenetic, and post-translational mechanisms. This chapter will focus on a few of the interesting open questions that have arisen from these findings.

5.1 Identification of genes involved in ATG12–ATG5-ATG16L1 complex assembly and turnover. We have shown that free, unbound ATG5, ATG12 and ATG16L1 are all inherently unstable and are rapidly ubiquitinated and degraded by the proteasome. However, the factors that mediate the ubiquitination and degradation are completely unknown. Additionally, it's not clear how the ATG12-ATG5-ATG16L1 complex can be assembled if all the free, unbound subunits are

rapidly and continuously degraded. Therefore, there might be unknown factors capable of stabilizing ATG5, ATG12 and ATG16L1 in specific contexts to mediate formation of the complex. To try and identify genes involved in complex assembly and turnover, we have developed a system that takes advantage of the unique instability of the complex subunits and allows for the screening of genes that affect turnover of ATG5, ATG12 and ATG16L1. Since expression of ATG5 stabilizes ATG16L1 and rescues the complex in DU145 cells, we have fused a fluorescent reporter to a version of ATG5 containing a mutation in the ATG16L1 binding region, which we have previously shown prevents stabilization and leads to proteasomal turnover. Therefore, the fluorescent reporter is continually suppressed by the ubiquitination and proteasomal degradation of its mutant ATG5 fusion partner. However, treatment with a proteasome inhibitor, or presumably the disruption of any gene involved in mediating that degradation, results in the accumulation of the mutant ATG5 along with the fluorescent signal.

On this basis, we plan to do an initial shRNA screen for E2 ubiquitin conjugating enzymes, of which there are approximately 40 (Komander, 2009), to identify which are essential for turnover of the fluorescent reporter-ATG5 fusion. The same principle will be applied to ATG12 and ATG16L1, since both are rapidly degraded in the absence of ATG5. Since free, unbound ATG5 is normally completely degraded, the system allows for a wide dynamic range of signal from the fluorescent reporter, which should allow detection of knockdowns with only partial or minimal effects on turnover.

Another advantage of this system is that it allows the screen to be scaled and modified. After the proof-of-principle E2 screen, we can use the same system to screen for E3 ligases, of which there are more than 600 (Komander, 2009), and even scale up to a genome-wide shRNA or CRISPR/Cas9 screen. The clustered regularly interspaced short palindromic repeats (CRISPR) system uses guide RNAs to target CRISPR associated protein 9 (Cas9) nuclease to specific DNA sequences where it creates double-strand breaks that are repaired through error-prone DNA repair pathways and lead to gene inactivation. Large-scale screens will involve stable infection with a library of shRNAs or CRISPR guide RNAs targeting specific genes, followed by fluorescence activated cell sorting (FACS) for cells with positive fluorescence signal. The specific shRNAs or CRISPR gRNAs that are enriched in the sorted population will be identified by deep sequencing and can then be confirmed in a smaller secondary screen. This method should identify genes directly involved in the ubiquitination and proteasomal degradation of ATG5, ATG12 and ATG16L1, as well as any upstream regulators of the process. This should provide valuable insight into how ubiquitination and proteasomal degradation regulate ATG12–ATG5-ATG16L1 complex formation.

Importantly, the same basic principle can also be used to screen for genes essential for ATG12–ATG5-ATG16L1 complex assembly. Wild-type ATG5 fused to a fluorescent reporter is incorporated into the ATG12–ATG5-ATG16L1 complex providing a stable fluorescent signal. However, disruption of the

complex leads to the ubiquitination and turnover of the ATG5-fluorescent reporter fusion. Therefore, the screen for genes mediating or maintaining complex assembly would be for the loss of fluorescent signal, rather than the gain. Regardless, the dynamic range of the fluorescent signal should be roughly the same as the gain-of-fluorescence screen. Together, these systems will serve as powerful tools for identifying the unknown factors involved in ATG12–ATG5-ATG16L1 complex assembly and disassembly.

5.2 Establishment of *ATG5*-deficient mouse models of PCa. We have fully characterized *ATG5* mutations identified in human tumors and found many of them are amorphic due to the disruption of the ATG16L1 interaction that is essential for ATG12 conjugation. This suggested that *ATG5* might function as a tumor suppressor gene. Using publicly available tumor data, we have shown that *ATG5* is downregulated in both primary human PCa as well as metastases. Along with *ATG5, PTEN* and *SMAD4* are significantly downregulated in PCa metastasis, which together have been shown to suppress metastasis in mice (Ding et al., 2011). Therefore, we are currently developing similar mouse models to test if prostate-specific *Atg5* knockout promotes tumorigenesis alone and/or if it promotes tumor progression and metastasis in well-established mouse models of PCa.

Currently, we are crossing $Atg5^{flox/flox}$ mice with mice expressing Cre recombinase under the control of the prostate-specific rat probasin (PB) promoter

to generate a novel prostate-specific *Atg5* knockout mouse model. These mice will be examined at various ages for the development of high-grade prostatic intraepithelial neoplasia (HGPIN), invasive adenocarcinoma and lymph node metastases. This model will determine if *Atg5* suppresses tumorigenesis in the mouse prostate. It will also indicate if *Atg5* is a haploinsufficient tumor suppressor gene, which has been proposed for *BECN1* (Beclin 1) and *AMBRA1* (Qu et al., 2003; Yue et al., 2003; Cianfanelli et al., 2015).

A liver-specific *Atg7* knockout mouse developed benign tumors that did not invade or progress into malignancy, which suggested that autophagy might suppress tumorigenesis, while also being essential for tumor progression (Takamura et al., 2011). If the prostate-specific *Atg5* knockout mice develop HGPIN, we can determine if *Atg5* suppresses or promotes progression of these lesions into malignant adenocarcinomas and potentially metastases. Even if *Atg5* deletion is insufficient on its own to generate HGPIN or adenocarcinoma, we also plan to cross the $Atg5^{flox/flox}$ mice to well-established PCa mouse models such as $Pten^{flox/flox}$ mice. This will allow us to determine if *Atg5* deletion affects the development and progression of prostate tumors with predictable kinetics (Grabowska et al., 2014).

These mouse models will prove if *ATG5*, and by extension autophagy, play opposing roles in PCa initiation and progression, which has been proposed for other cancer types (Galluzzi et al., 2015). However, based on our human tumor data and our PCa xenograft results, we expect that *ATG5* will be tumor

suppressive in both early and late stages of mouse PCa progression. This prediction does not agree with the currently accepted model for the role of autophagy in tumor progression; however, there might be cancer-specific effects related to the different genetic alterations that typically occur in certain cancer types. Regardless, these results will be invaluable to clinicians since the autophagy inhibitor, hydroxychloroquine, is currently being used in combination with a variety of different chemotherapies in clinical trials, including Phase 2 trials targeting castration-refractory and metastatic PCa (Jiang and Mizushima, 2014).

5.3 Mechanistic characterization of *ATG5* PCa tumor suppression. We have convincingly demonstrated that *ATG5* is a prostate tumor suppressor based on the suppression of PCa xenograft tumor growth, as well mutation, copy number, and mRNA expression data from human tumors. Since copy number and mRNA expression levels do not necessarily correlate with protein expression levels, we will determine if ATG5 protein is underexpressed in human PCa by immunohistochemistry. We expect that this will confirm that the multiple mechanisms of *ATG5* downregulation ultimately lead to the loss of ATG5 protein levels in human PCa.

Additionally, the exact mechanism of *ATG5* tumor suppression still remains to be determined. The simplest explanation is that autophagy suppresses tumor formation, growth and metastases. We confirmed that the ATG5-expressing xenograft tumors have functional autophagy due to the

dramatically lower levels of the autophagy substrate, p62. p62 is reported to have a number of oncogenic functions including stabilizing Twist-related protein 1 (Twist1) and c-Myc as well as stimulating mTORC1, nuclear factor kappa-light-chain-enhancer of activated B cells (NF-κB) and nuclear factor, erythroid 2-like 2 (NRF2) signaling (Moscat and Diaz-Meco, 2012; Qiang et al., 2014; Wei et al., 2014). Thus, *ATG5* may suppress tumor growth by facilitating autophagic elimination of p62. To test this possibility, we will knock down p62 using shRNAs or delete it using CRISPR/Cas9 in order to determine if it attenuates xenograft tumor growth. Conversely, we will stably infect ATG5-expressing DU145 cells with p62 containing a mutated LC3 interacting region (LIR) to prevent autophagic degradation. Together these experiments will show whether p62 accumulation is responsible for driving tumor growth in the absence of *ATG5* and autophagy.

Since the loss of ATG5 leads to proteasomal degradation of ATG12 and ATG16L1, and also affects expression of the ULK1 complex, *ATG5* tumor suppressive function could be related to any or all of these affected proteins rather than autophagy, per se. Since the expression of ATG5, ATG12 and ATG16L1 are interdependent, it remains a challenge to isolate their individual functions. Our findings regarding ATG12–ATG5-ATG16L1 complex stability have provided insight into how we can potentially uncouple and individually stabilize ATG5 and ATG16L1 to determine if the tumor suppressive function is dependent upon ATG16L1 or the fully assembled complex. Since ATG5 stability is dependent upon its interaction with ATG16L1, we have fused the N-terminus of

ATG16L1 directly to ATG5 and found that it prevents binding of endogenous ATG16L1, and presumably ATG16L2 and TECPR1 since they all share the same binding site. This results in the proteasomal turnover of endogenous ATG16L1 and the expression of a stable, free form of ATG5. Conversely, we have shown that removal of the ATG5-binding site from ATG16L1 prevents its ubiquitination and turnover, which is essential for stable ATG16L1 expression in the absence of ATG5 (Fig. 3.3*D*). With these approaches we can express ATG5 and ATG16L1 independently of one another in DU145 PCa cells to determine if either of these proteins alone is responsible for xenograft tumor suppression. This should determine if ATG5 tumor suppression is dependent upon formation of a functional ATG12–ATG5-ATG16L1 complex and autophagy or through an alternative, non-autophagic mechanism.

References

Antonioli, M., F. Albiero, F. Nazio, T. Vescovo, A. B. Perdomo, M. Corazzari, C. Marsella, P. Piselli, C. Gretzmeier, J. Dengjel, F. Cecconi, M. Piacentini and G. M. Fimia (2014). "AMBRA1 interplay with cullin E3 ubiquitin ligases regulates autophagy dynamics." Dev Cell **31**(6): 734-746.

Arredouani, M. S., B. Lu, M. Bhasin, M. Eljanne, W. Yue, J. M. Mosquera, G. J. Bubley, V. Li, M. A. Rubin, T. A. Libermann and M. G. Sanda (2009). "Identification of the transcription factor single-minded homologue 2 as a potential biomarker and immunotherapy target in prostate cancer." Clin Cancer Res **15**(18): 5794-5802.

Arstila, A. U. and B. F. Trump (1968). "Studies on cellular autophagocytosis. The formation of autophagic vacuoles in the liver after glucagon administration." Am J Pathol **53**(5): 687-733.

Avivar-Valderas, A., E. Bobrovnikova-Marjon, J. Alan Diehl, N. Bardeesy, J. Debnath and J. A. Aguirre-Ghiso (2013). "Regulation of autophagy during ECM detachment is linked to a selective inhibition of mTORC1 by PERK." Oncogene **32**(41): 4932-4940.

Axe, E. L., S. A. Walker, M. Manifava, P. Chandra, H. L. Roderick, A. Habermann, G. Griffiths and N. T. Ktistakis (2008). "Autophagosome formation from membrane compartments enriched in phosphatidylinositol 3-phosphate and dynamically connected to the endoplasmic reticulum." J Cell Biol **182**(4): 685-701.

Baba, M., M. Osumi and Y. Ohsumi (1995). "Analysis of the membrane structures involved in autophagy in yeast by freeze-replica method." Cell Struct Funct **20**(6): 465-471.

Baca, S. C., D. Prandi, M. S. Lawrence, J. M. Mosquera, A. Romanel, Y. Drier, K. Park, N. Kitabayashi, T. Y. MacDonald, M. Ghandi, E. Van Allen, G. V. Kryukov, A. Sboner, J. P. Theurillat, T. D. Soong, E. Nickerson, D. Auclair, A. Tewari, H. Beltran, R. C. Onofrio, G. Boysen, C. Guiducci, C. E. Barbieri, K. Cibulskis, A. Sivachenko, S. L. Carter, G. Saksena, D. Voet, A. H. Ramos, W. Winckler, M. Cipicchio, K. Ardlie, P. W. Kantoff, M. F. Berger, S. B. Gabriel, T. R. Golub, M. Meyerson, E. S. Lander, O. Elemento, G. Getz, F. Demichelis, M. A. Rubin and L. A. Garraway (2013). "Punctuated evolution of prostate cancer genomes." Cell **153**(3): 666-677.

Barbieri, C. E., S. C. Baca, M. S. Lawrence, F. Demichelis, M. Blattner, J. P. Theurillat, T. A. White, P. Stojanov, E. Van Allen, N. Stransky, E. Nickerson, S. S. Chae, G. Boysen, D. Auclair, R. C. Onofrio, K. Park, N. Kitabayashi, T. Y. MacDonald, K. Sheikh, T. Vuong, C. Guiducci, K. Cibulskis, A. Sivachenko, S. L. Carter, G. Saksena, D. Voet, W. M. Hussain, A. H. Ramos, W. Winckler, M. C. Redman, K. Ardlie, A. K. Tewari, J. M. Mosquera, N. Rupp, P. J. Wild, H. Moch, C. Morrissey, P. S.

Nelson, P. W. Kantoff, S. B. Gabriel, T. R. Golub, M. Meyerson, E. S. Lander, G. Getz, M. A. Rubin and L. A. Garraway (2012). "Exome sequencing identifies recurrent SPOP, FOXA1 and MED12 mutations in prostate cancer." Nat Genet **44**(6): 685-689.

Barbieri, C. E. and S. A. Tomlins (2014). "The prostate cancer genome: perspectives and potential." Urologic oncology **32**(1): 53 e15-22.

Barbosa, C., I. Peixeiro and L. Romao (2013). "Gene expression regulation by upstream open reading frames and human disease." PLoS Genet **9**(8): e1003529.

Behrends, C., M. E. Sowa, S. P. Gygi and J. W. Harper (2010). "Network organization of the human autophagy system." Nature **466**(7302): 68-76.

Beroukhim, R., C. H. Mermel, D. Porter, G. Wei, S. Raychaudhuri, J. Donovan, J. Barretina, J. S. Boehm, J. Dobson, M. Urashima, K. T. Mc Henry, R. M. Pinchback, A. H. Ligon, Y. J. Cho, L. Haery, H. Greulich, M. Reich, W. Winckler, M. S. Lawrence, B. A. Weir, K. E. Tanaka, D. Y. Chiang, A. J. Bass, A. Loo, C. Hoffman, J. Prensner, T. Liefeld, Q. Gao, D. Yecies, S. Signoretti, E. Maher, F. J. Kaye, H. Sasaki, J. E. Tepper, J. A. Fletcher, J. Tabernero, J. Baselga, M. S. Tsao, F. Demichelis, M. A. Rubin, P. A. Janne, M. J. Daly, C. Nucera, R. L. Levine, B. L. Ebert, S. Gabriel, A. K. Rustgi, C. R. Antonescu, M. Ladanyi, A. Letai, L. A. Garraway, M. Loda, D. G. Beer, L. D. True, A. Okamoto, S. L. Pomeroy, S. Singer, T. R. Golub, E. S. Lander, G. Getz, W. R. Sellers and M. Meyerson (2010). "The landscape of somatic copy-number alteration across human cancers." Nature **463**(7283): 899-905.

Betin, V. M. and J. D. Lane (2009). "Caspase cleavage of Atg4D stimulates GABARAP-L1 processing and triggers mitochondrial targeting and apoptosis." J Cell Sci **122**(Pt 14): 2554-2566.

Bowers, W. E. (1998). "Christian de Duve and the discovery of lysosomes and peroxisomes." Trends Cell Biol **8**(8): 330-333.

Boya, P., R. A. Gonzalez-Polo, N. Casares, J. L. Perfettini, P. Dessen, N. Larochette, D. Metivier, D. Meley, S. Souquere, T. Yoshimori, G. Pierron, P. Codogno and G. Kroemer (2005). "Inhibition of macroautophagy triggers apoptosis." Mol Cell Biol **25**(3): 1025-1040.

Cai, Q., L. Yan and Y. Xu (2014). "Anoikis resistance is a critical feature of highly aggressive ovarian cancer cells." Oncogene **0**.

Caminsky, N., E. J. Mucaki and P. K. Rogan (2014). "Interpretation of mRNA splicing mutations in genetic disease: review of the literature and guidelines for information-theoretical analysis." F1000Res **3**: 282.

Cerami, E., J. Gao, U. Dogrusoz, B. E. Gross, S. O. Sumer, B. A. Aksoy, A. Jacobsen, C. J. Byrne, M. L. Heuer, E. Larsson, Y. Antipin, B. Reva, A. P. Goldberg, C. Sander and N. Schultz (2012). "The cBio cancer genomics portal: an open platform for exploring multidimensional cancer genomics data." Cancer Discov **2**(5): 401-404.

Chan, E. Y., A. Longatti, N. C. McKnight and S. A. Tooze (2009). "Kinase-inactivated ULK proteins inhibit autophagy via their conserved C-terminal domains using an Atg13-independent mechanism." Mol Cell Biol **29**(1): 157-171.

Chandran, U. R., C. Ma, R. Dhir, M. Bisceglia, M. Lyons-Weiler, W. Liang, G. Michalopoulos, M. Becich and F. A. Monzon (2007). "Gene expression profiles of prostate cancer reveal involvement of multiple molecular pathways in the metastatic process." BMC Cancer **7**: 64.

Chen, D., W. Fan, Y. Lu, X. Ding, S. Chen and Q. Zhong (2012). "A mammalian autophagosome maturation mechanism mediated by TECPR1 and the Atg12-Atg5 conjugate." Mol Cell **45**(5): 629-641.

Cheong, H., T. Lindsten, J. Wu, C. Lu and C. B. Thompson (2011). "Ammonia-induced autophagy is independent of ULK1/ULK2 kinases." Proc Natl Acad Sci U S A **108**(27): 11121-11126.

Chiang, H. L. and J. F. Dice (1988). "Peptide sequences that target proteins for enhanced degradation during serum withdrawal." J Biol Chem **263**(14): 6797-6805.

Chiang, H. L., S. R. Terlecky, C. P. Plant and J. F. Dice (1989). "A role for a 70-kilodalton heat shock protein in lysosomal degradation of intracellular proteins." Science **246**(4928): 382-385.

Choi, A. M., S. W. Ryter and B. Levine (2013). "Autophagy in human health and disease." The New England journal of medicine **368**(7): 651-662.

Cianfanelli, V., C. Fuoco, M. Lorente, M. Salazar, F. Quondamatteo, P. F. Gherardini, D. De Zio, F. Nazio, M. Antonioli, M. D'Orazio, T. Skobo, M. Bordi, M. Rohde, L. Dalla Valle, M. Helmer-Citterich, C. Gretzmeier, J. Dengjel, G. M. Fimia, M. Piacentini, S. Di Bartolomeo, G. Velasco and F. Cecconi (2015). "AMBRA1 links autophagy to cell proliferation and tumorigenesis by promoting c-Myc dephosphorylation and degradation." Nat Cell Biol **17**(1): 20-30.

Ciechanover, A. (2005). "Proteolysis: from the lysosome to ubiquitin and the proteasome." Nat Rev Mol Cell Biol **6**(1): 79-87.

Ciechanover, A., S. Elias, H. Heller and A. Hershko (1982). ""Covalent affinity" purification of ubiquitin-activating enzyme." J Biol Chem **257**(5): 2537-2542.

Cigudosa, J. C., P. H. Rao, M. J. Calasanz, M. D. Odero, J. Michaeli, S. C. Jhanwar and R. S. Chaganti (1998). "Characterization of nonrandom chromosomal gains and losses in multiple myeloma by comparative genomic hybridization." Blood **91**(8): 3007-3010.

Clague, M. J. and S. Urbe (2010). "Ubiquitin: same molecule, different degradation pathways." Cell **143**(5): 682-685.

Cuervo, A. M. (2011). "Chaperone-mediated autophagy: Dice's 'wild' idea about lysosomal selectivity." Nat Rev Mol Cell Biol **12**(8): 535-541.

Cuervo, A. M. and J. F. Dice (1996). "A receptor for the selective uptake and degradation of proteins by lysosomes." Science **273**(5274): 501-503.

Cuervo, A. M. and E. Wong (2014). "Chaperone-mediated autophagy: roles in disease and aging." Cell Res **24**(1): 92-104.

De Duve, C., B. C. Pressman, R. Gianetto, R. Wattiaux and F. Appelmans (1955). "Tissue fractionation studies. 6. Intracellular distribution patterns of enzymes in rat-liver tissue." Biochem J **60**(4): 604-617.

De Duve, C. and R. Wattiaux (1966). "Functions of lysosomes." Annu Rev Physiol **28**: 435-492.

de Waal, E. J., H. Vreeling-Sindelarova, J. P. Schellens, J. M. Houtkooper and J. James (1986). "Quantitative changes in the lysosomal vacuolar system of rat hepatocytes during short-term starvation. A morphometric analysis with special reference to macro- and microautophagy." Cell Tissue Res **243**(3): 641-648.

Demichelis, F., S. R. Setlur, R. Beroukhim, S. Perner, J. O. Korbel, C. J. Lafargue, D. Pflueger, C. Pina, M. D. Hofer, A. Sboner, M. A. Svensson, D. S. Rickman, A. Urban, M. Snyder, M. Meyerson, C. Lee, M. B. Gerstein, R. Kuefer and M. A. Rubin (2009). "Distinct genomic aberrations associated with ERG rearranged prostate cancer." Genes Chromosomes Cancer **48**(4): 366-380.

Di Bartolomeo, S., M. Corazzari, F. Nazio, S. Oliverio, G. Lisi, M. Antonioli, V. Pagliarini, S. Matteoni, C. Fuoco, L. Giunta, M. D'Amelio, R. Nardacci, A. Romagnoli, M. Piacentini, F. Cecconi and G. M. Fimia (2010). "The dynamic interaction of AMBRA1 with the dynein motor complex regulates mammalian autophagy." J Cell Biol **191**(1): 155-168.

Ding, Z., C. J. Wu, G. C. Chu, Y. Xiao, D. Ho, J. Zhang, S. R. Perry, E. S. Labrot, X. Wu, R. Lis, Y. Hoshida, D. Hiller, B. Hu, S. Jiang, H. Zheng, A. H. Stegh, K. L. Scott, S. Signoretti, N. Bardeesy, Y. A. Wang, D. E. Hill, T. R. Golub, M. J. Stampfer, W. H. Wong, M. Loda, L. Mucci, L. Chin and R. A. DePinho (2011). "SMAD4-dependent barrier constrains prostate cancer growth and metastatic progression." Nature **470**(7333): 269-273.

Dooley, H. C., M. Razi, H. E. Polson, S. E. Girardin, M. I. Wilson and S. A. Tooze (2014). "WIPI2 links LC3 conjugation with PI3P, autophagosome formation, and pathogen clearance by recruiting Atg12-5-16L1." Mol Cell **55**(2): 238-252.

Dunlop, E. A., D. K. Hunt, H. A. Acosta-Jaquez, D. C. Fingar and A. R. Tee (2011). "ULK1 inhibits mTORC1 signaling, promotes multisite Raptor phosphorylation and hinders substrate binding." Autophagy **7**(7): 737-747.

Dunlop, E. A. and A. R. Tee (2013). "The kinase triad, AMPK, mTORC1 and ULK1, maintains energy and nutrient homoeostasis." Biochem Soc Trans **41**(4): 939-943.

Egan, D. F., D. B. Shackelford, M. M. Mihaylova, S. Gelino, R. A. Kohnz, W. Mair, D. S. Vasquez, A. Joshi, D. M. Gwinn, R. Taylor, J. M. Asara, J. Fitzpatrick, A. Dillin, B. Viollet, M. Kundu, M. Hansen and R. J. Shaw (2011). "Phosphorylation of ULK1 (hATG1) by AMP-activated protein

kinase connects energy sensing to mitophagy." Science **331**(6016): 456-461.
Elgendy, M., M. Ciro, A. K. Abdel-Aziz, G. Belmonte, R. Dal Zuffo, C. Mercurio, C. Miracco, L. Lanfrancone, M. Foiani and S. Minucci (2014). "Beclin 1 restrains tumorigenesis through Mcl-1 destabilization in an autophagy-independent reciprocal manner." Nat Commun **5**: 5637.
Eskelinen, E. L. (2008). "Fine structure of the autophagosome." Methods Mol Biol **445**: 11-28.
Etxebarria, A., O. Terrones, H. Yamaguchi, A. Landajuela, O. Landeta, B. Antonsson, H. G. Wang and G. Basanez (2009). "Endophilin B1/Bif-1 stimulates BAX activation independently from its capacity to produce large scale membrane morphological rearrangements." J Biol Chem **284**(7): 4200-4212.
Feng, Y., D. He, Z. Yao and D. J. Klionsky (2014). "The machinery of macroautophagy." Cell Res **24**(1): 24-41.
Forbes, S. A., N. Bindal, S. Bamford, C. Cole, C. Y. Kok, D. Beare, M. Jia, R. Shepherd, K. Leung, A. Menzies, J. W. Teague, P. J. Campbell, M. R. Stratton and P. A. Futreal (2011). "COSMIC: mining complete cancer genomes in the Catalogue of Somatic Mutations in Cancer." Nucleic acids research **39**(Database issue): D945-950.
Fujita, N., T. Saitoh, S. Kageyama, S. Akira, T. Noda and T. Yoshimori (2009). "Differential involvement of Atg16L1 in Crohn disease and canonical autophagy: analysis of the organization of the Atg16L1 complex in fibroblasts." The Journal of biological chemistry **284**(47): 32602-32609.
Funderburk, S. F., Q. J. Wang and Z. Yue (2010). "The Beclin 1-VPS34 complex--at the crossroads of autophagy and beyond." Trends Cell Biol **20**(6): 355-362.
Galluzzi, L., F. Pietrocola, J. M. Bravo-San Pedro, R. K. Amaravadi, E. H. Baehrecke, F. Cecconi, P. Codogno, J. Debnath, D. A. Gewirtz, V. Karantza, A. Kimmelman, S. Kumar, B. Levine, M. C. Maiuri, S. J. Martin, J. Penninger, M. Piacentini, D. C. Rubinsztein, H. U. Simon, A. Simonsen, A. M. Thorburn, G. Velasco, K. M. Ryan and G. Kroemer (2015). "Autophagy in malignant transformation and cancer progression." EMBO J.
Galluzzi, L., I. Vitale, J. M. Abrams, E. S. Alnemri, E. H. Baehrecke, M. V. Blagosklonny, T. M. Dawson, V. L. Dawson, W. S. El-Deiry, S. Fulda, E. Gottlieb, D. R. Green, M. O. Hengartner, O. Kepp, R. A. Knight, S. Kumar, S. A. Lipton, X. Lu, F. Madeo, W. Malorni, P. Mehlen, G. Nunez, M. E. Peter, M. Piacentini, D. C. Rubinsztein, Y. Shi, H. U. Simon, P. Vandenabeele, E. White, J. Yuan, B. Zhivotovsky, G. Melino and G. Kroemer (2012). "Molecular definitions of cell death subroutines: recommendations of the Nomenclature Committee on Cell Death 2012." Cell Death Differ **19**(1): 107-120.

Gammoh, N., O. Florey, M. Overholtzer and X. Jiang (2013). "Interaction between FIP200 and ATG16L1 distinguishes ULK1 complex-dependent and -independent autophagy." Nat Struct Mol Biol **20**(2): 144-149.

Gan, B. and J. L. Guan (2008). "FIP200, a key signaling node to coordinately regulate various cellular processes." Cell Signal **20**(5): 787-794.

Ganley, I. G., H. Lam du, J. Wang, X. Ding, S. Chen and X. Jiang (2009). "ULK1.ATG13.FIP200 complex mediates mTOR signaling and is essential for autophagy." J Biol Chem **284**(18): 12297-12305.

Geisler, S., K. M. Holmstrom, D. Skujat, F. C. Fiesel, O. C. Rothfuss, P. J. Kahle and W. Springer (2010). "PINK1/Parkin-mediated mitophagy is dependent on VDAC1 and p62/SQSTM1." Nat Cell Biol **12**(2): 119-131.

Gewirtz, D. A. (2014). "The four faces of autophagy: implications for cancer therapy." Cancer research **74**(3): 647-651.

Giannakopoulos, P., F. R. Herrmann, T. Bussiere, C. Bouras, E. Kovari, D. P. Perl, J. H. Morrison, G. Gold and P. R. Hof (2003). "Tangle and neuron numbers, but not amyloid load, predict cognitive status in Alzheimer's disease." Neurology **60**(9): 1495-1500.

Goldberg, A. L. and A. C. St John (1976). "Intracellular protein degradation in mammalian and bacterial cells: Part 2." Annu Rev Biochem **45**: 747-803.

Gomes, L. C. and I. Dikic (2014). "Autophagy in antimicrobial immunity." Mol Cell **54**(2): 224-233.

Grabowska, M. M., D. J. DeGraff, X. Yu, R. J. Jin, Z. Chen, A. D. Borowsky and R. J. Matusik (2014). "Mouse models of prostate cancer: picking the best model for the question." Cancer Metastasis Rev **33**(2-3): 377-397.

Grasso, C. S., Y. M. Wu, D. R. Robinson, X. Cao, S. M. Dhanasekaran, A. P. Khan, M. J. Quist, X. Jing, R. J. Lonigro, J. C. Brenner, I. A. Asangani, B. Ateeq, S. Y. Chun, J. Siddiqui, L. Sam, M. Anstett, R. Mehra, J. R. Prensner, N. Palanisamy, G. A. Ryslik, F. Vandin, B. J. Raphael, L. P. Kunju, D. R. Rhodes, K. J. Pienta, A. M. Chinnaiyan and S. A. Tomlins (2012). "The mutational landscape of lethal castration-resistant prostate cancer." Nature **487**(7406): 239-243.

Haller, M., A. K. Hock, E. Giampazolias, A. Oberst, D. R. Green, J. Debnath, K. M. Ryan, K. H. Vousden and S. W. Tait (2014). "Ubiquitination and proteasomal degradation of ATG12 regulates its proapoptotic activity." Autophagy **10**(12): 2269-2278.

Hamasaki, M., N. Furuta, A. Matsuda, A. Nezu, A. Yamamoto, N. Fujita, H. Oomori, T. Noda, T. Haraguchi, Y. Hiraoka, A. Amano and T. Yoshimori (2013). "Autophagosomes form at ER-mitochondria contact sites." Nature **495**(7441): 389-393.

Hanahan, D. and R. A. Weinberg (2011). "Hallmarks of cancer: the next generation." Cell **144**(5): 646-674.

Hara, T., K. Nakamura, M. Matsui, A. Yamamoto, Y. Nakahara, R. Suzuki-Migishima, M. Yokoyama, K. Mishima, I. Saito, H. Okano and N.

Mizushima (2006). "Suppression of basal autophagy in neural cells causes neurodegenerative disease in mice." Nature **441**(7095): 885-889.
Hershko, A., H. Heller, S. Elias and A. Ciechanover (1983). "Components of ubiquitin-protein ligase system. Resolution, affinity purification, and role in protein breakdown." J Biol Chem **258**(13): 8206-8214.
Hieronymus, H., N. Schultz, A. Gopalan, B. S. Carver, M. T. Chang, Y. Xiao, A. Heguy, K. Huberman, M. Bernstein, M. Assel, R. Murali, A. Vickers, P. T. Scardino, C. Sander, V. Reuter, B. S. Taylor and C. L. Sawyers (2014). "Copy number alteration burden predicts prostate cancer relapse." Proc Natl Acad Sci U S A **111**(30): 11139-11144.
Holzbeierlein, J., P. Lal, E. LaTulippe, A. Smith, J. Satagopan, L. Zhang, C. Ryan, S. Smith, H. Scher, P. Scardino, V. Reuter and W. L. Gerald (2004). "Gene expression analysis of human prostate carcinoma during hormonal therapy identifies androgen-responsive genes and mechanisms of therapy resistance." Am J Pathol **164**(1): 217-227.
Hong, S. B., B. W. Kim, K. E. Lee, S. W. Kim, H. Jeon, J. Kim and H. K. Song (2011). "Insights into noncanonical E1 enzyme activation from the structure of autophagic E1 Atg7 with Atg8." Nat Struct Mol Biol **18**(12): 1323-1330.
Hosokawa, N., T. Hara, T. Kaizuka, C. Kishi, A. Takamura, Y. Miura, S. Iemura, T. Natsume, K. Takehana, N. Yamada, J. L. Guan, N. Oshiro and N. Mizushima (2009a). "Nutrient-dependent mTORC1 association with the ULK1-Atg13-FIP200 complex required for autophagy." Mol Biol Cell **20**(7): 1981-1991.
Hosokawa, N., Y. Hara and N. Mizushima (2006). "Generation of cell lines with tetracycline-regulated autophagy and a role for autophagy in controlling cell size." FEBS Lett **580**(11): 2623-2629.
Hosokawa, N., T. Sasaki, S. Iemura, T. Natsume, T. Hara and N. Mizushima (2009b). "Atg101, a novel mammalian autophagy protein interacting with Atg13." Autophagy **5**(7): 973-979.
Ichimura, Y., T. Kirisako, T. Takao, Y. Satomi, Y. Shimonishi, N. Ishihara, N. Mizushima, I. Tanida, E. Kominami, M. Ohsumi, T. Noda and Y. Ohsumi (2000). "A ubiquitin-like system mediates protein lipidation." Nature **408**(6811): 488-492.
Ishibashi, K., N. Fujita, E. Kanno, H. Omori, T. Yoshimori, T. Itoh and M. Fukuda (2011). "Atg16L2, a novel isoform of mammalian Atg16L that is not essential for canonical autophagy despite forming an Atg12-5-16L2 complex." Autophagy **7**(12): 1500-1513.
Jiang, P. and N. Mizushima (2014). "Autophagy and human diseases." Cell research **24**(1): 69-79.
Joo, J. H., F. C. Dorsey, A. Joshi, K. M. Hennessy-Walters, K. L. Rose, K. McCastlain, J. Zhang, R. Iyengar, C. H. Jung, D. F. Suen, M. A. Steeves, C. Y. Yang, S. M. Prater, D. H. Kim, C. B. Thompson, R. J. Youle, P. A. Ney, J. L. Cleveland and M. Kundu (2011). "Hsp90-Cdc37 chaperone

complex regulates Ulk1- and Atg13-mediated mitophagy." Mol Cell **43**(4): 572-585.
Jung, C. H., C. B. Jun, S. H. Ro, Y. M. Kim, N. M. Otto, J. Cao, M. Kundu and D. H. Kim (2009). "ULK-Atg13-FIP200 complexes mediate mTOR signaling to the autophagy machinery." Mol Biol Cell **20**(7): 1992-2003.
Jung, C. H., M. Seo, N. M. Otto and D. H. Kim (2011). "ULK1 inhibits the kinase activity of mTORC1 and cell proliferation." Autophagy **7**(10): 1212-1221.
Kaiser, S. E., K. Mao, A. M. Taherbhoy, S. Yu, J. L. Olszewski, D. M. Duda, I. Kurinov, A. Deng, T. D. Fenn, D. J. Klionsky and B. A. Schulman (2012). "Noncanonical E2 recruitment by the autophagy E1 revealed by Atg7-Atg3 and Atg7-Atg10 structures." Nat Struct Mol Biol **19**(12): 1242-1249.
Kamada, N., M. Sakurai, K. Miyamoto, I. Sanada, N. Sadamori, S. Fukuhara, S. Abe, Y. Shiraishi, T. Abe, Y. Kaneko and et al. (1992). "Chromosome abnormalities in adult T-cell leukemia/lymphoma: a karyotype review committee report." Cancer Res **52**(6): 1481-1493.
Kan, Z., H. Zheng, X. Liu, S. Li, T. D. Barber, Z. Gong, H. Gao, K. Hao, M. D. Willard, J. Xu, R. Hauptschein, P. A. Rejto, J. Fernandez, G. Wang, Q. Zhang, B. Wang, R. Chen, J. Wang, N. P. Lee, W. Zhou, Z. Lin, Z. Peng, K. Yi, S. Chen, L. Li, X. Fan, J. Yang, R. Ye, J. Ju, K. Wang, H. Estrella, S. Deng, P. Wei, M. Qiu, I. H. Wulur, J. Liu, M. E. Ehsani, C. Zhang, A. Loboda, W. K. Sung, A. Aggarwal, R. T. Poon, S. T. Fan, J. Hardwick, C. Reinhard, H. Dai, Y. Li, J. M. Luk and M. Mao (2013). "Whole-genome sequencing identifies recurrent mutations in hepatocellular carcinoma." Genome research **23**(9): 1422-1433.
Kang, M. R., M. S. Kim, J. E. Oh, Y. R. Kim, S. Y. Song, S. S. Kim, C. H. Ahn, N. J. Yoo and S. H. Lee (2009). "Frameshift mutations of autophagy-related genes ATG2B, ATG5, ATG9B and ATG12 in gastric and colorectal cancers with microsatellite instability." The Journal of pathology **217**(5): 702-706.
Kaufmann, A., V. Beier, H. G. Franquelim and T. Wollert (2014). "Molecular mechanism of autophagic membrane-scaffold assembly and disassembly." Cell **156**(3): 469-481.
Kim, H. T., K. P. Kim, F. Lledias, A. F. Kisselev, K. M. Scaglione, D. Skowyra, S. P. Gygi and A. L. Goldberg (2007). "Certain pairs of ubiquitin-conjugating enzymes (E2s) and ubiquitin-protein ligases (E3s) synthesize nondegradable forked ubiquitin chains containing all possible isopeptide linkages." J Biol Chem **282**(24): 17375-17386.
Kim, J., M. Kundu, B. Viollet and K. L. Guan (2011). "AMPK and mTOR regulate autophagy through direct phosphorylation of Ulk1." Nat Cell Biol **13**(2): 132-141.
Kim, J. H., S. B. Hong, J. K. Lee, S. Han, K. H. Roh, K. E. Lee, Y. K. Kim, E. J. Choi and H. K. Song (2015). "Insights into autophagosome maturation revealed by the structures of ATG5 with its interacting partners." Autophagy **11**(1): 75-87.

Kim, P. K., D. W. Hailey, R. T. Mullen and J. Lippincott-Schwartz (2008). "Ubiquitin signals autophagic degradation of cytosolic proteins and peroxisomes." Proc Natl Acad Sci U S A **105**(52): 20567-20574.

Klionsky, D. J. (2007). "Autophagy: from phenomenology to molecular understanding in less than a decade." Nat Rev Mol Cell Biol **8**(11): 931-937.

Klionsky, D. J., J. M. Cregg, W. A. Dunn, Jr., S. D. Emr, Y. Sakai, I. V. Sandoval, A. Sibirny, S. Subramani, M. Thumm, M. Veenhuis and Y. Ohsumi (2003). "A unified nomenclature for yeast autophagy-related genes." Dev Cell **5**(4): 539-545.

Klionsky, D. J. and B. A. Schulman (2014). "Dynamic regulation of macroautophagy by distinctive ubiquitin-like proteins." Nat Struct Mol Biol **21**(4): 336-345.

Komander, D. (2009). "The emerging complexity of protein ubiquitination." Biochem Soc Trans **37**(Pt 5): 937-953.

Komatsu, M., S. Waguri, T. Chiba, S. Murata, J. Iwata, I. Tanida, T. Ueno, M. Koike, Y. Uchiyama, E. Kominami and K. Tanaka (2006). "Loss of autophagy in the central nervous system causes neurodegeneration in mice." Nature **441**(7095): 880-884.

Komatsu, M., S. Waguri, T. Ueno, J. Iwata, S. Murata, I. Tanida, J. Ezaki, N. Mizushima, Y. Ohsumi, Y. Uchiyama, E. Kominami, K. Tanaka and T. Chiba (2005). "Impairment of starvation-induced and constitutive autophagy in Atg7-deficient mice." J Cell Biol **169**(3): 425-434.

Korolchuk, V. I., A. Mansilla, F. M. Menzies and D. C. Rubinsztein (2009). "Autophagy inhibition compromises degradation of ubiquitin-proteasome pathway substrates." Mol Cell **33**(4): 517-527.

Koyama-Honda, I., E. Itakura, T. K. Fujiwara and N. Mizushima (2013). "Temporal analysis of recruitment of mammalian ATG proteins to the autophagosome formation site." Autophagy **9**(10): 1491-1499.

Kraft, C., M. Kijanska, E. Kalie, E. Siergiejuk, S. S. Lee, G. Semplicio, I. Stoffel, A. Brezovich, M. Verma, I. Hansmann, G. Ammerer, K. Hofmann, S. Tooze and M. Peter (2012). "Binding of the Atg1/ULK1 kinase to the ubiquitin-like protein Atg8 regulates autophagy." EMBO J **31**(18): 3691-3703.

Kristensen, A. R., S. Schandorff, M. Hoyer-Hansen, M. O. Nielsen, M. Jaattela, J. Dengjel and J. S. Andersen (2008). "Ordered organelle degradation during starvation-induced autophagy." Mol Cell Proteomics **7**(12): 2419-2428.

Kuma, A., M. Hatano, M. Matsui, A. Yamamoto, H. Nakaya, T. Yoshimori, Y. Ohsumi, T. Tokuhisa and N. Mizushima (2004). "The role of autophagy during the early neonatal starvation period." Nature **432**(7020): 1032-1036.

Laddha, S. V., S. Ganesan, C. S. Chan and E. White (2014). "Mutational landscape of the essential autophagy gene BECN1 in human cancers." Mol Cancer Res **12**(4): 485-490.

Lapointe, J., C. Li, J. P. Higgins, M. van de Rijn, E. Bair, K. Montgomery, M. Ferrari, L. Egevad, W. Rayford, U. Bergerheim, P. Ekman, A. M. DeMarzo, R. Tibshirani, D. Botstein, P. O. Brown, J. D. Brooks and J. R. Pollack (2004). "Gene expression profiling identifies clinically relevant subtypes of prostate cancer." Proc Natl Acad Sci U S A **101**(3): 811-816.

LaTulippe, E., J. Satagopan, A. Smith, H. Scher, P. Scardino, V. Reuter and W. L. Gerald (2002). "Comprehensive gene expression analysis of prostate cancer reveals distinct transcriptional programs associated with metastatic disease." Cancer Res **62**(15): 4499-4506.

Lee, H. K., L. M. Mattei, B. E. Steinberg, P. Alberts, Y. H. Lee, A. Chervonsky, N. Mizushima, S. Grinstein and A. Iwasaki (2010). "In vivo requirement for Atg5 in antigen presentation by dendritic cells." Immunity **32**(2): 227-239.

Lee, M. J., J. H. Lee and D. C. Rubinsztein (2013). "Tau degradation: the ubiquitin-proteasome system versus the autophagy-lysosome system." Prog Neurobiol **105**: 49-59.

Levine, B., N. Mizushima and H. W. Virgin (2011). "Autophagy in immunity and inflammation." Nature **469**(7330): 323-335.

Li, M., Y. Hou, J. Wang, X. Chen, Z. M. Shao and X. M. Yin (2011). "Kinetics comparisons of mammalian Atg4 homologues indicate selective preferences toward diverse Atg8 substrates." J Biol Chem **286**(9): 7327-7338.

Liang, C., P. Feng, B. Ku, I. Dotan, D. Canaani, B. H. Oh and J. U. Jung (2006). "Autophagic and tumour suppressor activity of a novel Beclin1-binding protein UVRAG." Nat Cell Biol **8**(7): 688-699.

Liu, H., Z. He, T. von Rutte, S. Yousefi, R. E. Hunger and H. U. Simon (2013a). "Down-regulation of autophagy-related protein 5 (ATG5) contributes to the pathogenesis of early-stage cutaneous melanoma." Sci Transl Med **5**(202): 202ra123.

Liu, J., H. Xia, M. Kim, L. Xu, Y. Li, L. Zhang, Y. Cai, H. V. Norberg, T. Zhang, T. Furuya, M. Jin, Z. Zhu, H. Wang, J. Yu, Y. Li, Y. Hao, A. Choi, H. Ke, D. Ma and J. Yuan (2011). "Beclin1 controls the levels of p53 by regulating the deubiquitination activity of USP10 and USP13." Cell **147**(1): 223-234.

Liu, L., D. Feng, G. Chen, M. Chen, Q. Zheng, P. Song, Q. Ma, C. Zhu, R. Wang, W. Qi, L. Huang, P. Xue, B. Li, X. Wang, H. Jin, J. Wang, F. Yang, P. Liu, Y. Zhu, S. Sui and Q. Chen (2012). "Mitochondrial outer-membrane protein FUNDC1 mediates hypoxia-induced mitophagy in mammalian cells." Nat Cell Biol **14**(2): 177-185.

Liu, P., S. Ramachandran, M. Ali Seyed, C. D. Scharer, N. Laycock, W. B. Dalton, H. Williams, S. Karanam, M. W. Datta, D. L. Jaye and C. S. Moreno (2006). "Sex-determining region Y box 4 is a transforming oncogene in human prostate cancer cells." Cancer Res **66**(8): 4011-4019.

Liu, W., S. Laitinen, S. Khan, M. Vihinen, J. Kowalski, G. Yu, L. Chen, C. M. Ewing, M. A. Eisenberger, M. A. Carducci, W. G. Nelson, S. Yegnasubramanian, J. Luo, Y. Wang, J. Xu, W. B. Isaacs, T. Visakorpi

and G. S. Bova (2009). "Copy number analysis indicates monoclonal origin of lethal metastatic prostate cancer." Nat Med **15**(5): 559-565.
Liu, Y. and B. Levine (2015). "Autosis and autophagic cell death: the dark side of autophagy." Cell Death Differ **22**(3): 367-376.
Liu, Y., S. Shoji-Kawata, R. M. Sumpter, Jr., Y. Wei, V. Ginet, L. Zhang, B. Posner, K. A. Tran, D. R. Green, R. J. Xavier, S. Y. Shaw, P. G. Clarke, J. Puyal and B. Levine (2013b). "Autosis is a Na+,K+-ATPase-regulated form of cell death triggered by autophagy-inducing peptides, starvation, and hypoxia-ischemia." Proc Natl Acad Sci U S A **110**(51): 20364-20371.
Loffler, A. S., S. Alers, A. M. Dieterle, H. Keppeler, M. Franz-Wachtel, M. Kundu, D. G. Campbell, S. Wesselborg, D. R. Alessi and B. Stork (2011). "Ulk1-mediated phosphorylation of AMPK constitutes a negative regulatory feedback loop." Autophagy **7**(7): 696-706.
Long, J., T. R. Gallagher, J. R. Cavey, P. W. Sheppard, S. H. Ralston, R. Layfield and M. S. Searle (2008). "Ubiquitin recognition by the ubiquitin-associated domain of p62 involves a novel conformational switch." J Biol Chem **283**(9): 5427-5440.
Lorin, S., A. Hamai, M. Mehrpour and P. Codogno (2013). "Autophagy regulation and its role in cancer." Semin Cancer Biol **23**(5): 361-379.
Lu, Z., R. Z. Luo, Y. Lu, X. Zhang, Q. Yu, S. Khare, S. Kondo, Y. Kondo, Y. Yu, G. B. Mills, W. S. Liao and R. C. Bast, Jr. (2008). "The tumor suppressor gene ARHI regulates autophagy and tumor dormancy in human ovarian cancer cells." J Clin Invest **118**(12): 3917-3929.
Luo, J. H., Y. P. Yu, K. Cieply, F. Lin, P. Deflavia, R. Dhir, S. Finkelstein, G. Michalopoulos and M. Becich (2002). "Gene expression analysis of prostate cancers." Mol Carcinog **33**(1): 25-35.
Luo, S. and D. C. Rubinsztein (2010). "Apoptosis blocks Beclin 1-dependent autophagosome synthesis: an effect rescued by Bcl-xL." Cell Death Differ **17**(2): 268-277.
Maes, H., A. Kuchnio, A. Peric, S. Moens, K. Nys, K. De Bock, A. Quaegebeur, S. Schoors, M. Georgiadou, J. Wouters, S. Vinckier, H. Vankelecom, M. Garmyn, A. C. Vion, F. Radtke, C. Boulanger, H. Gerhardt, E. Dejana, M. Dewerchin, B. Ghesquiere, W. Annaert, P. Agostinis and P. Carmeliet (2014). "Tumor vessel normalization by chloroquine independent of autophagy." Cancer Cell **26**(2): 190-206.
Malhotra, R., J. P. Warne, E. Salas, A. W. Xu and J. Debnath (2015). "Loss of Atg12, but not Atg5, in pro-opiomelanocortin neurons exacerbates diet-induced obesity." Autophagy **11**(1): 145-154.
Martinez-Vicente, M., Z. Talloczy, E. Wong, G. Tang, H. Koga, S. Kaushik, R. de Vries, E. Arias, S. Harris, D. Sulzer and A. M. Cuervo (2010). "Cargo recognition failure is responsible for inefficient autophagy in Huntington's disease." Nat Neurosci **13**(5): 567-576.
Maycotte, P., C. M. Gearheart, R. Barnard, S. Aryal, J. M. Mulcahy Levy, S. P. Fosmire, R. J. Hansen, M. J. Morgan, C. C. Porter, D. L. Gustafson and A.

Thorburn (2014). "STAT3-mediated autophagy dependence identifies subtypes of breast cancer where autophagy inhibition can be efficacious." Cancer Res **74**(9): 2579-2590.
McAlpine, F., L. E. Williamson, S. A. Tooze and E. Y. Chan (2013). "Regulation of nutrient-sensitive autophagy by uncoordinated 51-like kinases 1 and 2." Autophagy **9**(3): 361-373.
Mercer, C. A., A. Kaliappan and P. B. Dennis (2009). "A novel, human Atg13 binding protein, Atg101, interacts with ULK1 and is essential for macroautophagy." Autophagy **5**(5): 649-662.
Messer, J. S., S. F. Murphy, M. F. Logsdon, J. P. Lodolce, W. A. Grimm, S. J. Bartulis, T. P. Vogel, M. Burn and D. L. Boone (2013). "The Crohn's disease: associated ATG16L1 variant and Salmonella invasion." BMJ Open **3**(6).
Mijaljica, D., M. Prescott and R. J. Devenish (2011). "Microautophagy in mammalian cells: revisiting a 40-year-old conundrum." Autophagy **7**(7): 673-682.
Mizushima, N. and B. Levine (2010). "Autophagy in mammalian development and differentiation." Nat Cell Biol **12**(9): 823-830.
Mizushima, N., T. Noda, T. Yoshimori, Y. Tanaka, T. Ishii, M. D. George, D. J. Klionsky, M. Ohsumi and Y. Ohsumi (1998a). "A protein conjugation system essential for autophagy." Nature **395**(6700): 395-398.
Mizushima, N., H. Sugita, T. Yoshimori and Y. Ohsumi (1998b). "A new protein conjugation system in human. The counterpart of the yeast Apg12p conjugation system essential for autophagy." J Biol Chem **273**(51): 33889-33892.
Moscat, J. and M. T. Diaz-Meco (2012). "p62: a versatile multitasker takes on cancer." Trends Biochem Sci **37**(6): 230-236.
Moyzis, A. G., J. Sadoshima and A. B. Gustafsson (2015). "Mending a broken heart: the role of mitophagy in cardioprotection." Am J Physiol Heart Circ Physiol **308**(3): H183-192.
Mukherjee, S., R. N. Ghosh and F. R. Maxfield (1997). "Endocytosis." Physiol Rev **77**(3): 759-803.
Murphy, M. P., A. Holmgren, N. G. Larsson, B. Halliwell, C. J. Chang, B. Kalyanaraman, S. G. Rhee, P. J. Thornalley, L. Partridge, D. Gems, T. Nystrom, V. Belousov, P. T. Schumacker and C. C. Winterbourn (2011). "Unraveling the biological roles of reactive oxygen species." Cell Metab **13**(4): 361-366.
Murthy, A., Y. Li, I. Peng, M. Reichelt, A. K. Katakam, R. Noubade, M. Roose-Girma, J. DeVoss, L. Diehl, R. R. Graham and M. van Lookeren Campagne (2014). "A Crohn's disease variant in Atg16l1 enhances its degradation by caspase 3." Nature **506**(7489): 456-462.
Nair, U., W. L. Yen, M. Mari, Y. Cao, Z. Xie, M. Baba, F. Reggiori and D. J. Klionsky (2012). "A role for Atg8-PE deconjugation in autophagosome biogenesis." Autophagy **8**(5): 780-793.

Nakatogawa, H., Y. Ichimura and Y. Ohsumi (2007). "Atg8, a ubiquitin-like protein required for autophagosome formation, mediates membrane tethering and hemifusion." Cell **130**(1): 165-178.

Nazio, F., F. Strappazzon, M. Antonioli, P. Bielli, V. Cianfanelli, M. Bordi, C. Gretzmeier, J. Dengjel, M. Piacentini, G. M. Fimia and F. Cecconi (2013). "mTOR inhibits autophagy by controlling ULK1 ubiquitylation, self-association and function through AMBRA1 and TRAF6." Nat Cell Biol **15**(4): 406-416.

Nishimura, T., T. Kaizuka, K. Cadwell, M. H. Sahani, T. Saitoh, S. Akira, H. W. Virgin and N. Mizushima (2013). "FIP200 regulates targeting of Atg16L1 to the isolation membrane." EMBO Rep **14**(3): 284-291.

Noda, N. N., Y. Fujioka, T. Hanada, Y. Ohsumi and F. Inagaki (2013). "Structure of the Atg12-Atg5 conjugate reveals a platform for stimulating Atg8-PE conjugation." EMBO reports **14**(2): 206-211.

Noda, N. N., Y. Ohsumi and F. Inagaki (2010). "Atg8-family interacting motif crucial for selective autophagy." FEBS Lett **584**(7): 1379-1385.

Norman, J. M., G. M. Cohen and E. T. Bampton (2010). "The in vitro cleavage of the hAtg proteins by cell death proteases." Autophagy **6**(8): 1042-1056.

Novak, I., V. Kirkin, D. G. McEwan, J. Zhang, P. Wild, A. Rozenknop, V. Rogov, F. Lohr, D. Popovic, A. Occhipinti, A. S. Reichert, J. Terzic, V. Dotsch, P. A. Ney and I. Dikic (2010). "Nix is a selective autophagy receptor for mitochondrial clearance." EMBO Rep **11**(1): 45-51.

Novikoff, A. B., H. Beaufay and C. De Duve (1956). "Electron microscopy of lysosomerich fractions from rat liver." J Biophys Biochem Cytol **2**(4 Suppl): 179-184.

Ogawa, M., Y. Yoshikawa, T. Kobayashi, H. Mimuro, M. Fukumatsu, K. Kiga, Z. Piao, H. Ashida, M. Yoshida, S. Kakuta, T. Koyama, Y. Goto, T. Nagatake, S. Nagai, H. Kiyono, M. Kawalec, J. M. Reichhart and C. Sasakawa (2011). "A Tecpr1-dependent selective autophagy pathway targets bacterial pathogens." Cell Host Microbe **9**(5): 376-389.

Ohsumi, Y. (2014). "Historical landmarks of autophagy research." Cell Res **24**(1): 9-23.

Okamoto, K. (2014). "Organellophagy: eliminating cellular building blocks via selective autophagy." J Cell Biol **205**(4): 435-445.

Otomo, C., Z. Metlagel, G. Takaesu and T. Otomo (2013). "Structure of the human ATG12~ATG5 conjugate required for LC3 lipidation in autophagy." Nature structural & molecular biology **20**(1): 59-66.

Ouyang, D. Y., L. H. Xu, X. H. He, Y. T. Zhang, L. H. Zeng, J. Y. Cai and S. Ren (2013). "Autophagy is differentially induced in prostate cancer LNCaP, DU145 and PC-3 cells via distinct splicing profiles of ATG5." Autophagy **9**(1): 20-32.

Papinski, D., M. Schuschnig, W. Reiter, L. Wilhelm, C. A. Barnes, A. Maiolica, I. Hansmann, T. Pfaffenwimmer, M. Kijanska, I. Stoffel, S. S. Lee, A. Brezovich, J. H. Lou, B. E. Turk, R. Aebersold, G. Ammerer, M. Peter and

C. Kraft (2014). "Early steps in autophagy depend on direct phosphorylation of Atg9 by the Atg1 kinase." Mol Cell **53**(3): 471-483.
Park, C. and A. M. Cuervo (2013). "Selective autophagy: talking with the UPS." Cell Biochem Biophys **67**(1): 3-13.
Patel, A. A. and J. A. Steitz (2003). "Splicing double: insights from the second spliceosome." Nat Rev Mol Cell Biol **4**(12): 960-970.
Pickrell, A. M. and R. J. Youle (2015). "The Roles of PINK1, Parkin, and Mitochondrial Fidelity in Parkinson's Disease." Neuron **85**(2): 257-273.
Poole, B., S. Ohkuma and M. J. Warburton (1977). "The accumulation of weakly basic substances in lysosomes and the inhibition of intracellular protein degradation." Acta Biol Med Ger **36**(11-12): 1777-1788.
Pruitt, K. D., G. R. Brown, S. M. Hiatt, F. Thibaud-Nissen, A. Astashyn, O. Ermolaeva, C. M. Farrell, J. Hart, M. J. Landrum, K. M. McGarvey, M. R. Murphy, N. A. O'Leary, S. Pujar, B. Rajput, S. H. Rangwala, L. D. Riddick, A. Shkeda, H. Sun, P. Tamez, R. E. Tully, C. Wallin, D. Webb, J. Weber, W. Wu, M. DiCuccio, P. Kitts, D. R. Maglott, T. D. Murphy and J. M. Ostell (2014). "RefSeq: an update on mammalian reference sequences." Nucleic acids research **42**(Database issue): D756-763.
Qiang, L., B. Zhao, M. Ming, N. Wang, T. C. He, S. Hwang, A. Thorburn and Y. Y. He (2014). "Regulation of cell proliferation and migration by p62 through stabilization of Twist1." Proc Natl Acad Sci U S A **111**(25): 9241-9246.
Qu, X., J. Yu, G. Bhagat, N. Furuya, H. Hibshoosh, A. Troxel, J. Rosen, E. L. Eskelinen, N. Mizushima, Y. Ohsumi, G. Cattoretti and B. Levine (2003). "Promotion of tumorigenesis by heterozygous disruption of the beclin 1 autophagy gene." The Journal of clinical investigation **112**(12): 1809-1820.
Radoshevich, L., L. Murrow, N. Chen, E. Fernandez, S. Roy, C. Fung and J. Debnath (2010). "ATG12 conjugation to ATG3 regulates mitochondrial homeostasis and cell death." Cell **142**(4): 590-600.
Rao, S., L. Tortola, T. Perlot, G. Wirnsberger, M. Novatchkova, R. Nitsch, P. Sykacek, L. Frank, D. Schramek, V. Komnenovic, V. Sigl, K. Aumayr, G. Schmauss, N. Fellner, S. Handschuh, M. Glosmann, P. Pasierbek, M. Schlederer, G. P. Resch, Y. Ma, H. Yang, H. Popper, L. Kenner, G. Kroemer and J. M. Penninger (2014). "A dual role for autophagy in a murine model of lung cancer." Nature communications **5**: 3056.
Ravikumar, B., R. Duden and D. C. Rubinsztein (2002). "Aggregate-prone proteins with polyglutamine and polyalanine expansions are degraded by autophagy." Hum Mol Genet **11**(9): 1107-1117.
Ravikumar, B., C. Vacher, Z. Berger, J. E. Davies, S. Luo, L. G. Oroz, F. Scaravilli, D. F. Easton, R. Duden, C. J. O'Kane and D. C. Rubinsztein (2004). "Inhibition of mTOR induces autophagy and reduces toxicity of polyglutamine expansions in fly and mouse models of Huntington disease." Nat Genet **36**(6): 585-595.

Redon, R., S. Ishikawa, K. R. Fitch, L. Feuk, G. H. Perry, T. D. Andrews, H. Fiegler, M. H. Shapero, A. R. Carson, W. Chen, E. K. Cho, S. Dallaire, J. L. Freeman, J. R. Gonzalez, M. Gratacos, J. Huang, D. Kalaitzopoulos, D. Komura, J. R. MacDonald, C. R. Marshall, R. Mei, L. Montgomery, K. Nishimura, K. Okamura, F. Shen, M. J. Somerville, J. Tchinda, A. Valsesia, C. Woodwark, F. Yang, J. Zhang, T. Zerjal, J. Zhang, L. Armengol, D. F. Conrad, X. Estivill, C. Tyler-Smith, N. P. Carter, H. Aburatani, C. Lee, K. W. Jones, S. W. Scherer and M. E. Hurles (2006). "Global variation in copy number in the human genome." Nature **444**(7118): 444-454.

Reidick, C., F. El Magraoui, H. E. Meyer, H. Stenmark and H. W. Platta (2014). "Regulation of the Tumor-Suppressor Function of the Class III Phosphatidylinositol 3-Kinase Complex by Ubiquitin and SUMO." Cancers (Basel) **7**(1): 1-29.

Rodrigues, L. U., L. Rider, C. Nieto, L. Romero, A. Karimpour-Fard, M. Loda, M. S. Lucia, M. Wu, L. Shi, A. Cimic, S. J. Sirintrapun, R. Nolley, C. Pac, H. Chen, D. M. Peehl, J. Xu, W. Liu, J. C. Costello and S. D. Cramer (2015). "Coordinate Loss of MAP3K7 and CHD1 Promotes Aggressive Prostate Cancer." Cancer Res **75**(6): 1021-1034.

Rogov, V., V. Dotsch, T. Johansen and V. Kirkin (2014). "Interactions between autophagy receptors and ubiquitin-like proteins form the molecular basis for selective autophagy." Mol Cell **53**(2): 167-178.

Romanov, J., M. Walczak, I. Ibiricu, S. Schuchner, E. Ogris, C. Kraft and S. Martens (2012). "Mechanism and functions of membrane binding by the Atg5-Atg12/Atg16 complex during autophagosome formation." The EMBO journal **31**(22): 4304-4317.

Rosenfeldt, M. T., J. O'Prey, J. P. Morton, C. Nixon, G. MacKay, A. Mrowinska, A. Au, T. S. Rai, L. Zheng, R. Ridgway, P. D. Adams, K. I. Anderson, E. Gottlieb, O. J. Sansom and K. M. Ryan (2013). "p53 status determines the role of autophagy in pancreatic tumour development." Nature **504**(7479): 296-300.

Russell, R. C., Y. Tian, H. Yuan, H. W. Park, Y. Y. Chang, J. Kim, H. Kim, T. P. Neufeld, A. Dillin and K. L. Guan (2013). "ULK1 induces autophagy by phosphorylating Beclin-1 and activating VPS34 lipid kinase." Nat Cell Biol **15**(7): 741-750.

Russell, R. C., H. X. Yuan and K. L. Guan (2014). "Autophagy regulation by nutrient signaling." Cell Res **24**(1): 42-57.

Sabharwal, S. S. and P. T. Schumacker (2014). "Mitochondrial ROS in cancer: initiators, amplifiers or an Achilles' heel?" Nat Rev Cancer **14**(11): 709-721.

Sahu, R., S. Kaushik, C. C. Clement, E. S. Cannizzo, B. Scharf, A. Follenzi, I. Potolicchio, E. Nieves, A. M. Cuervo and L. Santambrogio (2011). "Microautophagy of cytosolic proteins by late endosomes." Dev Cell **20**(1): 131-139.

Saitoh, T., N. Fujita, M. H. Jang, S. Uematsu, B. G. Yang, T. Satoh, H. Omori, T. Noda, N. Yamamoto, M. Komatsu, K. Tanaka, T. Kawai, T. Tsujimura, O. Takeuchi, T. Yoshimori and S. Akira (2008). "Loss of the autophagy protein Atg16L1 enhances endotoxin-induced IL-1beta production." Nature **456**(7219): 264-268.

Sakoh-Nakatogawa, M., K. Matoba, E. Asai, H. Kirisako, J. Ishii, N. N. Noda, F. Inagaki, H. Nakatogawa and Y. Ohsumi (2013). "Atg12-Atg5 conjugate enhances E2 activity of Atg3 by rearranging its catalytic site." Nat Struct Mol Biol **20**(4): 433-439.

Schaeffer, V., I. Lavenir, S. Ozcelik, M. Tolnay, D. T. Winkler and M. Goedert (2012). "Stimulation of autophagy reduces neurodegeneration in a mouse model of human tauopathy." Brain **135**(Pt 7): 2169-2177.

Seibenhener, M. L., J. R. Babu, T. Geetha, H. C. Wong, N. R. Krishna and M. W. Wooten (2004). "Sequestosome 1/p62 is a polyubiquitin chain binding protein involved in ubiquitin proteasome degradation." Mol Cell Biol **24**(18): 8055-8068.

Shaid, S., C. H. Brandts, H. Serve and I. Dikic (2013). "Ubiquitination and selective autophagy." Cell Death Differ **20**(1): 21-30.

Shang, L., S. Chen, F. Du, S. Li, L. Zhao and X. Wang (2011). "Nutrient starvation elicits an acute autophagic response mediated by Ulk1 dephosphorylation and its subsequent dissociation from AMPK." Proc Natl Acad Sci U S A **108**(12): 4788-4793.

Shi, C. S. and J. H. Kehrl (2010). "Traf6 and A20 differentially regulate TLR4-induced autophagy by affecting the ubiquitination of Beclin 1." Autophagy **6**(7): 986-987.

Shibutani, S. T. and T. Yoshimori (2014). "A current perspective of autophagosome biogenesis." Cell Res **24**(1): 58-68.

Singh, D., P. G. Febbo, K. Ross, D. G. Jackson, J. Manola, C. Ladd, P. Tamayo, A. A. Renshaw, A. V. D'Amico, J. P. Richie, E. S. Lander, M. Loda, P. W. Kantoff, T. R. Golub and W. R. Sellers (2002). "Gene expression correlates of clinical prostate cancer behavior." Cancer Cell **1**(2): 203-209.

Sou, Y. S., S. Waguri, J. Iwata, T. Ueno, T. Fujimura, T. Hara, N. Sawada, A. Yamada, N. Mizushima, Y. Uchiyama, E. Kominami, K. Tanaka and M. Komatsu (2008). "The Atg8 conjugation system is indispensable for proper development of autophagic isolation membranes in mice." Mol Biol Cell **19**(11): 4762-4775.

Stanley, R. E., M. J. Ragusa and J. H. Hurley (2014). "The beginning of the end: how scaffolds nucleate autophagosome biogenesis." Trends Cell Biol **24**(1): 73-81.

Strohecker, A. M., J. Y. Guo, G. Karsli-Uzunbas, S. M. Price, G. J. Chen, R. Mathew, M. McMahon and E. White (2013). "Autophagy sustains mitochondrial glutamine metabolism and growth of BrafV600E-driven lung tumors." Cancer Discov **3**(11): 1272-1285.

Taherbhoy, A. M., S. W. Tait, S. E. Kaiser, A. H. Williams, A. Deng, A. Nourse, M. Hammel, I. Kurinov, C. O. Rock, D. R. Green and B. A. Schulman (2011). "Atg8 transfer from Atg7 to Atg3: a distinctive E1-E2 architecture and mechanism in the autophagy pathway." Mol Cell **44**(3): 451-461.

Takahashi, Y., D. Coppola, N. Matsushita, H. D. Cualing, M. Sun, Y. Sato, C. Liang, J. U. Jung, J. Q. Cheng, J. J. Mule, W. J. Pledger and H. G. Wang (2007). "Bif-1 interacts with Beclin 1 through UVRAG and regulates autophagy and tumorigenesis." Nat Cell Biol **9**(10): 1142-1151.

Takamura, A., M. Komatsu, T. Hara, A. Sakamoto, C. Kishi, S. Waguri, Y. Eishi, O. Hino, K. Tanaka and N. Mizushima (2011). "Autophagy-deficient mice develop multiple liver tumors." Genes Dev **25**(8): 795-800.

Takeshige, K., M. Baba, S. Tsuboi, T. Noda and Y. Ohsumi (1992). "Autophagy in yeast demonstrated with proteinase-deficient mutants and conditions for its induction." J Cell Biol **119**(2): 301-311.

Tamura, K., M. Furihata, T. Tsunoda, S. Ashida, R. Takata, W. Obara, H. Yoshioka, Y. Daigo, Y. Nasu, H. Kumon, H. Konaka, M. Namiki, K. Tozawa, K. Kohri, N. Tanji, M. Yokoyama, T. Shimazui, H. Akaza, Y. Mizutani, T. Miki, T. Fujioka, T. Shuin, Y. Nakamura and H. Nakagawa (2007). "Molecular features of hormone-refractory prostate cancer cells by genome-wide gene expression profiles." Cancer Res **67**(11): 5117-5125.

Tan, J. M., E. S. Wong, D. S. Kirkpatrick, O. Pletnikova, H. S. Ko, S. P. Tay, M. W. Ho, J. Troncoso, S. P. Gygi, M. K. Lee, V. L. Dawson, T. M. Dawson and K. L. Lim (2008). "Lysine 63-linked ubiquitination promotes the formation and autophagic clearance of protein inclusions associated with neurodegenerative diseases." Hum Mol Genet **17**(3): 431-439.

Taylor, B. S., N. Schultz, H. Hieronymus, A. Gopalan, Y. Xiao, B. S. Carver, V. K. Arora, P. Kaushik, E. Cerami, B. Reva, Y. Antipin, N. Mitsiades, T. Landers, I. Dolgalev, J. E. Major, M. Wilson, N. D. Socci, A. E. Lash, A. Heguy, J. A. Eastham, H. I. Scher, V. E. Reuter, P. T. Scardino, C. Sander, C. L. Sawyers and W. L. Gerald (2010). "Integrative genomic profiling of human prostate cancer." Cancer cell **18**(1): 11-22.

Thierry-Mieg, D. and J. Thierry-Mieg (2006). "AceView: a comprehensive cDNA-supported gene and transcripts annotation." Genome biology **7 Suppl 1**: S12 11-14.

Tomlins, S. A., R. Mehra, D. R. Rhodes, X. Cao, L. Wang, S. M. Dhanasekaran, S. Kalyana-Sundaram, J. T. Wei, M. A. Rubin, K. J. Pienta, R. B. Shah and A. M. Chinnaiyan (2007). "Integrative molecular concept modeling of prostate cancer progression." Nat Genet **39**(1): 41-51.

Tomlins, S. A., D. R. Rhodes, S. Perner, S. M. Dhanasekaran, R. Mehra, X. W. Sun, S. Varambally, X. Cao, J. Tchinda, R. Kuefer, C. Lee, J. E. Montie, R. B. Shah, K. J. Pienta, M. A. Rubin and A. M. Chinnaiyan (2005). "Recurrent fusion of TMPRSS2 and ETS transcription factor genes in prostate cancer." Science **310**(5748): 644-648.

Tsukada, M. and Y. Ohsumi (1993). "Isolation and characterization of autophagy-defective mutants of Saccharomyces cerevisiae." FEBS Lett **333**(1-2): 169-174.

Vanaja, D. K., J. C. Cheville, S. J. Iturria and C. Y. Young (2003). "Transcriptional silencing of zinc finger protein 185 identified by expression profiling is associated with prostate cancer progression." Cancer Res **63**(14): 3877-3882.

Varambally, S., J. Yu, B. Laxman, D. R. Rhodes, R. Mehra, S. A. Tomlins, R. B. Shah, U. Chandran, F. A. Monzon, M. J. Becich, J. T. Wei, K. J. Pienta, D. Ghosh, M. A. Rubin and A. M. Chinnaiyan (2005). "Integrative genomic and proteomic analysis of prostate cancer reveals signatures of metastatic progression." Cancer Cell **8**(5): 393-406.

Viale, A., P. Pettazzoni, C. A. Lyssiotis, H. Ying, N. Sanchez, M. Marchesini, A. Carugo, T. Green, S. Seth, V. Giuliani, M. Kost-Alimova, F. Muller, S. Colla, L. Nezi, G. Genovese, A. K. Deem, A. Kapoor, W. Yao, E. Brunetto, Y. Kang, M. Yuan, J. M. Asara, Y. A. Wang, T. P. Heffernan, A. C. Kimmelman, H. Wang, J. B. Fleming, L. C. Cantley, R. A. DePinho and G. F. Draetta (2014). "Oncogene ablation-resistant pancreatic cancer cells depend on mitochondrial function." Nature **514**(7524): 628-632.

Wallace, T. A., R. L. Prueitt, M. Yi, T. M. Howe, J. W. Gillespie, H. G. Yfantis, R. M. Stephens, N. E. Caporaso, C. A. Loffredo and S. Ambs (2008). "Tumor immunobiological differences in prostate cancer between African-American and European-American men." Cancer Res **68**(3): 927-936.

Wei, H., C. Wang, C. M. Croce and J. L. Guan (2014). "p62/SQSTM1 synergizes with autophagy for tumor growth in vivo." Genes Dev **28**(11): 1204-1216.

Weidberg, H., T. Shpilka, E. Shvets, A. Abada, F. Shimron and Z. Elazar (2011). "LC3 and GATE-16 N termini mediate membrane fusion processes required for autophagosome biogenesis." Dev Cell **20**(4): 444-454.

Weidberg, H., E. Shvets, T. Shpilka, F. Shimron, V. Shinder and Z. Elazar (2010). "LC3 and GATE-16/GABARAP subfamilies are both essential yet act differently in autophagosome biogenesis." EMBO J **29**(11): 1792-1802.

Welsh, J. B., L. M. Sapinoso, A. I. Su, S. G. Kern, J. Wang-Rodriguez, C. A. Moskaluk, H. F. Frierson, Jr. and G. M. Hampton (2001). "Analysis of gene expression identifies candidate markers and pharmacological targets in prostate cancer." Cancer Res **61**(16): 5974-5978.

Wilkinson, K. D., M. K. Urban and A. L. Haas (1980). "Ubiquitin is the ATP-dependent proteolysis factor I of rabbit reticulocytes." J Biol Chem **255**(16): 7529-7532.

Williams, J. L., P. A. Greer and J. A. Squire (2014). "Recurrent copy number alterations in prostate cancer: an in silico meta-analysis of publicly available genomic data." Cancer Genet **207**(10-12): 474-488.

Winslow, A. R., C. W. Chen, S. Corrochano, A. Acevedo-Arozena, D. E. Gordon, A. A. Peden, M. Lichtenberg, F. M. Menzies, B. Ravikumar, S. Imarisio, S. Brown, C. J. O'Kane and D. C. Rubinsztein (2010). "alpha-Synuclein

impairs macroautophagy: implications for Parkinson's disease." J Cell Biol **190**(6): 1023-1037.
Wirth, M., J. Joachim and S. A. Tooze (2013). "Autophagosome formation--the role of ULK1 and Beclin1-PI3KC3 complexes in setting the stage." Semin Cancer Biol **23**(5): 301-309.
Wong, E. and A. M. Cuervo (2010). "Autophagy gone awry in neurodegenerative diseases." Nat Neurosci **13**(7): 805-811.
Wu, M., L. Shi, A. Cimic, L. Romero, G. Sui, C. J. Lees, J. M. Cline, D. F. Seals, J. S. Sirintrapun, T. P. McCoy, W. Liu, J. W. Kim, G. A. Hawkins, D. M. Peehl, J. Xu and S. D. Cramer (2012). "Suppression of Tak1 promotes prostate tumorigenesis." Cancer Res **72**(11): 2833-2843.
Xia, P., S. Wang, Y. Du, Z. Zhao, L. Shi, L. Sun, G. Huang, B. Ye, C. Li, Z. Dai, N. Hou, X. Cheng, Q. Sun, L. Li, X. Yang and Z. Fan (2013). "WASH inhibits autophagy through suppression of Beclin 1 ubiquitination." EMBO J **32**(20): 2685-2696.
Xu, C., J. Liu, L. C. Hsu, Y. Luo, R. Xiang and T. H. Chuang (2011). "Functional interaction of heat shock protein 90 and Beclin 1 modulates Toll-like receptor-mediated autophagy." FASEB J **25**(8): 2700-2710.
Yamaguchi, M., N. N. Noda, H. Yamamoto, T. Shima, H. Kumeta, Y. Kobashigawa, R. Akada, Y. Ohsumi and F. Inagaki (2012). "Structural insights into Atg10-mediated formation of the autophagy-essential Atg12-Atg5 conjugate." Structure **20**(7): 1244-1254.
Yang, A., N. V. Rajeshkumar, X. Wang, S. Yabuuchi, B. M. Alexander, G. C. Chu, D. D. Von Hoff, A. Maitra and A. C. Kimmelman (2014). "Autophagy Is Critical for Pancreatic Tumor Growth and Progression in Tumors with p53 Alterations." Cancer discovery **4**(8): 905-913.
Yang, S., X. Wang, G. Contino, M. Liesa, E. Sahin, H. Ying, A. Bause, Y. Li, J. M. Stommel, G. Dell'antonio, J. Mautner, G. Tonon, M. Haigis, O. S. Shirihai, C. Doglioni, N. Bardeesy and A. C. Kimmelman (2011). "Pancreatic cancers require autophagy for tumor growth." Genes & development **25**(7): 717-729.
Young, A. R., E. Y. Chan, X. W. Hu, R. Kochl, S. G. Crawshaw, S. High, D. W. Hailey, J. Lippincott-Schwartz and S. A. Tooze (2006). "Starvation and ULK1-dependent cycling of mammalian Atg9 between the TGN and endosomes." J Cell Sci **119**(Pt 18): 3888-3900.
Young, A. R., M. Narita, M. Ferreira, K. Kirschner, M. Sadaie, J. F. Darot, S. Tavare, S. Arakawa, S. Shimizu, F. M. Watt and M. Narita (2009). "Autophagy mediates the mitotic senescence transition." Genes Dev **23**(7): 798-803.
Yousefi, S., R. Perozzo, I. Schmid, A. Ziemiecki, T. Schaffner, L. Scapozza, T. Brunner and H. U. Simon (2006). "Calpain-mediated cleavage of Atg5 switches autophagy to apoptosis." Nat Cell Biol **8**(10): 1124-1132.
Yu, Y. P., D. Landsittel, L. Jing, J. Nelson, B. Ren, L. Liu, C. McDonald, R. Thomas, R. Dhir, S. Finkelstein, G. Michalopoulos, M. Becich and J. H.

Luo (2004). "Gene expression alterations in prostate cancer predicting tumor aggression and preceding development of malignancy." J Clin Oncol **22**(14): 2790-2799.

Yu, Z. Q., T. Ni, B. Hong, H. Y. Wang, F. J. Jiang, S. Zou, Y. Chen, X. L. Zheng, D. J. Klionsky, Y. Liang and Z. Xie (2012). "Dual roles of Atg8-PE deconjugation by Atg4 in autophagy." Autophagy **8**(6): 883-892.

Yue, Z., S. Jin, C. Yang, A. J. Levine and N. Heintz (2003). "Beclin 1, an autophagy gene essential for early embryonic development, is a haploinsufficient tumor suppressor." Proceedings of the National Academy of Sciences of the United States of America **100**(25): 15077-15082.

Zhang, J. and P. A. Ney (2009). "Role of BNIP3 and NIX in cell death, autophagy, and mitophagy." Cell Death Differ **16**(7): 939-946.

Zhao, Z., Z. Zhang, Y. Li, M. Zhou, X. Li, B. Yu and R. Wang (2013). "Probing the key interactions between human Atg5 and Atg16 proteins: a prospective application of molecular modeling." ChemMedChem **8**(8): 1270-1275.

Zhu, Y., S. Massen, M. Terenzio, V. Lang, S. Chen-Lindner, R. Eils, I. Novak, I. Dikic, A. Hamacher-Brady and N. R. Brady (2013). "Modulation of serines 17 and 24 in the LC3-interacting region of Bnip3 determines pro-survival mitophagy versus apoptosis." J Biol Chem **288**(2): 1099-1113.